Department of Process Engineering

Final Year Project 478

Assessing the kinetics of steam distillation for essential oil (D-limonene) recovery from citrus peel waste.

TTJ Muzondidya (22708421)

3 November 2022

Plagiarism Declaration

I, T.T.J. Muzondidya (22708421), declare that:

- I have read and understood the Stellenbosch University Policy on Plagiarism and the definitions of plagiarism and self-plagiarism contained in the Policy [Plagiarism: The use of the ideas or material of others without acknowledgement, or the re-use of one's own previously evaluated or published material without acknowledgement or indication thereof (self-plagiarism or text recycling)].
- I also understand that direct translations are plagiarism unless accompanied by an appropriate acknowledgement of the source. I also know that verbatim copy that has not been explicitly indicated as such, is plagiarism.
- I know that plagiarism is a punishable offence and may be referred to the University's Central Disciplinary Committee (CDC) which has the authority to expel me for such an offence.
- I know that plagiarism is harmful to the academic environment and that it harms any profession.
- Accordingly, all quotations and contributions from any source whatsoever (including the internet) have been cited fully (acknowledged); further, all verbatim copies have been expressly indicated as such (e.g., through quotation marks) and the sources are cited fully.
- Except where a source has been cited, the work contained in this assignment is my work and I have not previously (in its entirety or part) submitted it for grading in this module/assignment or another module/assignment.

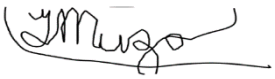

03/11/2022

Signed | Date

Acknowledgements

I could not have undertaken the journey of writing this thesis without the protection and strength of my loving God and Saviour. I would like to express my deepest gratitude to my Supervisor Mr Z. Mapholi for his guidance and feedback that has helped me to grow as a researcher.

Gratitude should also go to Ernst Kleynhans and Babylonstoren who were so kind to provide the raw clementine peel material used in this thesis.

I had the pleasure of working with Munae Troskie, Beatrice Mwamba, and co-Supervisor Mr. G. Teke who were in my research group.

Lastly, I cannot forget to mention my wonderful family who constantly provided emotional support and gave me the courage to continue moving forward.

Abstract

This study focused on investigating the effect of heating power and mass loading on the steam distillation of essential oils, with attention being given to D-Limonene. The study also focused on assessing the kinetics of the steam distillation process. D-Limonene has antibacterial qualities that can be utilised in the food, cosmetics, and pharmaceutical industries. Extraction of such a high-value product from citrus peel waste promotes a circular economy and could potentially aid in waste management, as anti-microbial properties prohibit composting. Knowledge of the kinetics of the extraction process not only leads to a better fundamental understanding and improvements that could be made to the extraction process but is also used to scale up experimental work to a larger industrial scale.

The current work aimed to fit a kinetic model to experimental data which would be used to describe the extraction of essential oils by steam distillation. The pseudo-first-order model was fit to the experimental data, and it was considered suitable to model the kinetics of steam distillation of essential oils from clementine peel because the observed coefficient of determination at the different extraction conditions was high ($R^2 > 0.85$). A study of the impact of heating power and mass loading on the kinetics of steam distillation using the one-factor-at-a-time approach concluded that the maximum equilibrium yield is obtained for a mass loading of 200g and the heating power of 1000 W. To obtain the equilibrium yield quickly a mass loading of 50 g and heating power of 1200 W were the suitable conditions. Taking into account both the equilibrium yield and how quickly the extraction process reaches this maximum. The optimal conditions for one factor at a time approach are a mass loading of 150 g and a heating power of 1000W.

Steam distillation of the crude essential oil and D-Limonene were optimised by response surface methodology. A central composite design based on the effect of heating power (between 800 W to 1400 W) and dry clementine peel mass loading (between 50 g to 200 g) was adopted with essential oil yields as the target function. Microsoft excel and STATISTICA Version 14 were used to process the data and carry out the central composite design-response surface methodology and the statistical analysis of data. The results of the analysis of variance showed that the model parameters were not statistically significant due to all of the probability values of the parameters being higher than the significance level of 0.05. The coefficient of determination (R^2) of the model was 0.836. The optimal conditions were heating power of 717.17 W and mass loading of 199.95 g which contributed an essential oil yield of 2.25%.

The chemical composition of the essential oil was analysed by Gas Chromatography-Flame Ionisation Detection which was used to determine the Concentration of D-limonene for the essential oil and observe whether the mass loading and/or heating power affect the concentration. The highest concentration of D-Limonene which was 106.97 mg/ml was observed for a heating power of 717.17 W and mass loading of 50.047 g. The concentration of D-Limonene decreased when the mass loading was increased. The effect of the heating power was statistically insignificant.

Table of Contents

Nomenclature

Symbols		
A	Area	m^2
f	fraction	
k	Rate constant	min^{-1}
m	Mass	kg
p	Probability	
q	Essential oil yield at time t	ml/g
R^2	Coefficient of determination	
t	Time	min
V	Volume	ml
W	Dry mass of material used	g
X_1	Heating Power	W
X_2	Mass loading	g
Y	Essential oil yield	ml/g
z	Number of factors	
Greek symbols		
ρ	Density	kg/m^3
β	regression model coefficients	
ϖ	Essential oil equilibrium yield	ml/g
α	Significance level	
ξ	Extent of reaction	mol
Subscripts and superscripts		
p	the essential oil obtained at time t	
in	Flow stream into the system	
out	Flow stream out of the system	
W	Washing process	
Acronyms		
ANOVA	Analysis of Variance	
CCD	Central composite design	
Df/DOF	Degrees of freedom	
d_1	Unhindered diffusion	
d_2	Hindered diffusion	
DOE	Design of Experiment	
EO	Essential Oil	
FID	Flame Ionisation Detection/Detector	
GC	Gas Chromatography	

MS	Mean square
SSE	Sum of square error
SST	The total sum of square
SSR	Sum of squared regression

1 Introduction

The citrus processing industry is a large global industry. It is estimated that more than 120 million tons of citrus are produced annually in both tropical and subtropical areas of the world (Mahato *et al.*, 2021). Focusing on South Africa's fruit sector, citrus is the primary export fruit in South Africa, accounting for 45 % of all fruit export revenues (Chisoro-Dube & Simon , 2021). This represents 32 % of the country's total fruit production (Chisoro-Dube & Simon , 2021). After Spain, South Africa is the world's second-largest supplier of citrus fruit, meeting 10% of worldwide demand in 2018 (Chisoro-Dube & Simon , 2021). Due to the magnitude of the mass production of citrus, it is naturally expected that large quantities of waste are produced from the citrus processing industry not only globally but in South Africa as well.

After processing, about 40-60% of citrus ends up as waste. Which contains peels, seeds, leftover pulp and pith (Mahato, Sharma, *et al.*, 2019). Landfill disposal of citrus waste is inappropriate since this waste biomass contains low pH, high water content, and high organic matter level of citrus waste, making them not environmentally friendly (Santiago *et al.*, 2020). In an attempt to compact citrus peel waste management, studies have been concentrated on recovering potentially high-value bioactive substances (pectin, hesperidin, and essential oils, particularly D-limonene) which promotes a circular economy.

Pectin is composed of 17 different monosaccharides (Mahato *et al.*, 2021). In the food industry, pectin is primarily used as a gelling agent and stabilizer (Palanisamy, Dhivya and Kuppamuthu, 2014). Conventionally, chemicals like strong acids are used to extract pectin, e.g., oxalic acid, hydrochloric acid, nitric acid, and sulphuric acid. Another valuable by-product is hesperidin (also known as vitamin P). Hesperidin is recovered from the solid residue and is present in the flavedo portions of the peels (Coll *et al.*, 1998). After an acidic pre-treatment of peel waste, it is collected in amounts between 3.7% and 4.5% of dry mass (Mahato, Sinha, *et al.*, 2019), (Mamma and Christakopoulos, 2014), (Fagbohungbe *et al.*, 2016). Hesperidin is an antioxidant that improves the ability of vitamin C (ascorbic acid) to reduce cholesterol levels (Sharma *et al.*, 2013)

The primary constituent of the essential oils in Citrus Peel Waste (CPW) is D-limonene, which is a terpene molecule with antibacterial qualities that can be used in the food, cosmetics, and pharmaceutical industries. Due to its organoleptic and antioxidant qualities as well as its low toxicity profile, D-limonene is used as a flavouring and scenting agent in a variety of items. These include perfumes, soaps, foods, and beverages (Ciriminna *et al.*, 2014). Numerous studies on the medicinal properties of limonene have demonstrated its anti-inflammatory (Kummer *et al.*, 2013), antioxidant (Murali, Karthikeyan and Saravanan, 2013), antinociceptive, anticancer (Russo *et al.*, 2013), antidiabetic (Kamalakkannan and Prince, 2004), antiviral, and gastroprotective properties, among other health-promoting properties (Vieira *et al.*, 2018). One such clinical application for limonene is the treatment of heartburn brought on by gastric acid(Sarpietro *et al.*, 2021).

D-Limonene finds wide application in many industries and as such extraction methods were developed to extract D-limonene from citrus material (Mahato, Sinha, *et al.*, 2019), (Negro *et al.*, 2017), (Ozturk,

Winterburn and Gonzalez-Miquel, 2019). The typical extraction method used to extract D-limonene from citrus peel includes cold press, solvent extraction, hydro/steam distillation or novel extraction methods such as microwave and ultrasound-assisted extraction(Siddiqui *et al.*, 2022). Conventional methods are typically used due to the simple and robust nature of the equipment setup that is required. There are several studies where steam distillation has been used to extract and maximise the yield of essential oils from plant material (Fitriady, Sulaswatty and Agustian, 2017), (Dao *et al.*, 2021), (Farhat *et al.*, 2011) and (Masango, 2005). It is crucial to comprehend the kinetics of essential oil steam distillation in addition to merely attempting to increase essential oil yields.

Investigation of steam distillation kinetics is not something new and authors such as (Milojević *et al.*, 2013), (Xavier *et al.*, 2011), (Koul, Gandotra, & Koul, 2004) have investigated and established kinetic models for extraction of essential oil from different plant material. However, the kinetics of steam distillation of clementine peels and the effect of mass loading and heating power together on the extraction process have not been investigated. In this paper, that is the focus of the study. Understanding the principles of the steam distillation process is necessary to operate, optimize, regulate, and design for industrial steam distillation by scaling up experimental essential oil extraction, which can only be known by understanding the kinetics of the process. From a technological and financial perspective, it is crucial to combine research into essential oil yield, composition, and kinetic models for steam distillation (Milojević *et al.*, 2013).

2 Aim and Objectives

The present study aimed to investigate the effect of heating power and mass loading on steam distillation and assess the kinetics of steam distillation for essential oil (D-Limonene) recovery from clementine peel. The aim of this study was fulfilled by fulfilling the following objectives:

- Investigate the impact of mass loading and heating power on steam distillation extraction of essential oils from clementine peels using a statistically valid experimental design.
- Assess the selection of a kinetic model to describe the steam distillation process of essential oils from clementine peels through the model fitting on a single factor and experimental design data.
- Investigate the effect of mass loading and heating power on the kinetics of steam distillation of essential oils from clementine peels.
- Explain the effect of mass loading and heating power conditions on the composition and subsequently concentration of the D-limonene.

2.1 Key Questions

1. How can the essential oil yield from clementine peels be optimised and maximised by optimising the mass loading and heating power during steam distillation?

2. Was the D-Limonene concentration impacted by the mass loading and heating power ranges that were selected?
3. Can the generated response surface methodology model be used to accurately predict essential oil from the studied factors?
4. Why is it important to study the kinetics of the extraction of D-limonene from citrus peel using steam distillation and what is the impact of heating power and mass loading on the extraction kinetics?

3 Theory / Literature

3.1 Citrus Peel

Citrus processing inducting is a large global industry where more than 120 million tons of citrus are produced annually in tropical and subtropical areas of the world (Mahato *et al.*, 2021). Every year, the industries that process citrus produce enormous volumes of waste, with citrus peel waste alone making up over 50% of the wet fruit mass (Sharma *et al.*, 2017). Due to the number of different flavonoids, carotenoids, dietary fibre, sugars, polyphenols, essential oils, ascorbic acid, and significant levels of some trace elements, citrus waste has enormous economic worth (Sharma *et al.*, 2017). Citrus waste also has a lot of sugars that are good for fermentation to make bioethanol. There are however problems associated with the processing or landfill disposal of citrus peel that needs to be addressed.

Citrus peel's high moisture content (75-85%) and the presence of essential oils make disposal extremely challenging. Due to the peel waste's high moisture content, it is challenging to dry it using standard, established techniques or commercial drying equipment (Sharma *et al.*, 2017). The majority of citrus wastes are currently dried to create cow feed pellets, which use a lot of energy(Mahato *et al.*, 2021).

Before being dumped in landfills or bioethanol production, peel waste must first be extracted from its oils since these oils harm bacterial and fermentation-based decomposition (Mahato *et al.*, 2021), (Sharma *et al.*, 2017). According to Murdock and Allen, orange peel oils are toxic to yeasts (Murdock and Allen, 1960). Orange peel essential oil has been discovered to have actions that hinder the growth of various beneficial bacteria, yeast, and moulds (e.g., Bacillus subtilis, Saccharomyces cerevisiae, Aspergillus awamori) (SUBBA, SOUMITHRI and RAO, 1967). In addition to reducing pollution, the process of extracting oil from peels yields beneficial by-products. As such, over the years, studies have concentrated on developing effective methods for obtaining bioactive substances (pectin, hesperidin, and essential oils, particularly D-limonene) (Sharma *et al.*, 2017), (Mahato, Sharma, *et al.*, 2019).

As was already noted, one of the most crucial procedures before the fermentation of biomass to produce biogas or biofuel is the removal and/or recovery of limonene. Aeration and biological treatment are the two main pre-treatment techniques for the elimination of limonene that have been documented. For the recovery of limonene, however, the primary pre-treatment techniques are cold pressing, dry distillation, filtering, sorption, centrifugation, steam distillation, steam explosion, and

liquid extraction with organic solvents (Mahato *et al.*, 2021). The details for the different D-Limonene recovery techniques are outlined in section 3.3.

After the bioactive compounds and limonene have been removed from the citrus waste, it is possible to use biotransformation to make ethanol, biogas, fuels, and bio sorbents (Mahato *et al.*, 2021). The latter comprises physical-chemical reactions and/or microbial fermentation (Fagbohungbe *et al.*, 2016), (Su, Tan and Xu, 2016), (Negro *et al.*, 2016), (Zema *et al.*, 2018). Citrus biomass is a renewable, sustainable, and affordable feedstock for making eco-friendly fuel because of its widespread production. Biogas and ethanol are produced by processing the citrus waste's carbohydrates and fermentable sugars. When compared to gasoline or petroleum fuel, the carbon dioxide emissions from biofuels can be reduced by 80% (Mark R Wilkins, Widmer and Grohmann, 2007), (Gunaseelan, 2004). Citrus waste can produce 1.2 billion litres (or 300 million gallons) of ethanol globally from its 70% carbohydrate content (Pourbafrani *et al.*, 2010).

The focus of this study was restricted to the extraction of citrus peel essential oil by steam distillation. As such, a further focus on the practical uses of citrus essential and the role of D-limonene and how steam distillation compares to the other extraction techniques was carried out.

3.2 D-Limonene

Essential oils (EOs) are aromatic molecules found in enormous quantities in oil sacs or oil glands located at various depths throughout the fruit peel, primarily in the flavedo portion and cuticles. These are water-insoluble but soluble in alcohol, ether, and natural oils (Mahato, Sharma, *et al.*, 2019). essential oils are particularly abundant in citrus peels. Citrus essential oils find practical application in flavouring ingredients in food products, cosmetics, perfumes, toiletries, and other personal sanitary products (Raeissi *et al.*, 2008). The primary constituent of citrus peel essential oils is limonene, which accounts for 91–95% of them. The remaining composition of the essential oil is Pinolene (1.83-2.61%), n-octanol (1.50–1.64%), myrcene (1.3%), a-pinene (0.28–0.5%), linalool (0.39%), b-pinene (0.38–1.05%), g-terpinene (0.41–1.09%), camphene (0.27–0.35%), and decanal (0.11–0.35%) (Mahato *et al.*, 2021). Due to its high composition in citrus essential oils, D-limonene is particularly useful when it comes to the extraction of essential oils from citrus peels.

D-Limonene has been utilized in aromatherapy, including massage, inhalations, and baths. It is used in the textile, plastics, and paint industries to hide undesirable odours (Mahato, Sharma, *et al.*, 2019). Due to rising consumer concerns and demand for food safety, Essential Oils as natural antimicrobial agents have recently attracted a lot of interest in the food and packaging industries (Calo *et al.*, 2015). D-limonene can be used instead of synthetic fungicides and antibacterial agents because it has a powerful antibacterial effect that destroys microbial cell integrity and prevents them from respiring (M'hiri *et al.*, 2016). The D-limonene percentage composition of total essential oils of different citrus fruit varieties is reported in table 1 below.

Table 1: D-limonene composition in various citrus fruit adapted from (Droby et al., 2008)

Genus, species, variety	D-limonene (% of total GC peak area)

Orange	86.80
Grapefruit	92.34
Clementine (Mandarin)	88.89

3.3 Conventional extraction methods of D-limonene

Each technique has particular advantages and disadvantages. Nevertheless, citrus peel oil is most frequently obtained by steam or hydro distillation. Mechanical cold pressing, water-based distillation or steam explosion, or solid-liquid extraction with organic solvents, traditionally carried out in a Soxhlet apparatus but also performed in agitated tanks to promote dissolution, are the most common D-Limonene extraction procedures (Siddiqui *et al.*, 2022). These traditional procedures are straightforward and effective, but they require a long extraction time (Khandare, Tomke and Rathod, 2021), a lot of energy (Ozturk, Winterburn and Gonzalez-Miquel, 2019), and a lot of money. This section details the extraction technology for each different technique and Table 2 gives the obtained yields and conditions that were used in various studies to extract D-Limonene essential oil from citrus peel.

3.3.1 Cold pressing

Cold pressing involves breaking the oil sacks off the husk and pressing the Citrus waste in a first press to obtain liquid and solid streams is how the oil is obtained. To separate any remaining peel from the oil, the liquid stream is delivered to the second press (Santiago *et al.*, 2020). Citrus essential oil is vigorously stirred with water during cold pressing, and the amount of citrus and terpene alcohols gradually decreases (Ferhat, Meklati and Chemat, 2007a). These cold-pressed oils have a significant concentration of other constituents besides D-limonene; therefore, they might not be appropriate for cases where maximizing D-Limonene yield is a priority (Dugo *et al.*, 1997).

3.3.2 Soxhlet extraction

A tried-and-tested technique for solid-liquid extraction, Soxhlet extraction has been around for a while. Hexane is the most frequently employed solvent in the context of plant oils (Siddiqui *et al.*, 2022). Soxhlet extraction entails that plant material must be placed in a thimble holder before a fresh solvent can be added. The solvent dissolves the solutes, and when it reaches an overflow level, it flows out of the thimble holder and into a distillation flask, where the solvent is separated. More fresh solvent is added to the thimble holder containing plant material as the solute builds up in the distillation flask, overflowing into the distillation flask until the extraction is finished (Siddiqui *et al.*, 2022). Although it is less complicated, more affordable, and performs better than other conventional techniques, Soxhlet extraction has a few drawbacks, including a lengthy extraction time, significant solvent consumption, the impossibility of speeding the process through agitation, energy expenditure for solvent evaporation, and heat degradation of the target molecules (Wang and Weller, 2006).

3.3.3 Distillation

Traditional techniques for obtaining bioactive substances and essential oils from plants include hydro distillation. It can be done before the dehydration of plant materials and does not require the use of organic solvents (Azmir *et al.*, 2013). Water distillation, water and steam distillation, and direct steam distillation are the three distinct kinds of hydro distillation (Vankar Padma S, 2004).

In the process of hydro distillation, the plant materials are first packed into a still compartment, and then enough water is added and brought to a boil. Another option is to introduce direct steam directly into the plant sample. The key influencing variables that liberate the bioactive chemicals from plant tissue are hot water and steam. The vaporized combination of water and oil is condensed by indirect water cooling. Oil and bioactive chemicals automatically separate from the water when the condensed mixture moves from the condenser to the separator (Silva *et al.*, 2005).

The hot temperatures and extended extraction times during steam and hydro distillation can chemically alter the oil components and frequently result in the loss of the most volatile compounds (Ferhat, Meklati and Chemat, 2007a).

Table 2: Extraction methods of D-limonene from the citrus peel in different studies

Technique	Reference	Fruit	Solvent	Extraction time	Temperature (°C)	Yield
Solid-liquid extraction	(Lopresto *et al.*, 2019)	Lemon	Hexane	30 min	100–200	2.97% w/w 0.95% w/w
Hydro distillation	(Chen *et al.*, 2014)	Orange peels				1.98% compared to 1% on a dried basis
Molecular distillation	(Rossi *et al.*, 2011)	Lemon			30	98.7%
Cold pressing	(Ferhat, Meklati and Chemat, 2007b)	Orange peels		30 min	100	86.3% 93.23%
Steam distillation	(Martín *et al.*, 2010)	Orange peels		1.0 h		70% w/w
Steam distillation	(Mark R. Wilkins, Widmer and Grohmann, 2007)	Citrus peel		1.0		90% w/w
Soxhlet extraction	(Jha *et al.*, 2019)	Citrus limetta		187 min	85	100% yield –33.78 mg/g
Hydrolysis	(Waheed *et al.*, 2020)	Orange	Enzyme-assisted hydro-distillation	3.8 h	55	66%

3.4 Kinetic modelling

The extraction of essential oil from citrus peel may be improved, created, and scaled up using mathematical modelling. Without having to conduct experimental methods, mathematical models are utilized to mimic a process and learn about the behaviour of the extraction process. To assess different techniques for selecting the process variable conditions, the steam distillation process must be mathematically modelled (Cassel *et al.*, 2009). One of the models that were utilized in this paper is based on a similar study that investigated the kinetics of hydro-distillation of juniper essential oil (Marković *et al.*, 2019).

3.4.1 Mechanism of Essential oil transfer

According to (Mahara & McGaw, 2020), there are three basic mechanisms relating to the transfer of oil from within the material to the steam passing through the bed as follows:

1. Diffusion of the oil onto the surface of the substance.
2. Oil vaporization on the surface
3. Convectional oil transfer from the material's surface to the steam

Considering the plant charge in terms of a series of vertical elements or layers (Mahara & McGaw, 2020), the mechanism of clementine essential oil transportation can be visually represented by Figure 1 below:

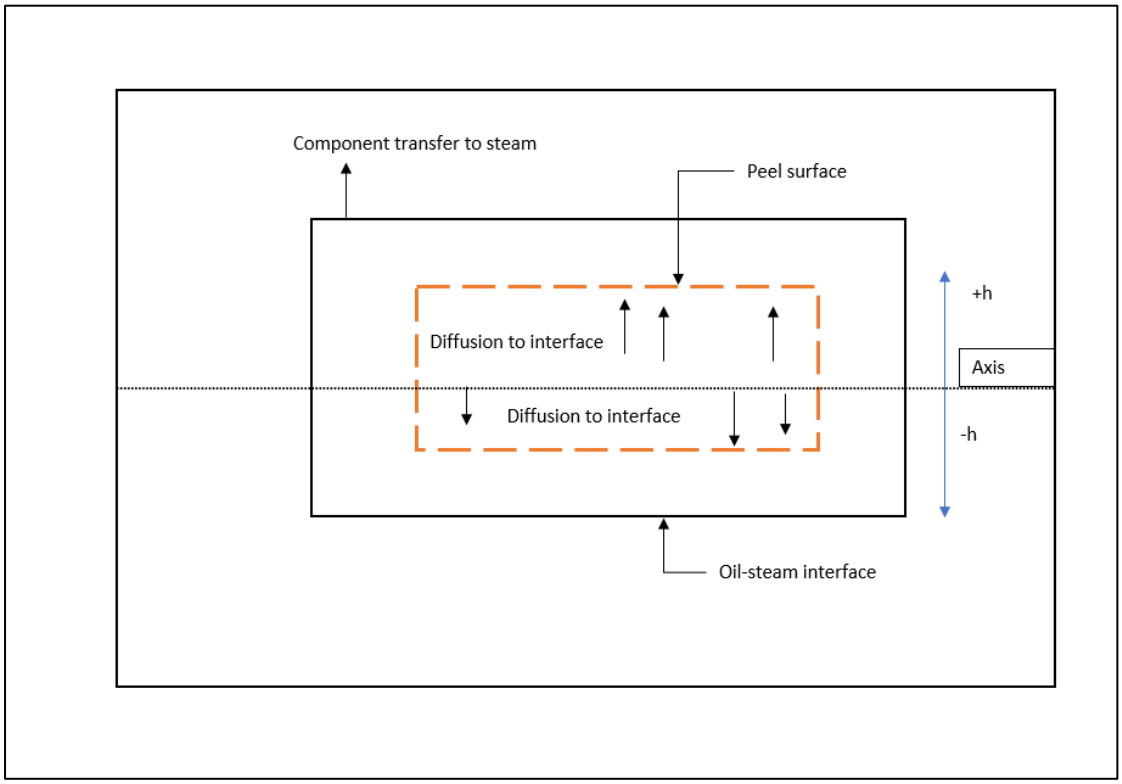

Figure 1: Essential oil transfer mechanism from clementine peel to steam

3.4.2 Published Steam distillation kinetic models

This section gives an overview of already published models which are listed in Table 3 and were adapted from references (Roth, Uhlenbrock and Strube, 2020). For the plant extraction portion of the models that are currently in use, two methods were used:

First-order kinetic: It is assumed that the separation of the essential oil from the plant particles follows a first-order kinetic model and the essential oil in the plant particle has a consistent composition (Cerpa, Mato and José Cocero, 2008), (Benyoussef *et al.*, 2002).

Diffusion: When diffusion is used to represent the extraction of the essential oil, Fick's second law is solved for a sphere or a slab. Washing and diffusion are two categories of extraction that result from varying extraction rates during steam distillation. Washing occurs when there are damaged plant cells and is realized by a high diffusion coefficient. Plant membrane causes diffusion, which occurs with plant cells but moves more slowly (Koudous *et al.*, 2014), (Sovová and Aleksovski, 2006).

In models listed in Table 3, most of the models assume that the evaporation of essential oil components is fast compared to diffusion in the particle. Evaporation is therefore neglected. For this reason, not all transport effects are taken into account in the corresponding models. Additionally, the models (except for the model presented by (Roth, Uhlenbrock and Strube, 2020)) treat the essential oil as a single pseudo-component and do not distinguish between other oil components.

Table 3: Published modelling approaches(Roth, Uhlenbrock and Strube, 2020)

Model	Plant Material	Particle Shape	Essential Oil	Mass Transport Inside Particle	Mass Transport into Steam	Author and year	Reference
Crude model	Lavandin	Glandular trichomes	Pseudo-single component	Not considered	Energy supply is limited	Denny 1979	(Denny, 1979)
Diffusional model and model based on first-order kinetics	Coriander fruits	Isotropic	Pseudo-single Component	Diffusion or diffusion with first-order kinetic	Not considered	Benyoussef 2002	(Benyoussef *et al.*, 2002)
First order kinetics	Lemon grass	Chopped or Un-chopped	Pseudo-single Component	First order kinetics	Not considered	Koul 2003	(Both, Chemat and Strube, 2014)
Diffusional model based on Fick's second law	Lemon grass, twigs and leaves	One-dimensional rectangle geometry	Pseudo-single Component	Unsteady-state diffusion (Fick's second law)	Not considered	Cassel 2006	(Cassel and Vargas, 2006)

Broken and intact cells	Creeping thyme leaves/intact coriander fruits	Spherical/slab	Pseudo-single component	First-order kinetics or linear	Not considered	Sovova 2006	(Sovová and Aleksovski, 2006)
Phenomenological model	Lavandin	Glandular trichomes	Individual oil components	First order kinetics	Vapour pressure is limiting	Cerpa 2008	(Cerpa, Mato and Cocero, 2008)
Diffusional model based on Fick's second law	Rosemary, basil, lavender	One-dimensional rectangle geometry	Pseudo-single component	Unsteady-state diffusion (Fick's second law)	Not considered	Cassel 2008	(Cassel *et al.*, 2009)
Model of Sovova based on mass transfer fundamentals	Asteraceae	Leaves/sticks	Pseudo-single component	Diffusion	Not considered	Xavier 2011	(Xavier *et al.*, 2011)
Washing and diffusion	Juniper berries	Isotropic	Pseudo-single component	Unsteady-state diffusion (Fick's second law)	Not considered	Milojevic 2008	(Milojević *et al.*, 2008)

3.4.3 Pseudo Non-Linear Model

According to (Marković *et al.*, 2019), it was assumed that the extraction of essential oil occurred through three simultaneous processes. The majority of the essential oil was dispersed throughout the plant particles with the remainder concentrated on their exterior surfaces. During the quick initial step of distillation, the so-called "washing," essential oil from the exterior surfaces was extracted. The remaining essential oil was extracted during the "unhindered" and "hindered" diffusions, i.e., the essential oil from ruptured and unruptured organs (Marković *et al.*, 2019). Both of these diffusional processes, which were crucial in the hydro distillation's latter stages but took far longer than washing, Unhindered diffusion was thought to be the quicker of the two diffusional processes. Regarding the essential oil contained in the plant particles, the kinetics of all three processes adhered to the first-order law:

$$-\frac{dq_p}{dt} = kq_p \qquad [1]$$

where q_p was the average content of essential oil in the plant particles (ml per 100 g) at time t, and k was the process rate constant.

To develop the mathematical model of this process, several assumptions were made, which have already been used for modelling the kinetics of Hydro-distillation (Milojević *et al.*, 2013)(Milojević *et al.*, 2008) and Microwave-assisted hydro-distillation (Pavi *et al.*, 2015):

1. Plant particles were similar in size, shape, and initial essential oil content, and they were isotropic.
2. The essential oil was regarded as a pseudo-single component;
3. Up until the system achieved equilibrium when no further distillation of essential oil took place, the amount of essential oil that could be retrieved matched the amount of essential oil that was distilled off;
4. It was assumed that the essential oil's washing, unimpeded, and hampered extraction fractions (f_w, f_{d1} and f_{d2}, respectively) would remain constant;
5. The rate constants for washing (k_w), unhindered diffusion (k_{d1}) and hindered diffusion (k_{d2}) were constant;
6. There did not impede the essential oil's mass transfer from the plant particles' exterior surfaces;
7. The water phase and the essential oil were completely immiscible;
8. Up until equilibrium, the amount of essential oil that was accessible for hydro distillation matched the amount of essential oil that was distilled off, i.e., t=0, $q_p=q_\infty$;
9. When the amount of plant material in the distillation vessel with a time delay was divided by the amount of essential oil collected in the separator, the result was equivalent to the essential oil yield from the plant material (Marković *et al.*, 2019).

For t = 0, $q_p = q_\infty$, so the integration of Equation [1] gave the following expressions for washing, unhindered diffusion and hindered diffusion, respectively:

$$q_{p,w} = q_\infty\left(e^{-k_w t}\right) \quad [\,2\,]$$

$$q_{p,d1} = q_\infty\left(e^{-k_{d1} t}\right) \quad [\,3\,]$$

$$q_{p,d2} = q_\infty\left(e^{-k_{d2} t}\right) \quad [\,4\,]$$

Taking into account assumption iv), the amount of essential oil that remained in the plant particles until time t was

$$\frac{q_p}{q_\infty} = f_w\left(e^{-k_w t}\right) + f_{d1}\left(e^{-k_{d1} t}\right) + f_{d2}\left(e^{-k_{d2} t}\right) \quad [\,5\,]$$

where $f_w=q_p$, w/q∞, fd1=q_p, d1/q_∞ and fd2=q_p, d2/q_∞,

$$f_w + f_{d1} + f_{d2} = 1 \quad [\,6\,]$$

Hence, the amount of essential oil extracted until time t, q(=q∞−q_p), was as follows

$$\frac{q}{q_\infty} = 1 - f_w\left(e^{-k_w t}\right) - f_{d1}\left(e^{-k_{d1} t}\right) - f_{d2}\left(e^{-k_{d2} t}\right) \quad [\,7\,]$$

$$q = q_\infty\left(1 - f_w\left(e^{-k_w t}\right) - f_{d1}\left(e^{-k_{d1} t}\right) - f_{d2}\left(e^{-k_{d2} t}\right)\right) \quad [\,8\,]$$

Equation [8] described the variation of the essential oil yield from the plant material with the progress of distillation.

If hindered diffusion was negligible (fd2 = 0), then Equation [7] was simplified to the following expression:

$$\frac{q}{q_\infty} = 1 - f_w\left(e^{-k_w t}\right) - (1 - f_w)\left(e^{-k_{d1} t}\right) \quad [\,9\,]$$

A simpler kinetic model was derived from Equation [9] by assuming instantaneous washing followed by diffusion ($k_w \rightarrow \infty$) and diffusion with no washing ($k_w \rightarrow \infty$ and $f_w=0$):

$$q = q_\infty\left(1 - e^{-kt}\right) \qquad [\ 10\ ]$$

Equation [10] was built around the hypothesis that the essential oil would still be present in the plant material after pseudo-first-order kinetics was applied(Marković *et al.*, 2019). This model was verified for the kinetics of HD (Morin, Gunther, Peyron, & Richard, 1985) and MAHD (Kapas, 2011). This model has been used for a steam distillation study by (Dao *et al.*, 2021).

Kinetics simulation revealed that in more than 75% of the analysed cases, a simple first-order model, equation [10] that only takes into account diffusion into the solid phase and makes several simplifying assumptions delivers findings that are in good agreement with the experimental data(Ait Amer Meziane *et al.*, 2020). According to the findings of the study conducted by (Ait Amer Meziane *et al.*, 2019), the model performs well under all operating situations and is independent of the type of plant substrate. Relatively complex models in the analysed cases converge to the first-order model. As a result, the straightforward first-order model is general and enables accurate prediction of the duration and yield of the extraction process in practice. In this model, the resistance in the solid phase is the only one that affects the rate of the entire process; the resistance in the fluid phase has no impact on the kinetics of extraction (Ait Amer Meziane *et al.*, 2019).

Due to the general applicability of Equation[10, this model was used to carry out the kinetic study of steam distillation of essential oil from clementine peels in this study. This model is simple with relatively high precision (P. T. Dao *et al.*, 2022).

4 Methodology

4.1 Materials and Equipment

4.1.1 Materials

The citrus peel waste used in this study was clementine collected from Babylonstoren juicer in June 2022. 50 kg of citrus peel was collected. The citrus peel consisted of clementine peels and left-over fibres and pulp in the peels. For steam distillation, the other raw material required is distilled water.

For the GC-FID analysis, the chemicals used were trichloromethane, 2-pentanol and D-Limonene. 99% Trichloromethane, which is an organic solvent was used as the Gas Chromatography (GC)-solvent. The internal standard used for the sample preparation for the GC-FID analysis was 98% 2-pentanol. 98% D-limonene was used to gain a reference for the GC-FID analysis of the samples. The chemicals were purchased from Sigma-Aldrich.

4.1.2 Equipment

A grinder was used to ground clementine peels into smaller particles and kept frozen in a plastic package. When required the material was thawed. The dry matter analysis was done with the KERN DBS moisture analyser. The moisture analyser reports the data in terms of solids %. The moisture content is then calculated using equation [11]:

$$Moisture\ content\ (\%) = 100 - solids\ \% \qquad [\ 11\ ]$$

Triplicate measurements for the moisture content were measured and the moisture content was 82.9 ± 2.3%. The steam Distillation set-up, depicted in Figure 2, consisted of a still pot, glass column, induction cooker heating mantle, and graham condenser.

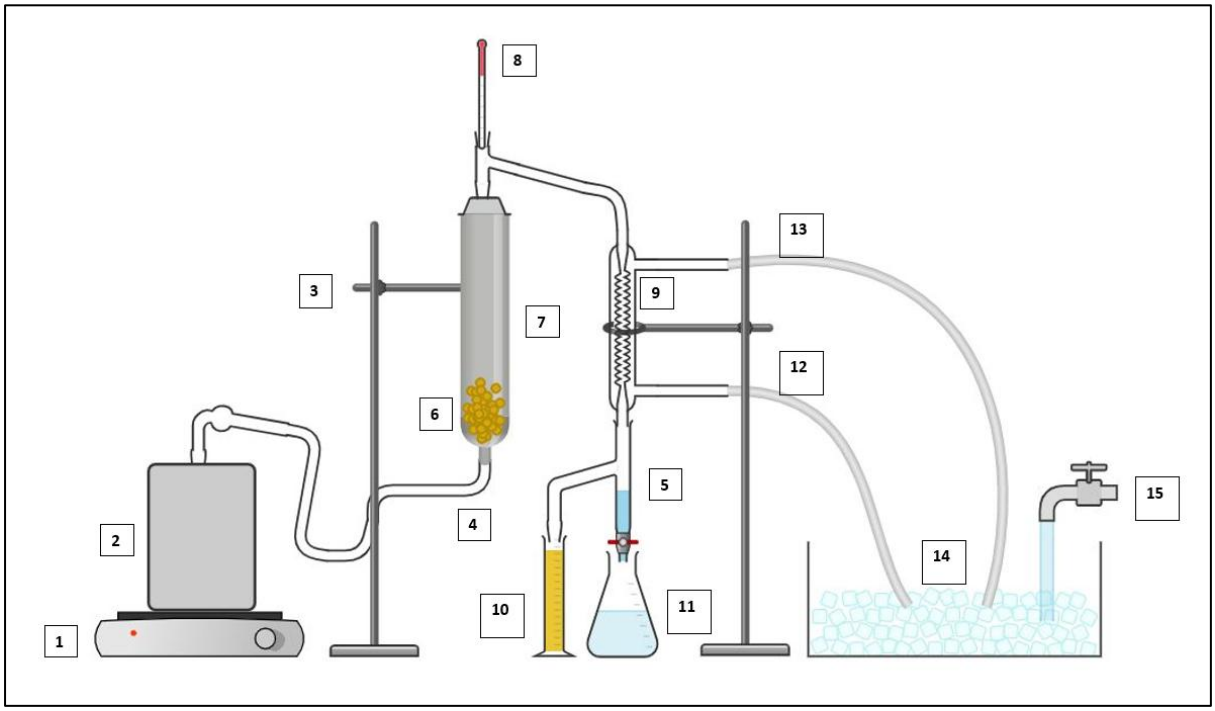

Figure 2: Steam Distillation Set up; 1 is the induction cooker, 2 is still pot,3 is the retort stand, 4 is the steam inlet, 5 is dean stark receiver, 6 is citrus peel,7 is a column, 8 is the thermometer, 9 is the condenser,10 is collected essential oil, 11 is condenser water, 12 is hot water out, 13 is cold water in, 14 is water and ice bath,15 is the cold-water source.

The still pot is a cylindrical vessel made of stainless steel which is the required material for construction that can be used for induction. The still pot has a capacity of 2L. During a steam distillation run, the distilled water within the pot must be replaced with a fresh feed of distilled water to continue the distillation process. The heating mantle used in this study is an induction cooker. the power ratings used were 800W, 1000W, 1200W and 1400W. Although the heating power goes up to 2000W it was noted from the calibration of the heating mantle that between 1400 W and 2000W, there was little change in the power. Power ratings below 800W were not used because below this rating, the heating mantle took too long to heat the distilled water and produce steam. This is undesirable because this

would result in increased electric power being used which is wasteful. The glass column where the citrus peel material is placed has a capacity of 2kg, which corresponds to a diameter of 9.5 cm and height of 38 cm. the mass loading of the column used for this study was at levels of dry citrus peel mass of 50g, 100g,150g and 200g. the maximum loading used was 200g because 200g of dry citrus peel corresponded to a weight basis of 1170g of citrus peel. Anything higher than this would cause overspilling of material out of the column which meant that not all the material would undergo steam distillation. The graham condenser used tap water at room temperature (25 C) to cool the water-essential oil vapour mixture. The essential oil was collected in 15 ml centrifuge tubes.

4.2 Steam distillation procedure

To extract the essential oil by steam distillation, citrus material was placed in a glass column with a diameter of 9.5 cm and 38 cm which corresponded to a volume of 0.269 m^3. Inside the column, the material is placed on top of the sieve located at the base. The lower part of the column is connected to the steam still pot by a pipe tube. The steam required for the steam distillation extraction is provided by distilled water which is heated in a still pot with a capacity of 2 L. The water is heated using an induction cooker.

The top of the column is connected to a graham condenser which is made out of glass also. The condensation was cooled and facilitated by a counter flow condenser that utilised water. The condenser has four openings: a vapour inlet, a cooling water inlet, an essential oil-water condensate outlet, and a hot water outlet. The condenser unit also consisted of a water tank that housed the cooling water. The cooling water used was tap water which was kept cool by adding ice to the water tank. Once the vapours are condensed, the essential oil-vapour mixture is collected using a dean stark receiver that is connected to the condenser. The dean stark receiver also facilitates oil-water separation.

The steam produced in the still pot penetrates the citrus peel material producing vapours consisting of essential oil and water vapour. These vapours are directed to the top of the column where they condense through a coil-condensing chamber. Once the vapours are condensed, density difference due to the buoyance permits complete separation of the essential oil water. After the condensation process, the oil is separated from water by decantation.

The volume of essential oil over time is measured using a collected using a measuring cylinder placed just below the steam distillation collecting reservoir. The steam distillation rate was calculated since the volume of the extracted oil measured over time (with the help of a stopwatch is known.

Each distillation run consists of taking samples of collected essential oil after every 10 minutes for 70 minutes. The time is started when the first drop is condensate is seen in the collecting vessel. For each run, the heating power and mass loading of citrus peel will be considered. The heating mantle power is varied in the range of 800 to 1400W. the mass loading of citrus peel is varied between 50g to 200g dry citrus peel mass.

The yield of limonene is calculated by:

$$Y\ (\%) = \frac{V}{W} * 100 \qquad [12]$$

where Y is the yield of essential oil (%, V/W), V is the volume of essential oil obtained (mL), and W is the dry mass of citrus peel (g).

The essential oils obtained by steam distillation are analysed by gas chromatography- flame ionisation detector (GC-FID). The details of the analysis procedure are detailed in section 4.5 and appendix B.

4.3 Single factor experiments

Single-factor experiments were utilised to determine the required factor values for the steam distillation central composite design. For these experiments, two factors were considered, the heating power and the mass loading of citrus peel in the column. The mass loading is expressed as the dry mass of clementine peels that were added. One factor was considered at a time by keeping one-factor constants while the other factor was varied. The procedure consisted of 8 runs that are listed in Table 4. For each run, the essential oil yield was collected and measured as a function of time for 70 minutes. The single-factor experiments were repeated in triplicate and presented as standard deviations.

Table 4: Single-factor experimental runs where one of the two factors(heating power/mass loading is kept constant) whilst the other factor is varied.

Run Number	Mass loading (g)	Heating Power(W)
1	50	1000
2	100	1000
3	150	1000
4	200	1000
5	150	800
6	150	1000
7	150	1200
8	150	1400

4.4 Experimental Design

Central composite design (CCD) statistical experimental design and the Response Surface methodology were used to study the effects of the two independent variables (heating power and material mass loading) on the response (yield, Y) to determine the optimal conditions which maximize the yield of essential oil from clementine peel. CCD was used to enable the estimation of regression parameters to fit a second-order polynomial regression model.

The variables, material mass and heating power were established based on the best conditions obtained from the single-factor survey. Experiments were established based on a Central composite design (CCD) with two factors at five levels and each independent variable was coded at five levels

between -α, −1, 0, 1 and + α. To maintain rotatability, the value of α depends on the number of experimental runs in the factorial portion of the central composite design:

$$\propto = [2^z]^{\frac{1}{4}} = 1.414 \qquad [\ 13\ ]$$

in this study, z represents the number of factors and in this study 2 factors are considered which means that α has a value of 1.414.

A total of 10 experimental runs were carried out in the central composite design which included duplicated centre point runs which allow for a more uniform estimate of the prediction variance over the entire design space. The factor levels for each run are listed in Table 5.

To carry out a complete central composite design, the following steps outlined in Figure 3 are required. The step that was not carried out in Figure 3 is the last step which was model validation/ confirmation of the experiment. This was not carried out due to a lack of time and material.

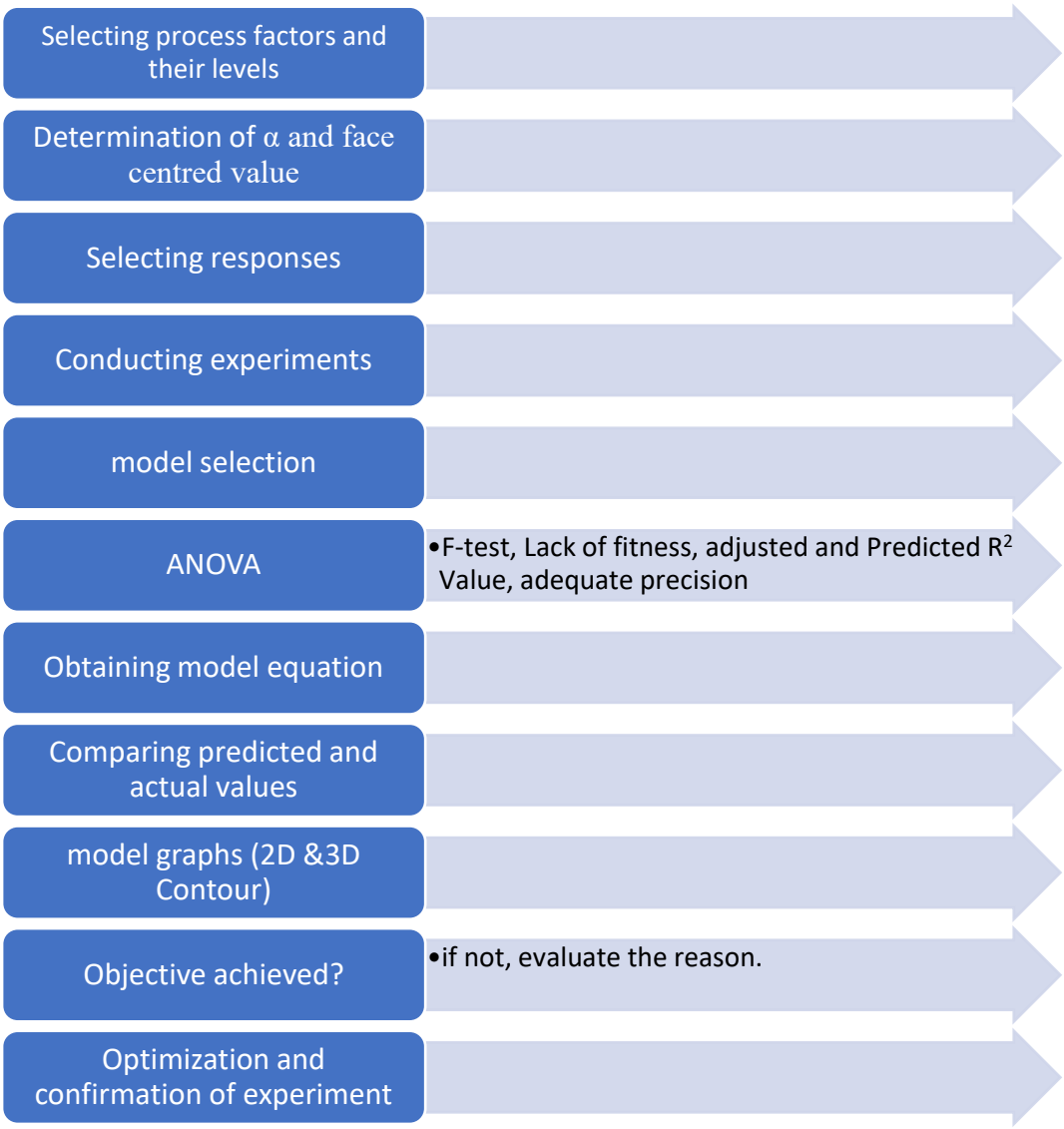

Figure 3: Steps required to be complete in the design of the experiment. Adapted from (Bhattacharya, 2021)

Table 5:Uncoded factor levels for a Central composite design of a two-variable system

Run #	Heating Power(W), X_1	Mass loading (g), X_2
1	800	72
2	800	178
3	1200	72
4	1200	178
5	717	125
6	1283	125
7	1000	50
8	1000	200
9	1000	125
10	1000	125

The model used in the optimization process was a quadratic or second-order model which follows the equation:

$$Y = \beta_0 + \beta_1 X_1 + \beta_2 X_2 + \beta_{12} X_1 X_2 + \beta_{11} X_1^2 + \beta_{22} X_2^2 \quad [14]$$

In this equation, Y = Dependent variables or Outcome variables or estimated responses, X_1 = the heating power(W), X_2 = the mass loading(g), β_0 = overall mean response or intercept constant, β_1 = regression model coefficients.

Put into words, a mathematical model of the observed values of the dependent variables y, that indicates:

1. Main effects for factor X_1……. X_k
2. Their interactions (X_1X_2, X_{k-1}, X_k)
3. Their quadratic components (X_1^2…X_k^2).

Response surface methodology (RSM, STATISTICA software) was utilized in this work as an optimization tool to conduct experimental design, execute statistical processing, and choose the best extraction conditions (Dao *et al.*, 2021).

4.5 GC-Analysis (D-Limonene quantification)

The quantity of D-Limonene present in the extracted essential oil from steam distillation was determined using Gas Chromatography- Flame Ionisation Detection (GC-FID) analysis. The information regarding the instrument Gas chromatography instrument is outlined in Table 6.

Table 6: Gas-Chromatography-Flame Ionisation Detection instrument information

Instrument:	**Thermo Trace GC Ultra Gas Chromatograph with FID detector**
Injector temp:	250°C PVT-Split
Injection Volume	1µl
Split ratio	67:1
Column	Zebron ZB-5ms (30m x 0.32mm x 0.25µm)
Carrier (He) flow	1.5 ml/min

Oven	Initial temp 45°C (2min), rate 15°C/min, final temp 250°C (2min)
FID detector	300°C
Calibration	The standard operating procedure is outlined in Appendix B. The internal standard is 2-Pentanol.

The quantification was done on the total collected essential oil from each design of experiment runs. The sample preparation procedure was followed. Approximately 1.5 ml of trichloromethane phase was added to the glass vial together with 30 µL of 2-pentanol. Trichloromethane(chloroform) was used as the gas chromatography solvent. The 2-pentanol was the internal standard used. The mass of 2-pentanol added must be recorded. For each sample, 80 µL of the extracted essential oil from each experimental design (CCD) run was used. The mass of the essential oil added was accurately recorded as this was the basis on which the GC-FID analysis was done. The composition of the D-limonene is measured in mg. once the composition of the D-Limonene was known, the concentration of D-limonene of the essential oils for each experimental design run was calculated. The equation used to calculate the concentration is given by equation [15]. The detailed step-by-step procedure of the method can be seen in Appendix B.

$$D - limonene\ concentration\left(\frac{mg}{ml}\right) = \frac{D - Limonene\ amount(mg)}{Volume\ of\ essential\ oil(ml)} \quad [15]$$

4.6 Statistical Analysis

4.6.1 Kinetic Model fitting

The model fitting was executed using Microsoft excel, the model parameters and constants are obtained by minimising the sum of the square difference between the theoretical and actual yield of Essential oil at the relevant time point.

$$Sum\ of\ Square\ Error(SSE) = \sum_{t=o}^{t=70} (y_{actual} - y_{model})^2 \quad [16]$$

The model fit is evaluated using the coefficient of determination, R^2. According to (Tripathi, 2021), the accuracy or precision of a model's performance may be evaluated directly by looking at its coefficient of determination. According to more precise terminology, the Coefficient of Determination

is a measurement of the variation in the response variable that can be predicted using the predictor variable. It is the most typical method of evaluating the model's robustness (Tripathi, 2021).

$$R^2 = \frac{SSR}{SST} \quad [17]$$

$$SSR = \sum_i (\hat{y}_i - \bar{y})^2 \quad [18]$$

$$SST = \sum_i (y_i - \bar{y})^2 \quad [19]$$

SSR is the sum of Squared regression which is known as the variation explained by the model.

SST is the total variation in the data also known as the sum of the squared total.

$\hat{y}_i$ is the predicted value of y for observation i

$\bar{y}$ is the mean of value y

y_i is the y value for observation, i.

If the fit is good, R^2 is close to 1.

4.6.2 Central composite design Statistical analysis

The STATISTICA software package software version 14.0 was used for experimental design analysis and subsequent regression analysis of the experimental data. Statistical analysis of the regression model was performed using analysis of variance(ANOVA) and evaluating the probability value, and p-value of each term in the model. The confidence interval was set to 95% and a significance(α) level of 5%. The quality of the regression polynomial model was evaluated by the coefficient of determination, R^2.

5 Results

5.1 Kinetic model study

5.1.1 Single factor data

The pseudo-first-order model, equation [10] was fit to the single factor experimental data where the heating power was varied from 800W to 1400 W whilst keeping the clementine peel loading constant at 100g dry mass. During the first 20 minutes of extraction, illustrated in Figure 4, at the heating power of 800W, 50.9% of available oil was extracted whilst at 1200W 92.4% of the available essential oil was extracted. In Figure 5**Error! Reference source not found.Error! Reference source not found.**, at the different mass loadings, 73% TO 100% of the available essential oil was extracted in the first 20 minutes of steam distillation. Typically, within the first 10 to 20 minutes of the extraction, more than 50% of the oil was already extracted.

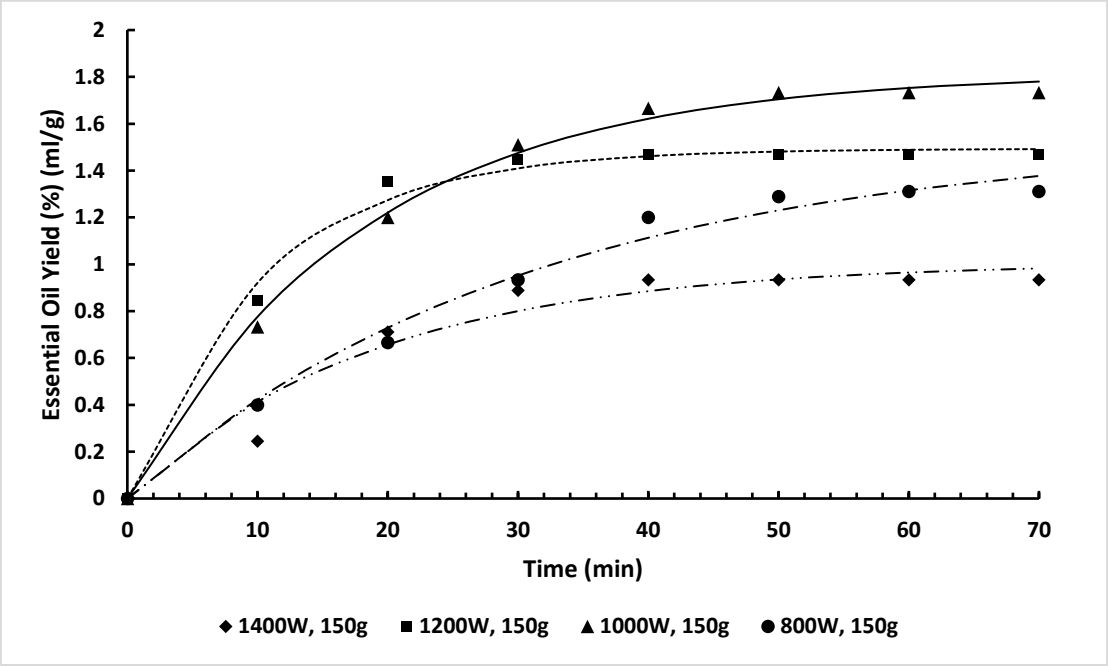

Figure 4: Kinetic model of steam distillation at different heating power and constant dry mass loading of 150 g clementine peel with the pseudo-first model.

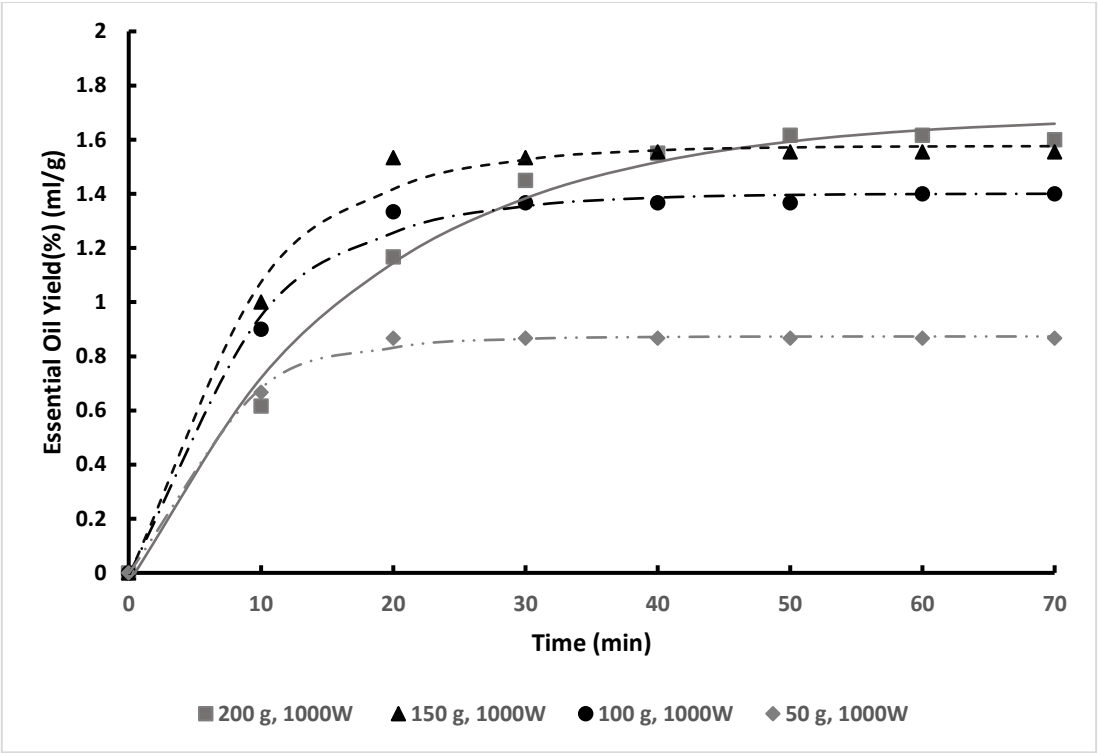

Figure 5:Kinetic model of steam distillation at different mass loading with the pseudo-non-linear model.

5.1.1.1 Heating power model fit

It was illustrated in Figure 4**Error! Reference source not found.** that the model fits very well with the e xperimental data and it is further proven by the coefficient of determination(R^2) listed in Table 7. The model fit was extremely well, especially for the heating powers from 800 W to 1200 W where the R^2 was above 0.95. The model did not fit as well at the highest heating power (1400 W) where the R^2 was 0.867, but the value was still adequately high to give a reasonable fit. The sum of square error (SSE) at each heating power was also very low and close to 0, which indicated that the residual difference between experimental data and the data predicted from the model were very similar which meant that the model predicted the experimental data well. It can also be concluded that the pseudo-nonlinear model fit well to the single factor experiments where the mass loading of clementine was increased whilst the heating power was kept constant at 1000W which was selected as the optimal heating power. 1000 W was selected as the optimum power because it had the largest end point yield of essential oil of 1.73 ± 0.11% after 70 minutes from the single-factor experiments where heating power was varied as illustrated in Figure 4.

Table 7: Variation in the kinetic constant, equilibrium yield, coefficient of determination and sum of square error as the heating power was increased.

Heating Power	Process constant (k_1)	Equilibrium yield (q_∞)	Coefficient of Determination (R^2)	Sum of Square error(SSE)
800	0.032	1.54	0.959	0.020
1000	0.056	1.82	0.979	0.009
1200	0.096	1.49	0.973	0.015

1400	0.053	1.01	0.867	0.045

5.1.1.2 Mass loading model fit

In Table 8, the coefficient of determination for all the mass loadings runs was very close to 1 and all above 0.95. There was minimal error in the model fit at all the mass loadings because the sum of square error was very small and all close to 0 which meant there was a minimal deviation in the predicted and experimental data. The combination of both a very high coefficient of determination and a very small sum of square error indicated that the pseudo-non-linear model was suitable to model the steam distillation of essential oil from clementine's. A dry mass loading of 150 g was selected as the optimum mass loading because in this condition the end point yield was the highest at 1.56 ± 0.03% in Figure 5.

Table 8:Variation in the kinetic constant, equilibrium yield, coefficient of determination and sum of square error as the mass loading was increased.

Mass loading (g)	Process constant k_1	Equilibrium yield q_∞	Coefficient of Determination R^2	Sum of Square error (SSE)
50	0.15	0.87	0.994	0.00163
100	0.11	1.40	0.983	0.00991
150	0.11	1.58	0.976	0.0203
200	0.056	1.69	0.952	0.0238

5.1.1.3 Heating power effect on equilibrium yield and process constant

In **Error! Reference source not found.** Figure 6**Error! Reference source not found.**, there was a notable trend in how the equilibrium yield varied as the heating power was increased. As the heating power was increased, the equilibrium yield, q_∞ increased from 1.54% up to a maximum value of 1.82%

at 1000W before decreasing as the heating power further increased above 100W to a low equilibrium yield of 1.01 % at 1400 W.

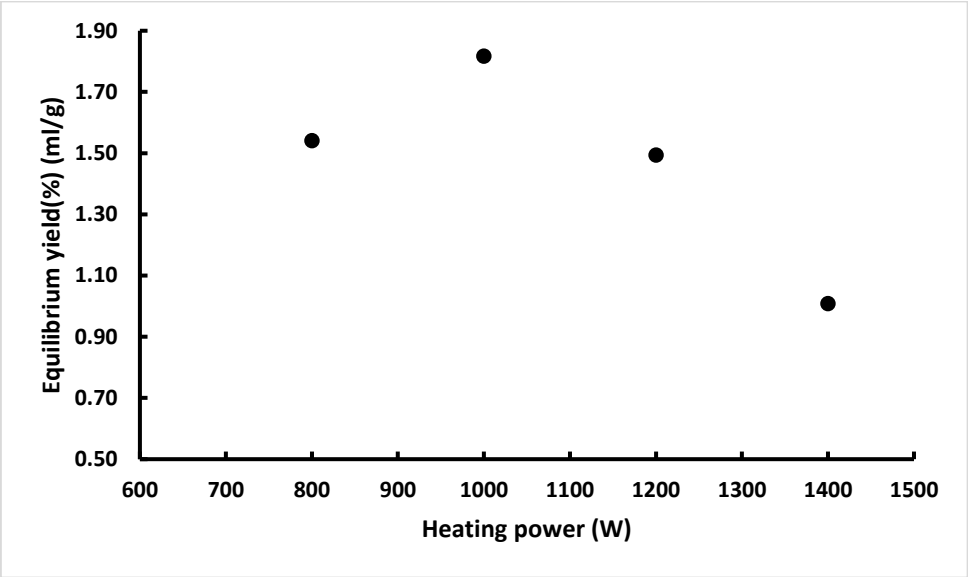

Figure 6: The variation in the equilibrium yield as the heating power was increased whilst the mass loading was kept constant at a dry mass loading of 150 g clementine peel.

A trend was also observed for the process constant,k_1 in Figure 7**Error! Reference source not found.**. The process constant increased when the heating power was increased up to a maximum heating power of 1200 W where the value of k_1 was 0.096. Beyond this heating power, the process constant decreased to 0.053 at the maximum heating power of 1400 W.

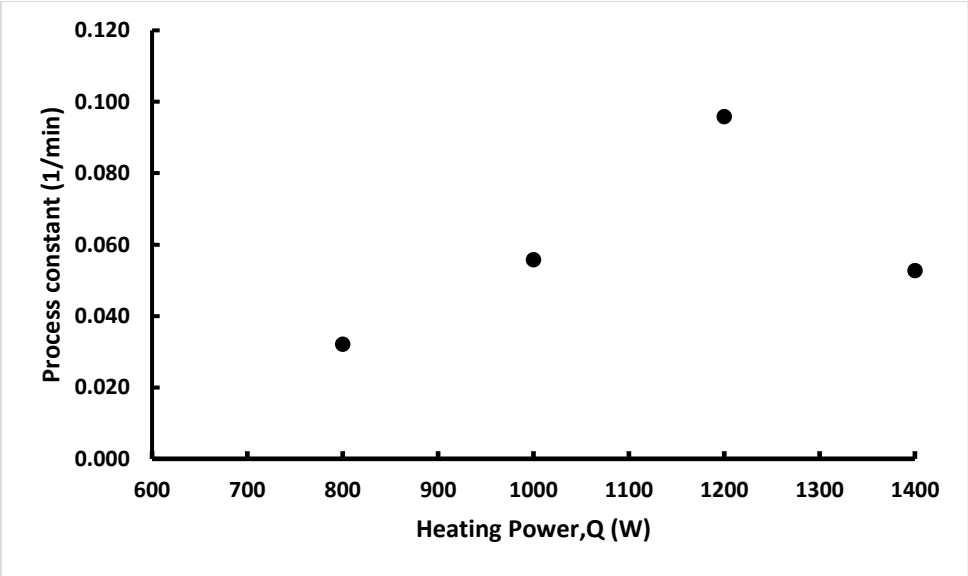

Figure 7: The variation in the process constant as the heating power was increased whilst the constant at a dry mass loading of 150 g clementine peel.

5.1.1.4 Mass loading effect on equilibrium yield and process constant

Although the equilibrium yield increased at elevated mass loading, it can also be deduced from Figure 8 that at very high mass loadings, the equilibrium yield is reaching a point whereby increasing the mass loading further will only slightly increase the equilibrium yield compared to changing the mass loading from 50 to 100 g dry clementine peel which caused a greater increase in the equilibrium yield. Although the highest equilibrium yield was observed at the highest mass loading of 200 g, this mass loading also took the longest to reach its equilibrium yield which means that there is a trade-off between obtaining a high yield and still trying to obtain the equilibrium yield as quickly as possible.

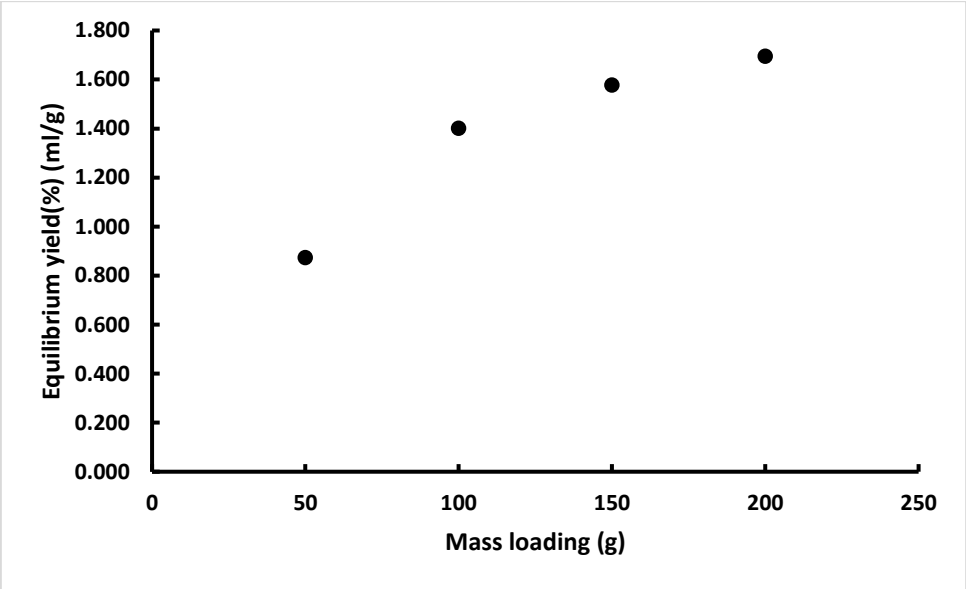

Figure 8: The variation in the equilibrium yield as the mass loading was increased whilst the heating power was kept constant at 1000W.

From Table 8 and Figure 9, it can be seen that process constant, k_1 decreased at elevated mass loading. The decrease in the kinetic constant indicated that the extraction process took longer to reach the equilibrium yield at that particular mass loading. The equilibrium yields as shown increased as the

mass loading was increased with the highest observed equilibrium yield of 1.69 % for a mass loading of 200 g dry clementine peel.

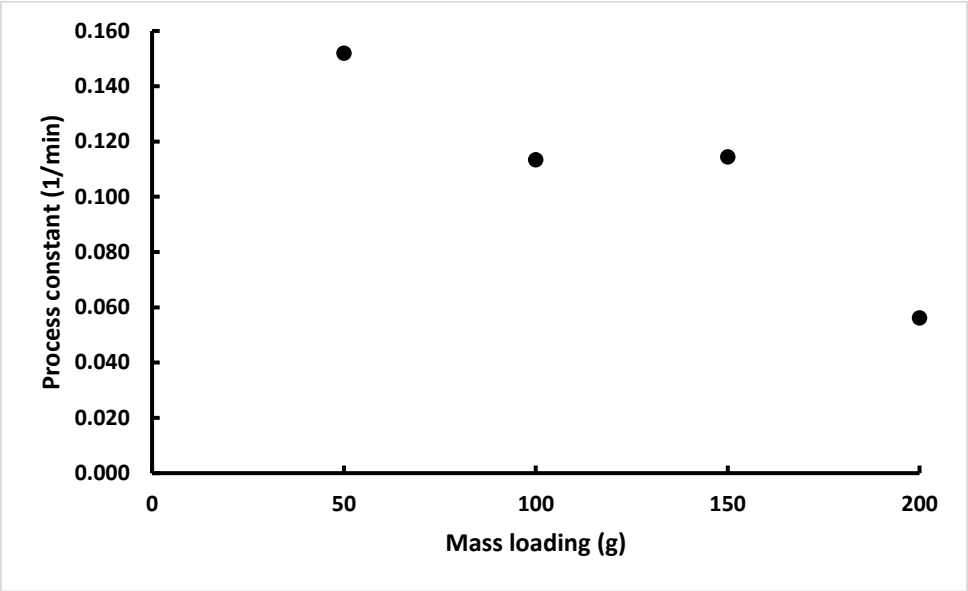

Figure 9: The variation in the process constant as the mass loading was increased whilst the heating power was kept constant at 1000W.

5.1.2 Central composite design data

The pseudo-first model, equation [10 was used to plot the central composite design data of essential oil yield collected as a function of time. The effect that the mass loading and heating power have on the model was investigated using a central composite experimental design. Models of the kinetic parameters, the process constant, k_1 and q_∞, the equilibrium yield of essential oil, as a function of the mass loading and heating power, was also obtained. The significance of these factors (the heating power and mass loading) on the model parameters was also investigated through statistical analysis.

The first-order model generally fit well for each run with a high coefficient of determination values that were close to 1 except for run three and run four which had R^2 of 0.722 and 0.765 respectively. From the model, the highest equilibrium yield was observed for run 2 (800 W heating and 178 g mass loading) where the yield was 3.04 %. This lowest equilibrium yield, 0.87 % was observed for run 7 (1000 W and 50 g mass loading).

Table 9: Experimental and predicted Kinetic process constant and equilibrium yield constant for the central composite design data

Run #	X1	X2	Experimental Process constant	Predicted Process constant	Experimental Equilibrium Yield	Predicted Equilibrium yield	Coefficient of Determination, R^2 for the first-order model
1	**800**	**72**	0.02	0.09	2.03	1.66	0.807
2	**800**	**178**	0.02	0.05	3.04	2.54	0.873

3	**1200**	**72**	0.05	0.09	1.82	1.58	0.722
4	**1200**	**178**	0.03	0.04	2.51	2.13	0.765
5	**717**	**125**	0.12	0.07	1.99	2.46	1.004
6	**1283**	**125**	0.07	0.06	1.83	2.11	0.916
7	**1000**	**50**	0.15	0.10	0.87	1.16	0.994
8	**1000**	**200**	0.06	0.04	1.70	2.17	0.954
9	**1000**	**125**	0.09	0.07	1.81	1.71	0.937
10	**1000**	**125**	0.05	0.07	1.62	1.71	0.912

5.1.2.1 Equilibrium yield as a function of heating power and mass loading

The equilibrium yield was then modelled as a function of the heating power and the mass loading to understand what effect these two factors had on this constant. The test for the significance of the model factors is performed using an analysis of variance(ANOVA) by determining the probability value(p-value). The obtained p-value was compared to the significance value which was set to 0.05. if the p-value was less than 0.05 that factor is significant.

A summary of the ANOVA is shown in Table 10 and it was seen that none of the factors was considered significant because all of the p-values were larger than 0.05. the factors that were considered close to significant were the linear mass loading with a p-value of 0.0929 and the quadratic power term with a p-value of 0.153. the factor that was considered least significant was the quadratic mass loading term which had a huge p-value of 0.702. the level of significance of the factors and the ranking of the factors from most to least significant is illustrated in the Pareto chart, Figure 10.

Table 10: Summary of the ANOVA of equilibrium yield as a function of heating power and mass loading

	SS	Df	MS	F	p
Heating Power (L)	0.119847	1	0.119847	6.35707	0.240379
Heating Power (Q)	0.314650	1	0.314650	16.69000	0.152825
Mass loading (L)	0.873351	1	0.873351	46.32513	0.092870
Mass loading (Q)	0.004810	1	0.004810	0.25516	0.702224
1L by 2L	0.029421	1	0.029421	1.56058	0.429745
Lack of Fit	1.097088	3	0.365696	19.39760	0.165024
Pure Error	0.018853	1	0.018853		
Total SS	2.489049	9			

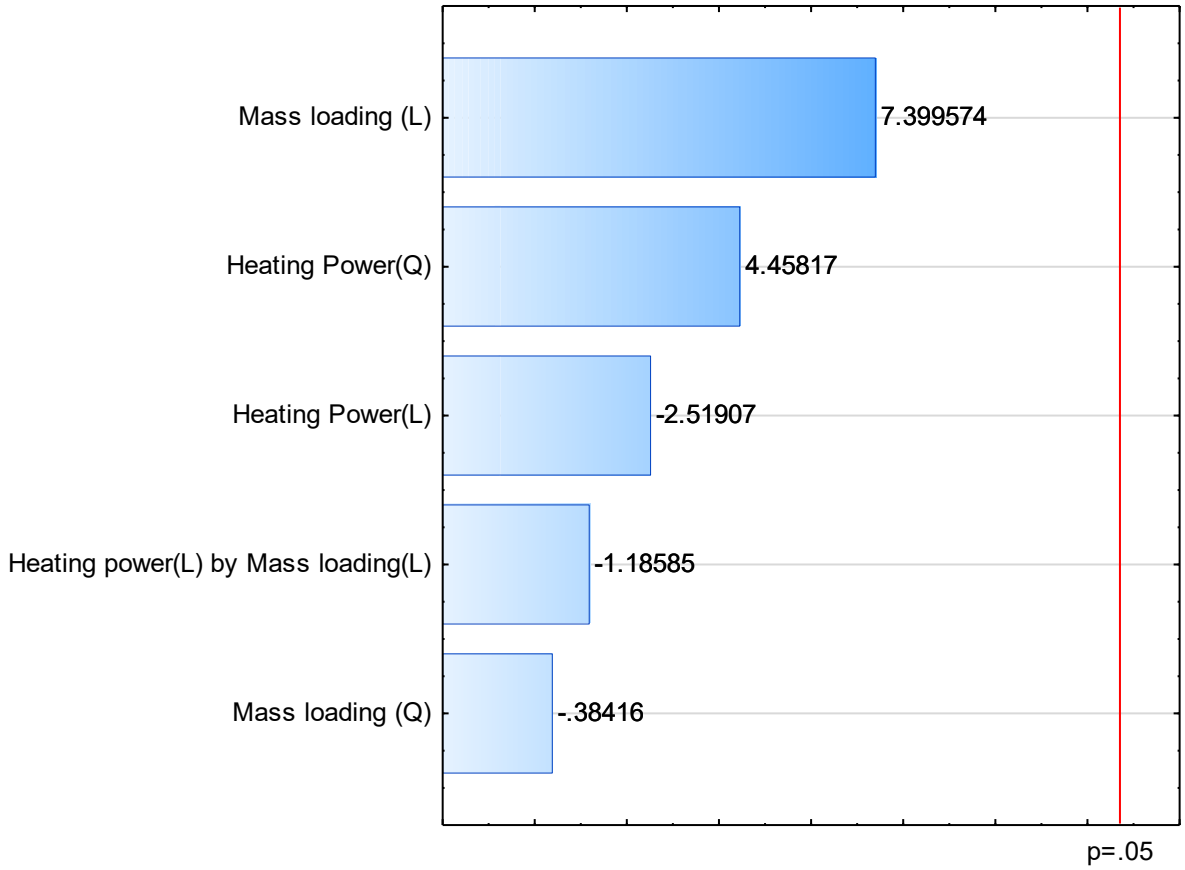

Figure 10: Pareto chart of the Standardized Effect Estimate (Absolute Value) of the equilibrium yield as a function of heating power and mass loading

The goodness of the fit of the models was also checked by the R^2 value. The coefficient of determination (R^2) of the model was 0.578 which suggests that the model does not fit the parameter well since R^2 is not close to 1. The low R^2 also suggested that there was high variation around the mean explained by the proposed regression model. The model obtained for q_∞ as a function of the mass loading and the heating, power is illustrated by equation [20]. The values obtained for the equilibrium yield are listed in Table 9.

$$q_\infty(\%) = 7.5384 - 1.40 * 10^{-2} X_1 + 7.16 * 10^{-6} X_1^2 + 1.67 * 10^{-2} X_2 - 8.78 * 10^{-5} X_2^2 - 7.68 * 10^{-6} X_1 X_2 \quad [20]$$

The regression model was then visually illustrated as a 3-D surface plot to show how the mass and power influenced the equilibrium yield in Figure 11. As the mass loading is increased, the equilibrium yields increased. This is different however with the heating power because as the heating power is increased, the equilibrium yields, q_∞ decreases to a minimum and then beyond the minimum point, q_∞ increases as the heating power is increased. The highest equilibrium yield (q_∞) observed was 2.54

% at a heating power of 717 W and mass loading of 178 g. whilst the lowest yield was 1.16 % for a mass loading of 50 g and 1000W heating power.

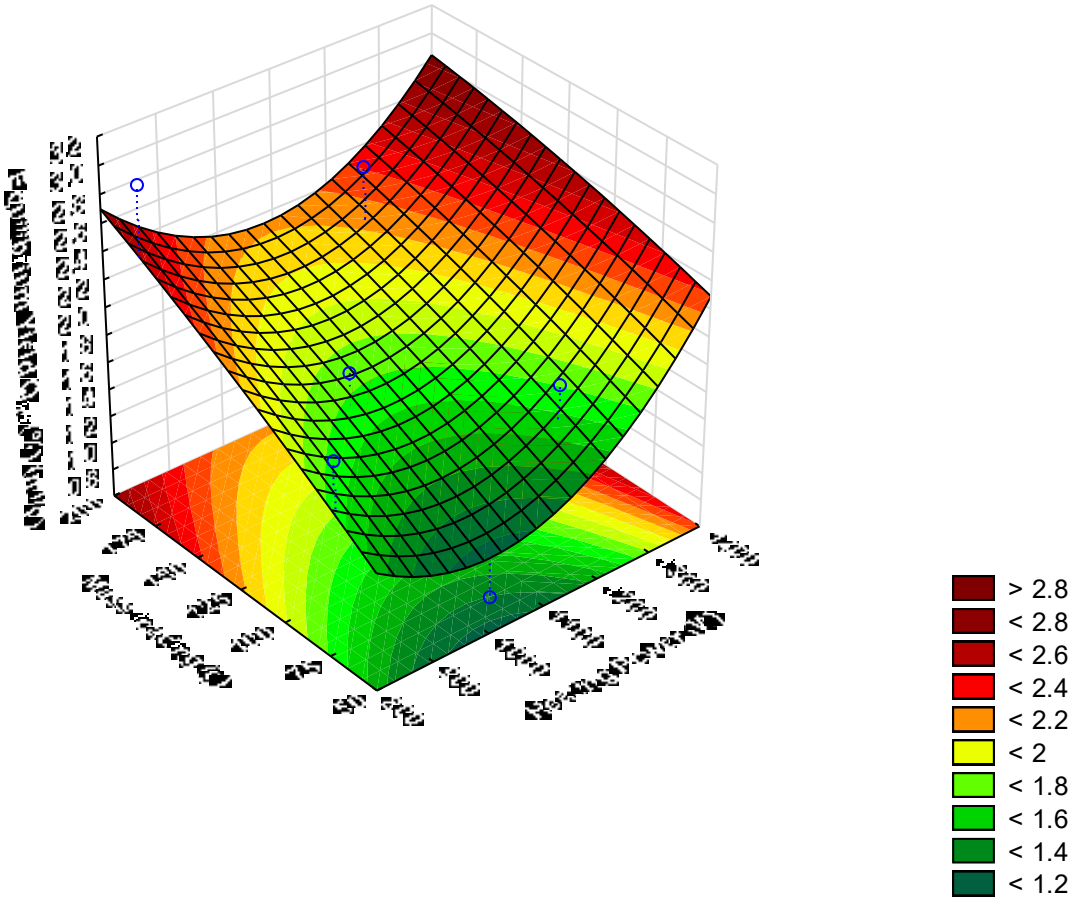

Figure 11: 3D Fitted surface plot showing the effect of mass and power on equilibrium yield

5.1.2.2 Process constant as a function of heating power and mass loading

The same statistical analysis using ANOVA was carried out for the process constant, k_1 and is summarized in Table 11. The p-values of all the factors were greater than 0.05 and considered statistically insignificant. The factor that was closest to being significant is the linear mass loading which had a p-value of 0.203. all the others had extremely high p-value greater than 0.65. The factors were ranked in terms of significance in the Pareto chart, Table 11. Due to the terms being highly

insignificant, adjusting the confidence interval to 90 % and the significance level to 0.1 had little effect to no effect in changing the significance of the factors.

Table 11: ANOVA of process constant as a function of heating power and mass loading

	SS	Df	MS	F	p
Heating Power(L)	0.000125	1	0.000125	0.212778	0.724857
Heating Power (Q)	0.000169	1	0.000169	0.286494	0.687133
Mass loading (L)	0.005407	1	0.005407	9.175143	0.202999
Mass loading (Q)	0.000098	1	0.000098	0.166356	0.753456
1L by 2L	0.000091	1	0.000091	0.154043	0.761898
Lack of Fit	0.015989	3	0.005330	9.044077	0.238624
Pure Error	0.000589	1	0.000589		
Total SS	0.022663	9			

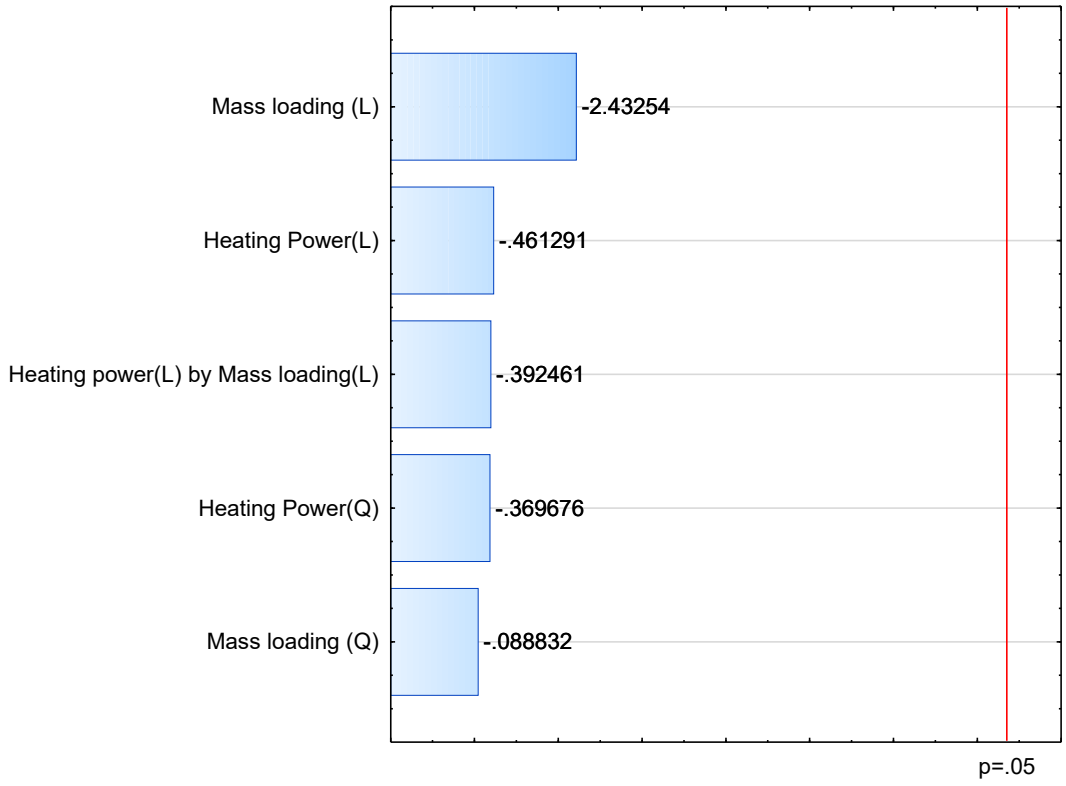

Figure 12: Pareto chart of the Standardized Effect Estimate (Absolute Value) of the process constant as a function of heating power and mass loading

The variation of the model to the mean and fit of the regression model which plotted the process constant as a function of the mass loading and heating power was evaluated using R^2. The coefficient of determination (R^2) of the model was 0.2685 which suggests that the model does not fit the parameter well since R^2 is not close to 1. It also means there was very high variability between the predicted process constant and the actual process constant. The regression model which is a quadratic model is illustrated by an equation [21 and the predicted constants are listed in Table 9. Once the model was obtained, a 3-D surface plot Figure 13, was used to illustrate certain trends of the kinetic constant as it was influenced by the factors.

$$k_1 = -2.67 * 10^{-2} + 2.46 * 10^{-4} X_1 - 1.05 * 10^{-7} X_1^2 + 1.45 * 10^{-4} X_2 - 3.59 * 10^{-7} X_2^2 - 4.4942 * 10^{-7} X_1 X_2 \quad [21]$$

The predicted kinetic constant ranged between the lowest which was 0.04 min^{-1} which was observed for a heating power of 1200 W and mass loading of 178 g whereas the highest kinetic constant, 0.10 min^{-1} was observed at a mass loading of 50 g and heating power of 1000 W. The general trends as depicted in Figure 13 were that as the mass loading increased, process parameter k_1 decreased. This is different however with the heating power because as the heating power is increased, k_1 increases to a maximum and then beyond the maximum point, k_1 decreases as the heating power is increased.

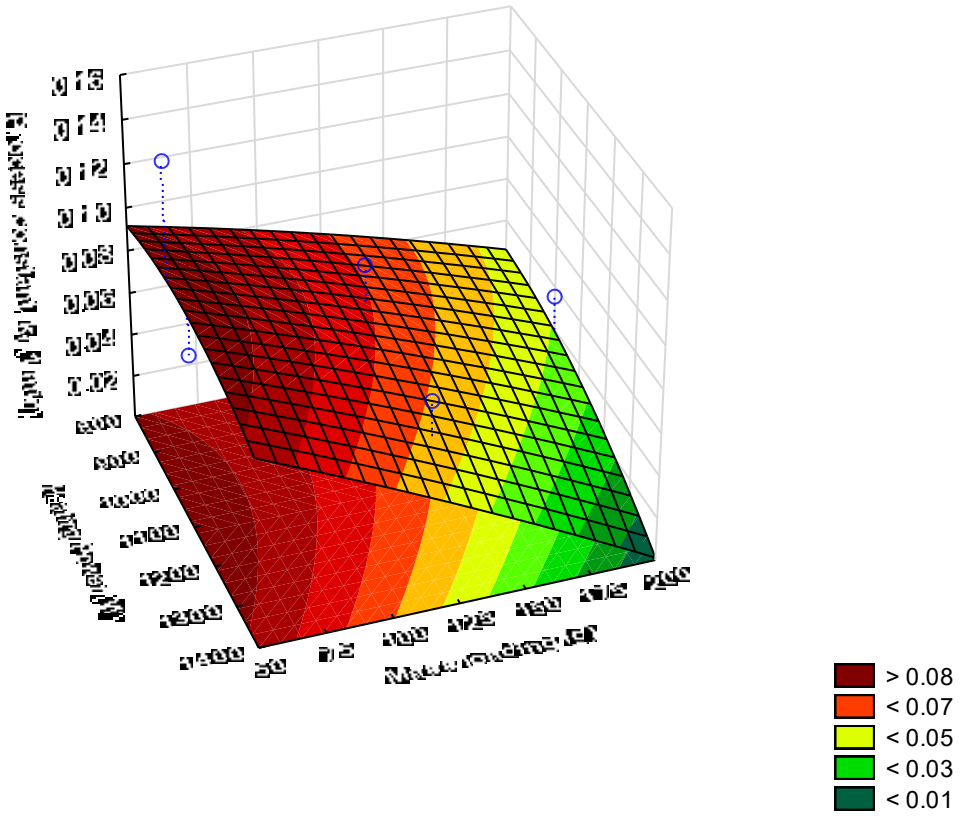

Figure 13: 3D Fitted surface plot showing the effect of mass and power on process constant

5.1.3 Globalized model

Combining the model for the predicted equilibrium yield constant and process constant as a function of the two factors, heating power and mass loading, a globalized model for the pseudo-first-order model was obtained. The model is given by equation [22] below:

$$q(\%) = (7.5384 - 1.40 * 10^{-2} X_1 + 7.16 * 10^{-6} X_1^2 + 1.67 * 10^{-2} X_2 - 8.78 * 10^{-5} X_2^2 - 7.68 * 10^{-6} X_1 X_2) e^{-(-2.67*10^{-2} + 2.46*10^{-4} X_1 - 1.05*10^{-7} X_1^2 + 1.45*10^{-4} X_2 - 3.59*10^{-7} X_2^2 - 4.4942*10^{-7} X_1 X_2) t} \quad [22]$$

5.2 Single factor experiments

The single-factor experiments were used to observe what effect the mass loading or heating power would have on the essential oil yield as well as the kinetics of the essential oil yield over time. The results from the single-factor experiments were used to decide on the range of required levels for the two factors (heating power and mass loading) to use in the central composite experimental design.

5.2.1 Mass loading effect

Figure 14 depicts how the essential oil yield after 70 minutes varied as the loading of citrus peel mass in the column was increased. It can be seen that as the mass loading is increased, the essential oil yield also increased. However, due to the high variability indicated by the high error bars at each mass loading, this trend cannot be considered truly conclusive.

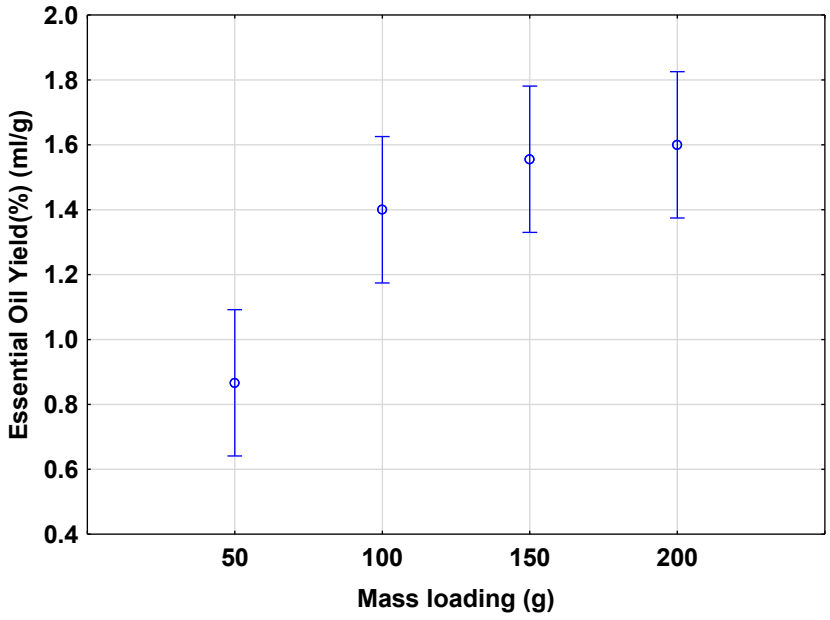

Figure 14: Essential Oil yield as a function of mass loading whilst the heating power was kept constant at 1000W

To determine whether mass loading was a significant effect on the essential oil yield, one-way ANOVA was used and carried out in STATISTICA Version 14. The results of the ANOVA are in Table 12. The mass loading was deemed significant because the value of p (0.00257) was less than the set alpha level (0.05) with a 95% confidence interval.

Table 12: Summary of the ANOVA for the effect of mass loading and the heating power kept constant at 1000W.

	SS	Degrees of Freedom	MS	f	p	
Intercept	22.05037	1		22.05037	768.2065	0.000000
Mass (g)	1.02222	3		0.34074	11.8710	0.002573
Error	0.22963	8		0.02870		

Once the significance of mass loading was established, the ideal conditions to get desirable essential oil yield was established. The desired essential oil is determined by selecting a mass loading that results in the highest essential oil yield possible as depicted in Figure 15. In Figure 15, the ideal mass loading that gives desirable essential oil yield(1.6 %) is a mass loading of 200g with a desirability of 68.1%.

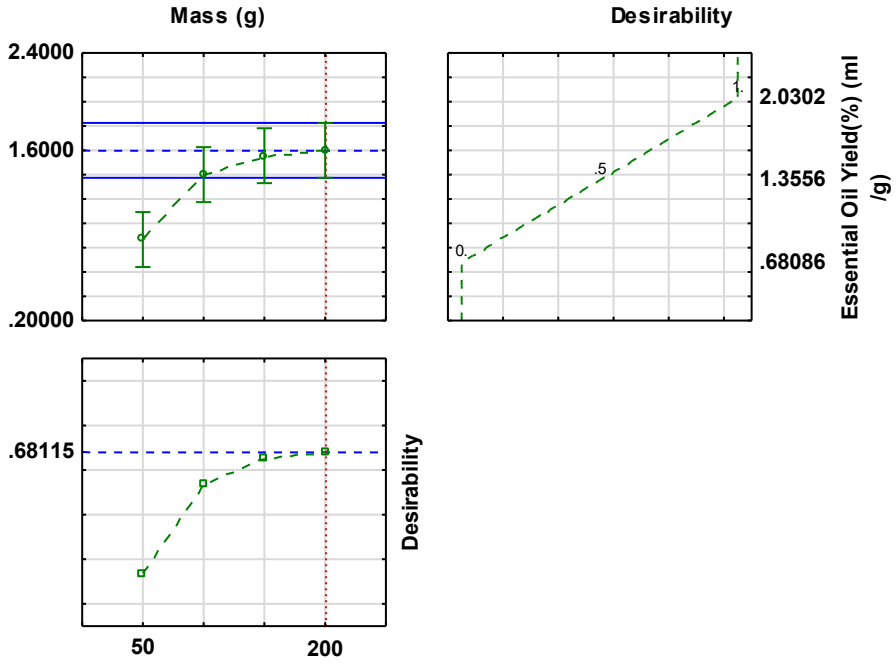

Figure 15: Profiles for Predicted Values and Desirability of essential oil yield as a function of mass loading whilst the heating power was kept constant at 1000W.

5.2.2 Heating power effect

A similar procedure to what was done in section 5.2.1 investigated the effect of heating power on essential oil yield and the statistical significance of the factor was done. Figure 16 depicts how the end point essential oil yield varied as the heating power was increased. As the heating power increased, the essential oil yield also increased up to a maximum yield of 1.73% at 1000W and then starts to

decrease. The lowest yield is 0.93 % which occurred at the highest heating power that was considered, 1400W.

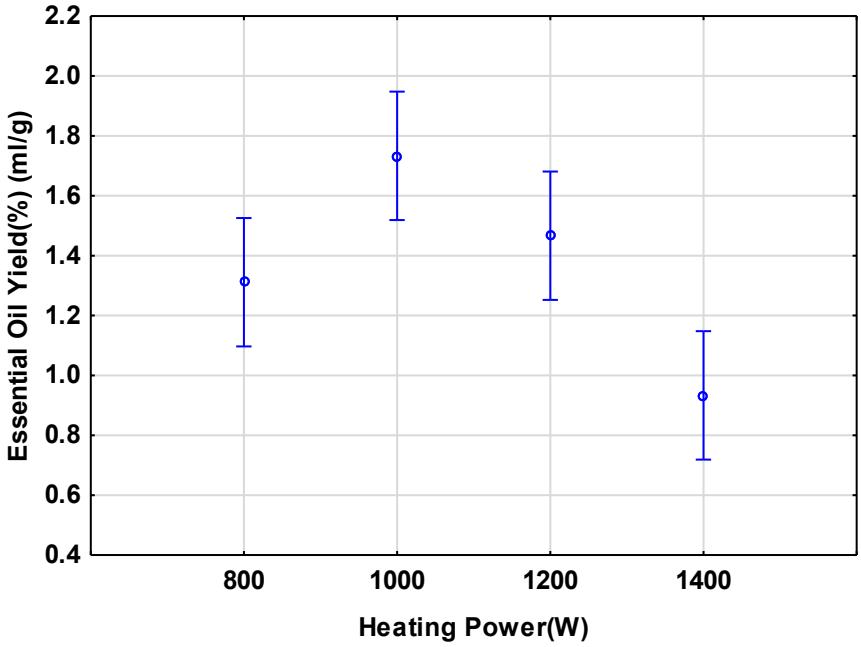

Figure 16: Essential Oil yield as a function of heating power whilst the dry mass loading was kept constant at 150 g clementine peel

A summary of the ANOVA used for the statistical analysis of the effect of heating power is given in Table 15. The heating power was deemed significant because the value of p (0.00195) was less than the set alpha level (0.05).

Table 13: Summary of the ANOVA for the effect of heating power and the mass loading kept constant at 150g.

Effect	SS	Degrees of Freedom	MS	f	p
Intercept	22.23148	1	22.23148	857.5000	0.000000
Power(W)	1.00556	3	0.33519	12.9286	0.001954
Error	0.20741	8	0.02593		

The optimal heating power to obtain a high yield was determined using the desirability function in STATISTICAL Version 14. The results of this function are illustrated in Figure 17. In Figure 17, the ideal heating power that gives desirable essential oil yield(1.73 %) is a heating power of 1000W with a desirability of 78.0%.

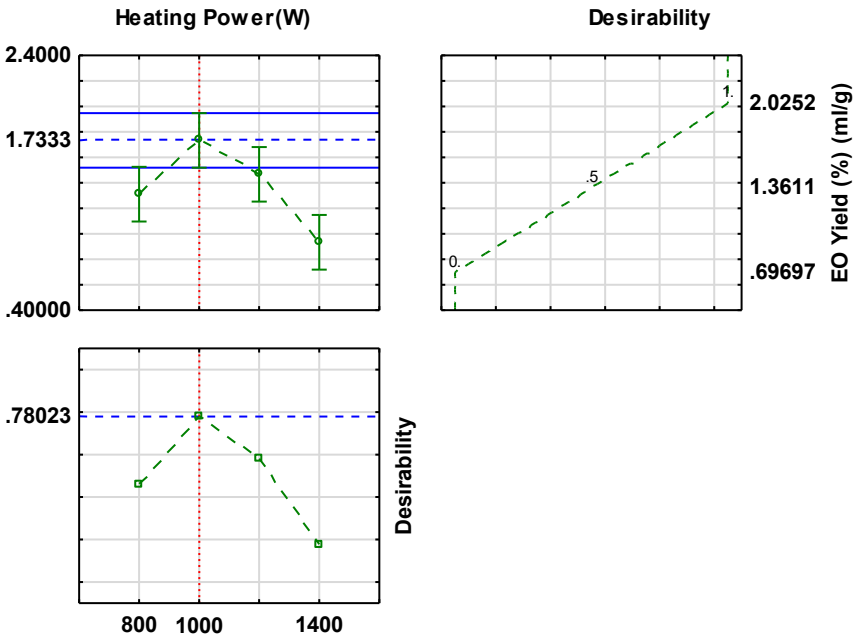

Figure 17: Profiles for Predicted Values and Desirability of essential oil yield as a function of heating power whilst the dry mass loading was kept constant at 150 g clementine peel

5.3 Optimising Essential oil yield using Central Composite Design

5.3.1 Statistical Significance

The statistical significance of the central composite design-Response surface methodology on the effect of heating power and mass loading on the essential oil yield was evaluated using the analysis of variance (ANOVA). The confidence interval of the data was set to 95% and the significance value was set to 0.05. A factor was considered significant if the p-value was less than 0.05. Table 14 presents the results of the analysis of variance. According to the p-values presented in Table 14, none of the factors was statistically significant. The linear mass loading term was the closest to being considered significant with a p-value of 0.157 whereas the linear heating power term was the least significant with a p-value of 0.632. A Pareto chart, Figure 18, was also used to rank the factors from most significant to the least significant. The factor which showed the greatest effect on the yield was the linear term of the mass followed by the quadratic term of heating power. The linear heating power term had the least effect on the yield of essential oil. The data was highly statistically insignificant and even when the confidence interval and significance were set to 90% and 0.1 respectively, the factors were still insignificant. The quality of fit of the polynomial equation was then evaluated and expressed by the coefficient of determination(R^2). The R^2 was also used to measure the amount of variation around the mean explained by the model.

Table 14: Summary of the ANOVA of percentage yield as a function of heating power and mass loading

Factor	SS	Df	MS	F	p
Heating Power (L)	0.012237	1	0.012237	0.42489	0.632247
Heating Power (Q)	0.151846	1	0.151846	5.27243	0.261483
Mass loading (L)	0.456566	1	0.456566	15.85300	0.156651
Mass loading (Q)	0.085692	1	0.085692	2.97543	0.334468
1L by 2L	0.015781	1	0.015781	0.54797	0.594327
Lack of Fit	0.146276	3	0.048759	1.69301	0.501879
Pure Error	0.028800	1	0.028800		
Total SS	1.070419	9			

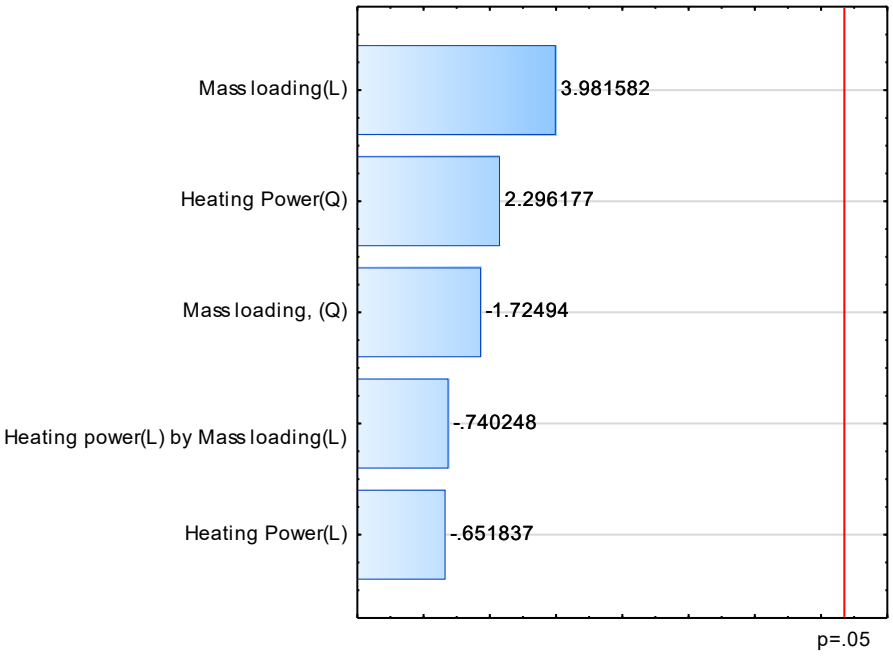

Figure 18: Pareto chart of the standardized effects of the factors on the essential oil yield

5.3.2 Variability of the regression model

The coefficient of determination (R^2) of the model was 0.836 which suggests that the model fits the experimental data well since R^2 is almost close to 1. The regression model expressed as a quadratic model, equation [23 was used to mathematically define the essential oil yield as a function of the mass loading and the heating power. The proposed model follows the same trend as the experimental data.

$$q_p(\%) = 4.326 - 8.5675 * 10^{-3}X_1 + 4.556 * 10^{-6}{X_1}^2 + 2.262 * 10^{-2}X_2 - 4.874 * 10^{-5}{X_2}^2 - 5.926 * 10^{-6}X_1X_2 \quad [23]$$

In Table 15, the experimental essential oil yield is compared to the yield predicted by the regression model by the percentage difference between the two. The experimental yield data showed that the lowest essential oil yield was 0.87% observed for run 7 and the highest yield was 2.08% seen for run 2, whilst for the predicted yield, the highest oil yield was 2.06 which was also for run 5 and the lowest yield was 1.03% observed at run 7. The percentage differences ranged from 18.65% to 2.52% but generally, the percentage differences were below 10% which indicated that the model was able to predict essential yield. The regression model was then visually represented by a 3-D surface plot to observe the interaction between the factors and their effect on yield.

Table 15: Predicted and experimental Percentage yield of essential oil for the central composite design

Run #	Heating power (W)	Mass loading (g)	Experimental Essential oil Yield (%) (ml/g)	Predicted Essential oil Yield (%) (ml/g)	% Difference
1	**800**	**72**	1.53	1.42	6.87
2	**800**	**178**	2.08	2.03	2.52
3	**1200**	**72**	1.67	1.47	11.79
4	**1200**	**178**	1.97	1.82	7.32
5	**717**	**125**	2.00	2.06	2.99
6	**1283**	**125**	1.76	1.95	10.75
7	**1000**	**50**	0.87	1.03	18.65
8	**1000**	**200**	1.62	1.70	5.40
9	**1000**	**125**	1.76	1.64	6.82
10	**1000**	**125**	1.52	1.64	7.90

5.3.2.1 effect of mass loading and heating power on essential oil yield

The surface plot, Figure 19 showed how the yield of essential oil is influenced by the dry mass loading of citrus peel. In Figure 19, red areas indicated higher essential oil yields whilst dark green areas indicated lower yields. What is reflected in Figure 19 is that as the mass loading of citrus peel was increased, the yield of essential oil also increased. It was not conclusive because the essential oil yield decreased as the heating power was increased up to 1000 W, and a minimum yield was reached. Beyond the minimum essential oil point, the essential oil yield increased as the heating power increased. However, the effect of the heating power on the essential oil was not conclusive. This has to do with how the effect of power was considered statistically insignificant due to the high variability of the data. In Figure 19, the predicted oil yield is the highest when the heating power is low (717 W) and the mass loading is high 200 g.

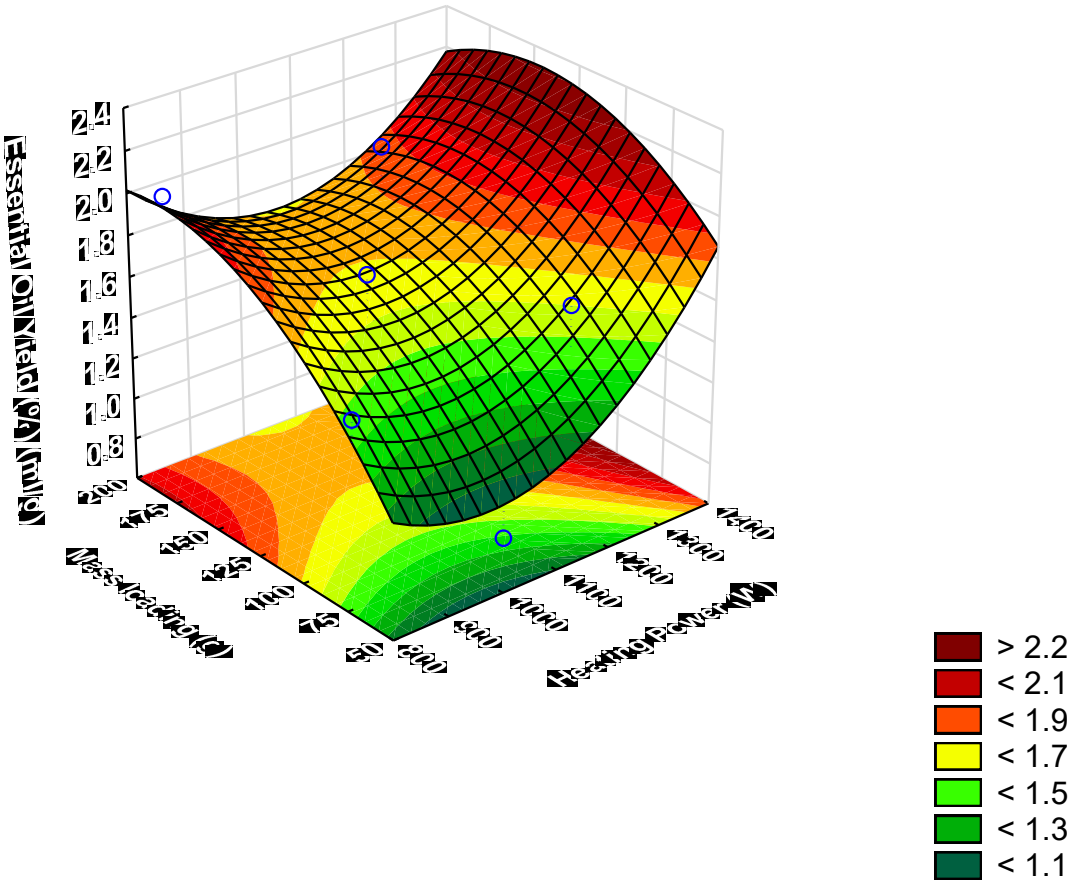

Figure 19: 3D Fitted surface plot showing the effect of mass loading and heating power on the yield of essential oil

5.3.3 Optimisation

One of the goals of the design of the experiment is to determine the optimal conditions that will result in a high yield of essential oil. The desired conditions for optimal yield are illustrated in Figure 20. The highest yield of essential was obtained when the heating power was set to 717 W and the mass loading was 199.95 g which yielded a percentage essential oil yield of 2.26 ml/g with desirability of 1.00.

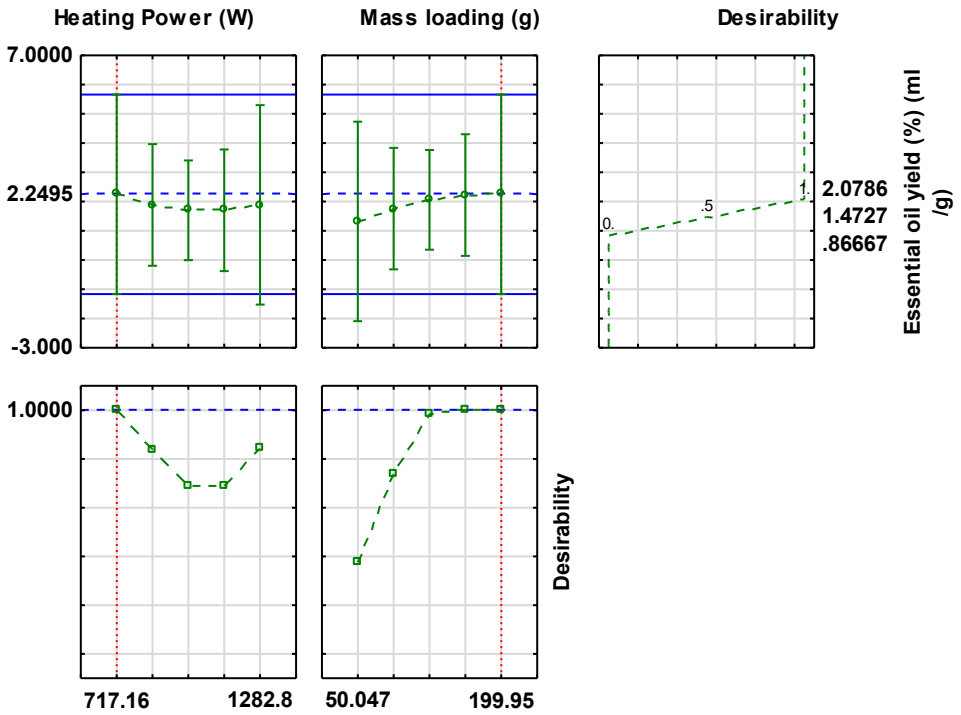

Figure 20: Profiles for Predicted Values and Desirability of essential oil yield as a function of both heating power and mass loading

5.4 D-Limonene Concentration

5.4.1 Statistical significance of factors on D-Limonene concentration

The effect of mass loading and heating power on the D-Limonene Concentration of extracted essential oil was evaluated using central composite design-response surface methodology. The analysis of variance (ANOVA) was used to determine the statistical significance of the experimental design. The conditions that were used initially were a confidence interval of 95% and a significance level of 5%. A factor was considered significant if the probability(p) level was less than the significance(α) level. A summary of the ANOVA is given in Table 16. The significant factors were the linear mass loading and quadratic mass loading which had p-values of 0.0210 and 0.0474 respectively. The term that was close to being significant is the quadratic heating power term which had a p-value of 0.0880. The least significant terms were the linear heating term and the interaction term which had very high p-values of 0.765 and 0.373 respectively. Due to the high insignificance of this term, when improving the models, this term was disregarded from the model and a different significant level of 10% and confidence interval of 90% was used. The linear heating term was also removed from the regression model because the presence of this term was predicting negative D-limonene concentration which is not physically possible. A different analysis of variance was carried out with these conditions and the results of this are listed in Table 17.

Table 16: Analysis of Variance results for the effect of heating power and mass loading on the D-limonene Concentration of the essential oils using a 95% confidence interval and an alpha level of 5%.

Factor	SS	Df	MS	F	p
Heating Power (L)	0.91	1	0.915	0.1493	0.765293
Heating Power (Q)	316.82	1	316.818	51.6926	0.087981
Mass loading (L)	5611.95	1	5611.947	915.6555	0.021031
Mass loading (Q)	1101.53	1	1101.534	179.7283	0.047399
1L by 2L	13.93	1	13.930	2.2729	0.372846
Lack of Fit	2359.82	3	786.608	128.3444	0.064775
Pure Error	6.13	1	6.129		
Total SS	10350.51	9			

Table 17:Analysis of Variance results for the effect of heating power and mass loading on the D-limonene Concentration of the essential oils using a 90% confidence interval and an alpha level of 10%.

Factor	SS	Df	MS	F	p
Heating Power (W)(Q)	316.82	1	316.818	51.6926	0.087981
(2)Mass loading (g)(L)	5611.95	1	5611.947	915.6555	0.021031
Mass loading (g)(Q)	1101.53	1	1101.534	179.7283	0.047399
1L by 2L	13.93	1	13.930	2.2729	0.372846
Lack of Fit	2360.74	4	590.185	96.2956	0.076264
Pure Error	6.13	1	6.129		
Total SS	10350.51	9			

The level of statistical significance for each factor was also evaluated using the Pareto chart, Figure 21, which lists the factors from most significant to least significant. The most statistically significant factor that influences the D-limonene Concentration is the mass loading of clementine peel. It is also noted that in the Pareto chart, the linear mas loading, quadratic mass loading and quadratic heating power factor are the ones that are significant because they cross the red line in Figure 21 and the probability levels were all less than the set alpha level of 10% which are given in Table 17. Once the significance of each factor was evaluated the next step was to evaluate the variability of the quadratic regression model in predicting the D-Limonene essential oil yield.

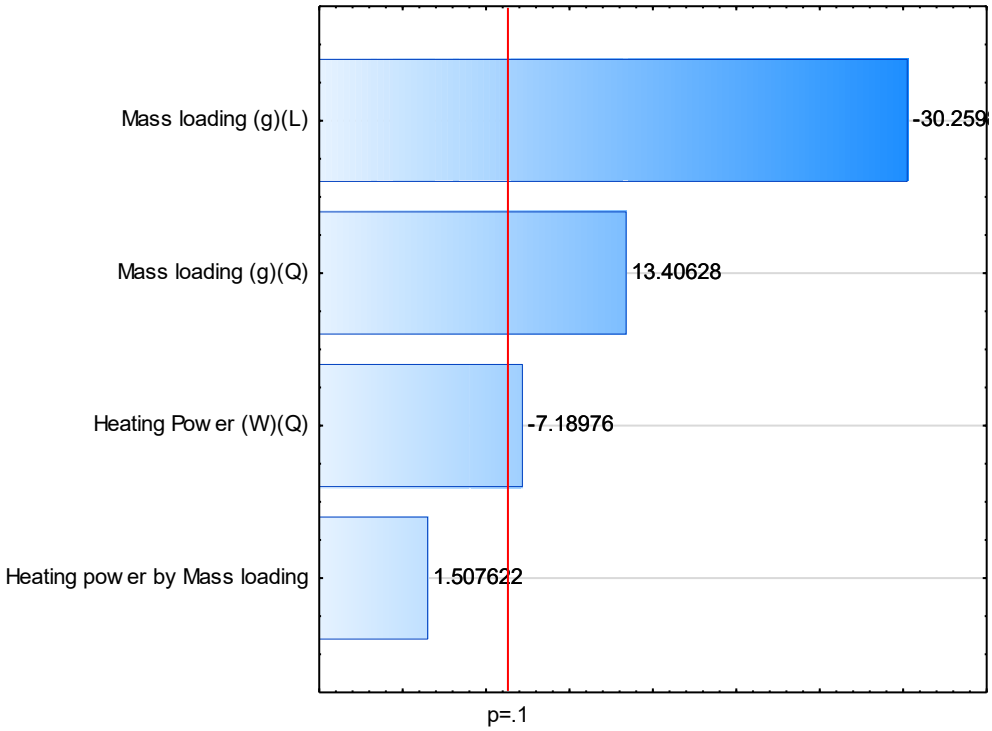

Figure 21:Figure 18: Pareto chart of the standardized effects of the factors on the concentration of D-Limonene in the essential oil

5.4.2 Variability of the regression model to predict D-limonene concentration

The regression model for the D-Limonene concentration is given by equation [25]. The variation of the model fit to experimental data was evaluated using the coefficient of determination for this model(R^2) is 0.77133. This meant that although not close to 1, the model was able to predict the D-limonene concentration at some conditions and at other conditions it did not predict the Concentration very well and led to very high variability in the experimental data. The regression model was then plotted as a 3-D surface plot of the oil in Figure 22. Equation [24] and Figure 22 indicated certain trends of how the D-limonene concentration varied. It was seen that the concentration of D-Limonene decreased as the mass loading increased. However, the trend of the D-Limonene concentration to the heating power could not be distinguished due to the linear heating power term being removed from the regression model to improve the fit of the model as well as its accuracy.

$$D - Limonene\ concentration\ (mg/ml) = 216.263 - 2.457 * 10^{-5}{X_1}^2 - 2.524X_2 + 6.646 * 10^{-3}{X_2}^2 + 3.627 * 10^{-4}X_1X_2 \quad [24]$$

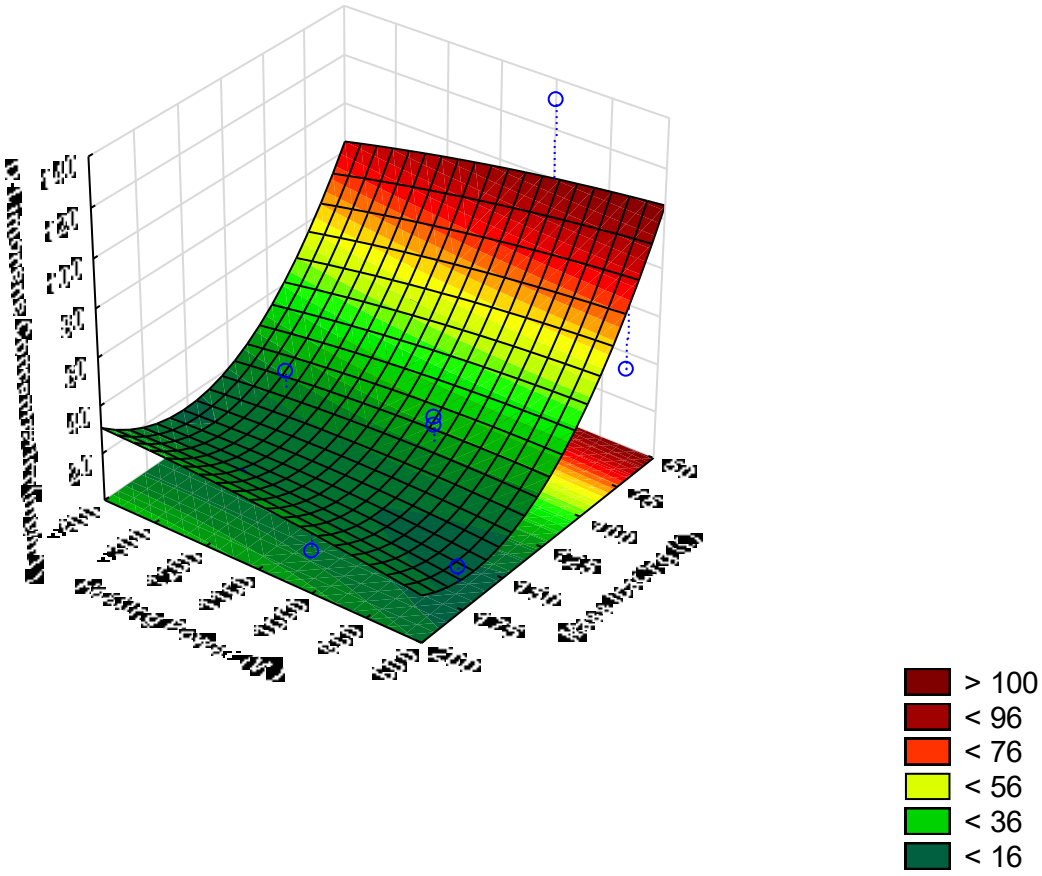

Figure 22:3D Fitted surface plot showing the effect of mass loading and heating power on the Concentration of D-Limonene in extracted essential oil

5.4.3 Optimisation of the factors to obtain high D-Limonene concentration

Once the regression model was obtained, optimisation was carried out by using the desirability function to determine which conditions for the heating power and mass loading give the highest D-Limonene concentration. The results of the optimisation are in Figure 23, and it was noted that the highest D-Limonene concentration, 106.97 mg/ml was obtained for a heating power of 7171.17 W and mass loading of 50.047 g with desirability of 78.317%.

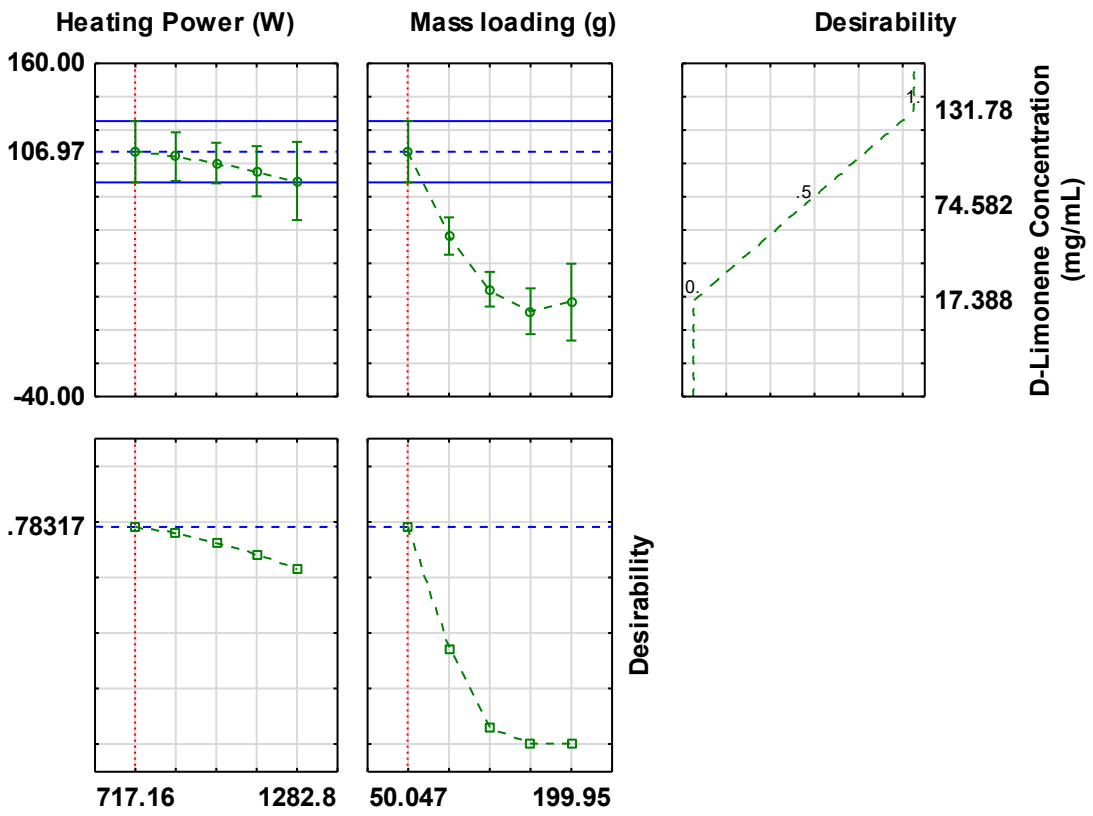

Figure 23: Profiles for Predicted Values and Desirability of D-Limonene concentration as a function of both heating power and mass loading

6 Discussion

6.1 Essential oil yield

The highest yield obtained from the central composite design runs was a yield of 2.08 % (ml/g) which is roughly 1.75% (g/100 g of dry peel) assuming that the density of the essential oil is roughly that of D-Limonene. In a study carried out by (Farhat *et al.*, 2011) with steam distillation, the overall yield observed after 40 minutes was 1.51% (g/100 g dry orange peel). In another different study done by (DO, PHAM, & LAM, 2019) that used hydro-distillation to extract essential oils from orange peels, the maximum yield was 1.2384 % g/100 g dry peel. An even lower yield of 0.42 ± 0.02% by Microwave Assisted hydro distillation and 0.39 ± 0.02% (yields are expressed as in grams of essential oil per 100 g of orange fruit) by Hydro distillation of orange peels was observed in a study by (Ferhat *et al.*, 2006). In comparison to the literature data, the observed highest yield from the central composite data was higher.

It must also be mentioned that from the literature there is a lot of variability within the highest yields obtained due to the differences in the extraction conditions observed for particular studies and in most cases, the plant used is not the same citrus plant species used in this paper.

6.2 Kinetic model

The pseudo-first-order model which was fit to the single factor experimental kinetic data fit very well to the data which was proven by the high coefficient of determination (R^2) which ranged from 0.85 TO 0.99) for each run. (Milojević *et al.*, 2013) fit the same model to different types of plant material which are included In these studies (Cerpa, Mato and José Cocero, 2008), (Romdhane and Tizaoui, 2005), (Koul, Gandotra, & Koul, 2004), (Cassel *et al.*, 2009) and (Xavier *et al.*, 2011), and it was concluded by (Milojević *et al.*, 2013) that this model was the best generally for steam distillation. The same model also showed good compatibility with the hydro distillation or orange-peel essential oils with an R^2 greater than 0.95 (DO, PHAM, & LAM, 2019).

(Cerpa, Mato and José Cocero, 2008) used the same first-order model, equation [10] to investigate the effect of flow rate on the kinetic process constant. It was seen that the kinetic constant increases when the flow rate is increased. Assuming that the heating power can be related to the steam flow rate, a similar effect was seen in this study. As mentioned in the single factor experiments under the results section, an increase in heating power (from 800W to 1000W) also had an increasing effect on the process constant. This same increasing trend was also seen in other studies (Nazlina, Chan, & Angelynn, 2017),(Malekydozzadeh *et al.*, 2012).

The increase in the kinetic constant means that during that extraction process, the equilibrium yield was reached quickly. This is ideal behaviour because if less time is required to reach the maximum, a decrease in extraction time means that the extraction of all essential oil would not need to be unnecessarily prolonged or delayed. Above 1200W, the kinetic constant did decrease which meant that a long time was required to reach the equilibrium yield. This meant that the kinetic constant could only be kept high at an optimal heating power which in this case was 1200 W.

In Figure 8 and Figure 9, the effect of mass loading on the kinetic constant and equilibrium yield is illustrated. Although the equilibrium yield did however increase with higher mass loading, the process constant decreased. As mentioned before, this meant it took longer for the extraction process to reach the equilibrium yield. The extraction process was longer because the steam could not access all the material uniformly. This happened as a result of the steam being unable to penetrate through the plant material bed due to dense packing caused by a higher mass loading. The effect of mass loading on the kinetics of the process indicated how there is a trade-off between obtaining a high equilibrium essential oil yield and reaching that equilibrium yield in a reasonable amount of time. Taking these two ideas into account, the ideal mass loading was 150g. A 150 g mass loading was still high enough to ensure that the equilibrium yield could be kept high but also since its process constant was identical to that of the 100g mass loading in Figure 8, the extraction kinetics were still fast enough to reach the high equilibrium yield.

For the same model, the pseudo-first-order model,(Ait Amer Meziane *et al.*, 2020) obtained an equilibrium yield of 1.66 % and a process constant of 0.0625 min^{-1} for a study by (Farhat *et al.*, 2011) which considered steam distillation extraction kinetics of sweet orange(citrus Sinensis). These values matched well for the equilibrium yield of 1.69% and kinetic constant of 0.056 min^{-1} that was obtained for a mass loading of 200g and heating power of 1000 W(from the single factor experimental data).

The similar kinetic constants are also due to the maximum yield in the study by (Farhat *et al.*, 2011) being obtained after 40 minutes which is similar to the 70 minutes that it took for the yield to reach a maximum in this study. This once again showed that the kinetic parameters obtained in this study compared well to the observed literature.

In similar studies that considered hydro-distillation of citrus but with longer run times, there was a notable difference in the kinetic constant obtained from this study. The literature considered was studied by (Atti-Santos *et al.*, 2005) who considered lime extraction and (Ferhat, Meklati and Chemat, 2007b) who considered lemon extraction. The kinetic constants for the studies were 0.0087 and 0.011 min^{-1} respectively. These values are much smaller than those observed which were between 0.11 to 0.056 min^{-1}. This difference was largely because in those studies the run time was up to five hours and it was established that the longer it takes a process to reach the equilibrium yield, the smaller the value of the kinetic constant would be.

Regression models to predict the process constant and the equilibrium yield developed from the central composite design response surface methodology were also developed in this study. These models were then used to modify the pseudo-first-order kinetic model so that the process constant and the equilibrium yield can be predicted in terms of the heating power and mass loading. This globalized model, equation [22], was not suitable for predicting the essential oil yield. This was the case because the regression models developed for both the process constant and equilibrium yield showed high variability shown by the low coefficients of determination(R^2) of 0.2685 and 0.578 respectively. The factors in these models were also considered not statistically significant by the analysis of variance (ANOVA) which was used to do the statistical analysis. The high variability in the regression models can be explained by the data used in forming the regression model. The process constant and equilibrium yield data used were based on fitting the pseudo kinetic model to the central composite experimental run data and when that was done, the fitting of this kinetic model already had high variability as it was not a perfect fit to the experimental data. By then doing another regression to obtain the models of these kinetic model constants as a function of the heating power and mass loading these previous errors and variability in the data was carried over into the regression and as a result, meant very high variance in these regression models.

6.3 Mass loading effect on essential oil yield

The mass of the raw material is one of the primary influencing aspects in the steam distillation process because a sufficient mass assures that there will be enough steam to draw out all of the essential oils(Dao *et al.*, 2021). As noted in this study, the yield of essential oil increased when the mass loading of clementine peels was increased and these results were in agreement with a study done by (Radwan *et al.*, 2020). In that study, the yield of lavender oil increased when the batch mass was increased from 400, 600 and 800g where the highest yield was 0.791 % (w/w) for a batch mass of 800g. However, in a different study which was carried out by (Dao *et al.*, 2021) the essential oil content decreased as the mass loading of raw material citrus peel was increased. The explanation brought forward by (Alam, Husin and Asnawi, 2018), this trend was caused by the larger input volume, which resulted in denser material density and lower water vapour pressure from the heater, making it more challenging to

carry out the release of essential oils from the steam feedstock. What was concluded in that study (Alam, Husin and Asnawi, 2018) is that at a lower bed volume (less packing of the column), essential oil yield would be higher.

Overall, in this study, the increase in clementine essential oil yield with an increase in the mass loading can be explained by the reasoning that the column had enough volume available to accommodate the increased mass of raw material added and was not densely packed. Although the essential oil yield does increase with increased mass loading of the column, between the change in mass from 150g to 200g, the change in oil yield does start to the plateau which suggests that at the higher mass loading the column is overloaded and the yield would start to decrease.

6.4 Heating power effect on essential oil yield

In a similar study that assessed the effect of heating power, the results from that study showed that the extraction power affects the yield(T. P. Dao *et al.*, 2022). In that study, as the power was increased (from 170W to 204 W), there was an increase in the amount of oil extracted from 3.0% to 3.8%. This was similar to results shown in the single factor experiments, which indicated that when the power was increased from 800W to 1000 W, the yield also increased from 1.31 to 1.73%. However in that same study by (T. P. Dao *et al.*, 2022), when the power was increased to 238 W, the process efficiency decreased as the yield decreased to 2.8%. Again, this same trend was also shown in the result of this study because when the increased to 1000W and higher, the yield decreased from 1.73% to 1.47% in the single factor experiments.

The effect of the heating power on the essential oil yield when optimised using the central composite resulted in a minimum saddle point. Once again, assuming that changing the heating power corresponds to a change in the steam flow rate, (Masango, 2005) claimed that using less steam flow rate boosted the output and that steam in steam distillation serves two purposes: to produce heat energy and to carry distillate. The effect of steam flow rate can be explained by thinking of the total pressure inside the column which is affected by the pressure of water vapour and essential oil vapour. The pressure inside the steam distillation column is described by the following equation

$$P_{tot} = P_{org} + P_w \qquad [25]$$

The total pressure (atmospheric pressure) is denoted by P_{tot}, P_{org} is the partial pressure caused by the essential oil and P_w is the partial pressure caused by the steam.

To obtain a high yield of essential oil, it would be necessary to make P_{org} large. The only way to increase the partial pressure caused by the essential is by decreasing the partial pressure generated by the steam because the total pressure is always constant at atmospheric pressure. By decreasing the steam flow rate, the partial pressure brought on by the steam can be attenuated. Increased p_w and decreased p_{org} due to excessive steaming rate result in short steam residence times in extractors and poor oil isolation. The steaming flow rate, however, cannot be too low. This is true because, without increasing operational pressure and temperature, the steam flow rate must be high enough to give the required enthalpy for vaporizing the oil and the required energy to account for heat losses

from the still (Masango, 2001)(Masango, 2001). As a result, the best steam flow rate, or heating power, must be established.

What must also be noted with the effect of heating power is that the induction cooker which provided the heating of the still pot to produce steam did not operate at ideal conditions. In the calibration of the induction cooker, it was not those power ratings of 800 W,1000 W, 1200 W and 1400 W the actual power was not these values but instead lower values of 531 W, 882 W, 922 W and 986 W respectively. The actual values are very different from the rate power conditions which would also explain why the effect of heating power on the extraction of essential oils showed high variability and was considered statistically insignificant by the experimental design.

6.5 Raw material

6.5.1 Particle size

In this study, one of the assumptions that were made was that the clementine peel particles are homogenous and of the same size. Although the clementine peels were subjected to the same amount of time during grinding and comminution, a portion of the clementine peels was subjected to different degrees of crushing. Zones in the column bed that are less densely packed than the remainder of the bed result from peel particles that are larger than the average particle size. These zones are porous, and steam preferentially travels through them. This effect, known as channelling, results in an unequal distribution of the flow of steam in the bed (Masango, 2001) (Guenther, 1948). The particle bed of clementine peels can also be tightly packed which would be due to particle sizes that are fine sized. Tightly packed zones also have less steam flowing through them, which prevents steam from making contact with the particles there (Masango, 2001) (Guenther, 1948). The maximum amount of essential oil extraction is reduced in conditions where particles are both closely packed and of different sizes. To carry out an ideal steam distillation process even steam distribution must be maintained throughout the column, and this may be done by utilizing peel particles that are as homogeneous as possible and making sure they are the correct size such that the plant material is penetrated evenly and completely by steam (Guenther, 1948). To determine the appropriate particle size at which the clementine peels should be crushed, further research must be done to investigate the impact of particle sizes on the steam distillation extraction of clementine peel essential oils. In a study carried out by (JALGAONKAR, JHA, & PAL, 2013) that considered the grapefruit citrus species, where particle sizes of 1.4 mm, 1.1 mm and 0.5 mm were considered, the yield increased as the particle sizes were decreased. The highest essential oil yield 7.92% dry basis was obtained for the smallest particle size of 0.5 mm.

It should be emphasized that (Guenther, 1948) asserts that the plant material must be promptly distilled after it has been crushed or reduced in size. Otherwise, the essential oils will partially evaporate because they are rather volatile, which would diminish the overall output of oil by the amount corresponding to the quantity of evaporation.

6.5.2 Bed Height

When incoming steam makes contact with plant material during the first stage of steam distillation, a water film is created on the surface of the raw vegetable material (Masango, 2001). Depending on the cross-sectional area of the column, the bed height could be large which would also mean that this film of water would also be large. To be vaporized, the oil from the peel matrices must pass through this film. Theoretically, when the oil comes into contact with the vegetable raw material above it, it may condense. The height of the bed shouldn't be too high to guarantee that the oils condensate as little as possible. Heat and mass transfer will be hampered by an excessive height, which will reduce the rate of extraction and the maximum yield that can be obtained. In this study, the effect of bed height was noted during the single factor runs where mass was varied but kept constant at 1000W. after 10 minutes the essential oil yield at a mass of 200 g stood at 0.62% whereas at 150 g and 100g it was 1% and 0.9% respectively. As a possible explanation this means that due to the large bed height caused by the higher mass loading, the rate of extraction (mass transfer) was affected. There is a range of bed heights that is properly determined to ensure an acceptable temperature differential throughout the bed as well as adequate heat and mass transport (DeWasch & Froment, 1972). To obtain an ideal bed height without needing to change the amount of material used, different column diameters would need to be considered through a series of further experimental works.

7 Conclusion and Recommendations

7.1 Conclusion

In the present study, central composite experimental design and response surface methodology were used to determine the optimal heating power of a heater (induction cooker) and the dry mass loading of clementine citrus peel required to extract essential oil from clementine peels using steam distillation. The results of the optimisation indicated that a heating power of 717.17 W and mass loading of 199.96 g was required to achieve the maximum yield of 2.25 % of essential oil. A quadratic regression model was obtained which was able to predict the essential oil yield as a function of mass loading and heating power. The model was sufficiently suitable for simulating steam distillation of peels of clementine based on the coefficient of determination (R^2) of the model which was 0.836. The statistical significance of each term in the model was evaluated using an Analysis of variance (ANOVA). The results of the ANOVA, at a significance level of 0.05 indicated that all the terms of the ANOVA were not statistically significant. The p-values observed for the linear heating power factor and the linear mass loading factor were 0.632 and 0.157 respectively. In an attempt to improve the significance of the factors, the significance level was changed to 0.10, this however did not change the significance of the factors and was still statistically insignificant. Despite this, trends could still be noted between the essential oil yield and these variables. It was seen that an increase in the mass loading had an increasing effect on the essential oil yield. The mass loading had the most notable effect on the essential oil yield. The interaction effect of heating power and mass loading was considered to be insignificant and had the least effect on the essential oil yield.

The nature of the steam distillation extraction process of essential oil was also evaluated by fitting a pseudo-first-order model to the experimental data. Different kinetic parameters, the equilibrium yield and the process constant were estimated corresponding to this model and evaluated based on the coefficient of determination and the sum of square error between the calculated and experimental extraction yield kinetic data. Overall, the pseudo-nonlinear model was found suitable for describing the process at different extraction conditions which included varying heating power and mass loading. The model was found to fit well with the experimental data according to the high R^2 values (0.85 to 0.99) that were observed at the different extraction conditions.

The kinetic modelling of the process displayed trends as the heating power and the mass loading varied. The process constant, k_1 is an indication of how quickly the equilibrium yield of essential oil for the process is reached. It was seen that with an increase in the mass loading, this constant decreased which indicated that due to greater mass loading, the extraction kinetics were slower. It was seen however that with the heating power, the kinetic constant increased up to a maximum point as the heating power was increased which indicated that the extraction kinetics did increase. However, beyond a maximum heating power, the kinetic constant decreased. According to the kinetic modelling of the steam distillation process, the optimum conditions to obtain maximum essential oil yield would be a dry mass loading of 150 g of clementine peel and a heating power of 1000 W.

The study also attempted to formulate a globalized model for the first-order kinetic model using a central composite experimental design and response surface methodology. Regression models for the process constant and equilibrium as a function of the mass loading and heating power were formulated and then combined into the first-order kinetic model. Both regression models were considered to be statistically insignificant as the factors in both models were not statistically significant. The models also showed high variability to the experimental data shown by the very low R^2 of for the process constant and equilibrium yield models respectively. The models did however still show trends and similarly to the essential oil yield, the mass loading had the most significant effect on the kinetic model parameters. Similarly, an increasing mass loading increased the equilibrium yield while an increase in the mass loading decreased the kinetic constant. This was in agreement with the trend reflected in the single-factor experiments.

The effect of investigated factors, mass loading and heating power on the end point D-Limonene concentration was also studied using central composite design and response surface methodology. To predict the D-Limonene concentration as a function of mass loading and heating power, a quadratic regression model was obtained. The statistical significance and variability of the model were then evaluated. At the initial set significance level(α=0.05), the linear and quadratic terms of the mass loading factor were statistically significant with probability values of 0.0210 and 0.0474 respectively. The significance of the factors was improved by changing the α level to 0.10. At this condition, the linear mass loading, quadratic mass loading and quadratic heating power were considered statistically significant because the probability value for each of these factors was less than the new significance level of 10%. Although statistically significant, the regression model shows some level of variability with an R^2 value of 0.7713. Notably, the largest D-limonene concentration 131.8 mg/ml was observed for a mass loading of 50g of clementine peel and a heating power of 1000 W. the optimisation of the

factors however showed that to obtain a high concentration of D-Limonene, a low heating power, 717.17 W and mass loading of 50.07 g dry clementine peel should be used.

7.2 Recommendations

The essential oil yield data that was generated for the central composite design had high variability. With the data being highly variable, it became difficult to formulate a model that can consistently or accurately predict the essential oil yield as a function of the heating power and mass loading. To reduce the variability observed in the essential oil yield data it was recommended that the effect of the particle sizes must be taken into account in a future study. According to (Guenther, 1948), steam distillation must be carried out by making sure that particle size is uniform/homogenous and that there must be sufficiently large interfaces for rising steam to flow. This must be done to ensure steam can pass through all material and ensure all possible essential oil can be extracted. The clementine's were ground to make all peels smaller than the size that they were collected but the size of the particles was not considered in this study. It was however recommended by (Guenther, 1948) that as the material is ground, extraction must be done immediately to reduce the loss of essential oils due to the volatility of essential oils. In a future study, it would be important to consider this. It was also observed in a study by (DO, PHAM, & LAM, 2019), that yield of essential oil decreased as the number of days it was kept stored increased. In the present study when the clementine peels were ground to smaller particles, extraction was not carried out immediately. The delay in the extraction might have played a part in affecting the yield of essential oil and it would be recommended once again to use the raw material as soon as it is ground. The actual heating power that was provided by the induction did not align with the rated values on the equipment. It would be worth using a different source of heating to further improve the investigation of the effect of heating power on the steam distillation process of essential oils from clementine peels. Model validation of the models obtained from the central composite design-response surface methodology was not carried out in this study and it is recommended to see if the model can predict experimental data carried out at the optimum heating power and mass loading conditions.

8 References

Ait Amer Meziane, I. *et al.* (2019) 'The first-order model in the simulation of essential oil extraction kinetics', *Journal of Applied Research on Medicinal and Aromatic Plants*, 15, p. 100226. doi:10.1016/J.JARMAP.2019.100226.

Ait Amer Meziane, I. *et al.* (2020) 'Modelling and optimization of energy consumption in essential oil extraction processes', *Food and Bioproducts Processing*, 119, pp. 373–389. doi:10.1016/J.FBP.2019.11.018.

Alam, P.N., Husin, H. and Asnawi, T.M. (2018) 'Extraction of citral oil from lemongrass (Cymbopogon Citratus) by steam-water distillation technique', *IOP Conference Series: Materials Science and Engineering*, 345, pp. 1–7. doi:10.1088/1757-899X/345/1/012022.

Atti-Santos, A.C. *et al.* (2005) 'Extraction of essential oils from lime (Citrus latifolia Tanaka) by hydrodistillation and supercritical carbon dioxide', *Brazilian Archives of Biology and Technology*, 48(1), pp. 155–160. doi:10.1590/S1516-89132005000100020.

Azmir, J. *et al.* (2013) 'Techniques for extraction of bioactive compounds from plant materials: A review', *Journal of Food Engineering*, 117(4), pp. 426–436. doi:10.1016/J.JFOODENG.2013.01.014.

Benyoussef, E.H. *et al.* (2002) 'Modélisation du transfert de matiére lors de l'extraction de l'huile essentielle des fruits de coriandre', *Chemical Engineering Journal*, 85(1), pp. 1–5. doi:10.1016/S1385-8947(01)00134-6.

Both, S., Chemat, F. and Strube, J. (2014) 'Extraction of polyphenols from black tea – Conventional and ultrasound assisted extraction', *Ultrasonics Sonochemistry*, 21(3), pp. 1030–1034. doi:https://doi.org/10.1016/j.ultsonch.2013.11.005.

Calo, J.R. *et al.* (2015) 'Essential oils as antimicrobials in food systems – A review', *Food Control*, 54, pp. 111–119. doi:10.1016/J.FOODCONT.2014.12.040.

Cassel, E. *et al.* (2009) 'Steam distillation modeling for essential oil extraction process', *Industrial Crops and Products*, 29(1), pp. 171–176. doi:10.1016/J.INDCROP.2008.04.017.

Cassel, E. and Vargas, R.M.F. (2006) 'Experiments and Modeling of the Cymbopogon winterianus Essential Oil Extraction by Steam Distillation', *Revista de la Sociedad Química de Mexico*, 50, pp. 126–129.

Cerpa, M.G., Mato, R.B. and Cocero, M.J. (2008) 'Modeling steam distillation of essential oils: Application to lavandin super oil', *AIChE Journal*, 54(4), pp. 909–917. doi:10.1002/aic.11438.

Cerpa, M.G., Mato, R.B. and José Cocero, M. (2008) 'Modeling steam distillation of essential oils: Application to lavandin super oil', *AIChE Journal*, 54(4), pp. 909–917. doi:https://doi.org/10.1002/aic.11438.

Chen, Y. *et al.* (2014) 'Effect of Second Cooling on the Chemical Components of Essential Oils from Orange Peel (Citrus sinensis)', *Journal of Agricultural and Food Chemistry*, 62(35), pp. 8786–8790. doi:10.1021/jf501079r.

Ciriminna, R. *et al.* (2014) 'Limonene: a versatile chemical of the bioeconomy', *Chem. Commun.*, 50(97), pp. 15288–15296. doi:10.1039/C4CC06147K.

Coll, M.D. *et al.* (1998) 'Recovery of flavanones from wastes of industrially processed lemons', *Zeitschrift für Lebensmitteluntersuchung und -Forschung A*, 206(6), pp. 404–407. doi:10.1007/s002170050282.

Dao, P.T. *et al.* (2022) 'Kinetics of pilot-scale essential oil extraction from pomelo (Citrus maxima)

peels: Comparison between linear and nonlinear models', *Alexandria Engineering Journal*, 61(3), pp. 2564–2572. doi:10.1016/J.AEJ.2021.07.002.

Dao, T.P. *et al.* (2021) 'Central Composite Design, Kinetic Model, Thermodynamics, and Chemical Composition of Pomelo (Citrus Maxima (Burm.) Merr.) Essential Oil Extraction by Steam Distillation'. doi:10.3390/pr9112075.

Dao, T.P. *et al.* (2022) 'Assessing the kinetic model on extraction of essential oil and chemical composition from lemon peels (Citrus aurantifolia) by hydro-distillation process', *Materials Today: Proceedings*, 51, pp. 172–177. doi:10.1016/j.matpr.2021.05.069.

Droby, S. *et al.* (2008) 'Role of citrus volatiles in host recognition, germination and growth of Penicillium digitatum and Penicillium italicum', *Postharvest Biology and Technology*, 49(3), pp. 386–396. doi:10.1016/J.POSTHARVBIO.2008.01.016.

Dugo, P. *et al.* (1997) *Characterization of Cold-Pressed Key and Persian Lime Oils by Gas Chromatography, Gas Chromatography/Mass Spectroscopy, High-Performance Liquid Chromatography, and Physicochemical Indices*. Available at: https://pubs.acs.org/sharingguidelines.

Fagbohungbe, M.O. *et al.* (2016) 'Impact of biochar on the anaerobic digestion of citrus peel waste', *Bioresource Technology*, 216, pp. 142–149. doi:https://doi.org/10.1016/j.biortech.2016.04.106.

Farhat, A. *et al.* (2011) 'Microwave steam diffusion for extraction of essential oil from orange peel: Kinetic data, extract's global yield and mechanism', *Food Chemistry*, 125(1), pp. 255–261. doi:10.1016/j.foodchem.2010.07.110.

Ferhat, M.A. *et al.* (2006) 'An improved microwave Clevenger apparatus for distillation of essential oils from orange peel', *Journal of Chromatography A*, 1112(1–2), pp. 121–126. doi:10.1016/J.CHROMA.2005.12.030.

Ferhat, M.A., Meklati, B.Y. and Chemat, F. (2007a) 'Comparison of different isolation methods of essential oil from Citrus fruits: cold pressing, hydrodistillation and microwave "dry" distillation', *J*, 22, pp. 494–504. doi:10.1002/ffj.

Ferhat, M.A., Meklati, B.Y. and Chemat, F. (2007b) 'Comparison of different isolation methods of essential oil from Citrus fruits: cold pressing, hydrodistillation and microwave "dry" distillation', *J*, 22, pp. 494–504. doi:10.1002/ffj.

Fitriady, M.A., Sulaswatty, A. and Agustian, E. (2017) 'Steam distillation extraction of ginger essential oil: Study of the effect of steam flow rate and time process ARTICLES YOU MAY BE INTERESTED IN', p. 20033. doi:10.1063/1.4973159.

Gunaseelan, V.N. (2004) 'Biochemical methane potential of fruits and vegetable solid waste feedstocks', *Biomass and Bioenergy*, 26(4), pp. 389–399. doi:https://doi.org/10.1016/j.biombioe.2003.08.006.

Jha, P. *et al.* (2019) 'Valorisation of orange peel: supplement in fermentation media for ethanol production and source of limonene', *Environmental Sustainability*, 2(1), pp. 33–41. doi:10.1007/s42398-019-00048-2.

Kamalakkannan, N. and Prince, P.S.M. (2004) 'Antidiabetic and anti-oxidant activity of Aegle marmelos extract in streptozotocin-induced diabetic rats', *Pharmaceutical Biology*, 42(2), pp. 125 – 130. doi:10.1080/13880200490510937.

Khandare, R.D., Tomke, P.D. and Rathod, V.K. (2021) 'Kinetic modeling and process intensification of ultrasound-assisted extraction of d-limonene using citrus industry waste', *Chemical Engineering and Processing - Process Intensification*, 159(September 2020), p. 108181. doi:10.1016/j.cep.2020.108181.

Koudous, I. *et al.* (2014) 'Process design based on physicochemical properties for the example of obtaining valuable products from plant-based extracts', *Comptes Rendus Chimie*, 17(3), pp. 218–231.

doi:https://doi.org/10.1016/j.crci.2013.11.003.

Kummer, R. *et al.* (2013) 'Evaluation of Anti-Inflammatory Activity of *Citrus latifolia* Tanaka Essential Oil and Limonene in Experimental Mouse Models', *Evidence-Based Complementary and Alternative Medicine*. Edited by J.-H. Lee, 2013, p. 859083. doi:10.1155/2013/859083.

Lopresto, C.G. *et al.* (2019) 'Process-intensified waste valorization and environmentally friendly d-limonene extraction', *Euro-Mediterranean Journal for Environmental Integration*, 4(1), p. 31. doi:10.1007/s41207-019-0122-0.

M'hiri, N. *et al.* (2016) 'Food Reviews International Phytochemical characteristics of citrus peel and effect of conventional and nonconventional processing on phenolic compounds: A review'. doi:10.1080/87559129.2016.1196489.

Mahato, N., Sharma, K., *et al.* (2019) 'Citrus essential oils: Extraction, authentication and application in food preservation', *Critical Reviews in Food Science and Nutrition*, 59(4), pp. 611–625. doi:10.1080/10408398.2017.1384716.

Mahato, N., Sinha, M., *et al.* (2019) 'Modern Extraction and Purification Techniques for Obtaining High Purity Food-Grade Bioactive Compounds and Value-Added Co-Products from Citrus Wastes', *Foods*, 8(11). doi:10.3390/foods8110523.

Mahato, N. *et al.* (2021) 'processes Biotransformation of Citrus Waste-I: Production of Biofuel and Valuable Compounds by Fermentation'. doi:10.3390/pr9020220.

Malekydozzadeh, M. *et al.* (2012) 'Application of Multistage Steam Distillation Column for Extraction of Essential Oil of Rosemarinus officinialis L', *IAChE*, 9(4), pp. 54 – 64. Available at: https://www.scopus.com/inward/record.uri?eid=2-s2.0-85028762478&partnerID=40&md5=7c94a934007197278459ffcb085a2320.

Mamma, D. and Christakopoulos, P. (2014) 'Biotechnological Potential of Citrus Peels', in *Industrial Microbiology : Microbes in Process*. Nova Science Publishers, Incorporated, pp. 59–92.

Marković, M.S. *et al.* (2019) 'A new kinetic model for the common juniper essenstial oil extraction by microwave hydrodistillation', *Chinese Journal of Chemical Engineering*, 27(3), pp. 605–612. doi:10.1016/J.CJCHE.2018.06.022.

Martín, M.A. *et al.* (2010) 'Biomethanization of orange peel waste', *Bioresource Technology*, 101(23), pp. 8993–8999. doi:https://doi.org/10.1016/j.biortech.2010.06.133.

Masango, P. (2005) 'Cleaner production of essential oils by steam distillation', *Journal of Cleaner Production*, 13(8), pp. 833–839. doi:10.1016/J.JCLEPRO.2004.02.039.

Milojević, S.Ž. *et al.* (2008) 'Kinetics of distillation of essential oil from comminuted ripe juniper (Juniperus communis L.) berries', *Biochemical Engineering Journal*, 39(3), pp. 547–553. doi:10.1016/J.BEJ.2007.10.017.

Milojević, S.Ž. *et al.* (2013) 'Modelovanje kinetike hidrodestilacije etarskog ulja iz biljnih materijala', *Hemijska Industrija*, 67(5), pp. 843–859. doi:10.2298/HEMIND121026009M.

Murali, R., Karthikeyan, A. and Saravanan, R. (2013) 'Protective Effects of d-Limonene on Lipid Peroxidation and Antioxidant Enzymes in Streptozotocin-Induced Diabetic Rats', *Basic and Clinical Pharmacology and Toxicology*, 112(3), pp. 175 – 181. doi:10.1111/bcpt.12010.

Murdock, D.I. and Allen, W.E. (1960) 'Germicidal effect of orange peel oil and d-limonene in water and orange juice', *Food Technol*, 14(9), pp. 441 – 445. Available at: https://www.scopus.com/inward/record.uri?eid=2-s2.0-0038735144&partnerID=40&md5=7bd933c998250eb2cf38dceb9f0e9723.

Negro, V. *et al.* (2016) 'Citrus waste as feedstock for bio-based products recovery: Review on limonene

case study and energy valorization', *Bioresource Technology*, 214, pp. 806–815. doi:10.1016/J.BIORTECH.2016.05.006.

Negro, V. *et al.* (2017) 'Recovery of D-limonene through moderate temperature extraction and pyrolytic products from orange peels', *Journal of Chemical Technology and Biotechnology*, 92(6), pp. 1186–1191. doi:10.1002/jctb.5107.

Ozturk, B., Winterburn, J. and Gonzalez-Miquel, M. (2019) 'Orange peel waste valorisation through limonene extraction using bio-based solvents', *Biochemical Engineering Journal*, 151, p. 107298. doi:10.1016/J.BEJ.2019.107298.

Palanisamy, K., Dhivya, J. and Kuppamuthu, K. (2014) 'Extraction and Analysis of Pectin from Citrus Peels: Augmenting the Yield from Citrus limon Using Statistical Experimental Design', *Iranica Journal of Energy & Environment*, 5, pp. 303–312. doi:10.5829/idosi.ijee.2014.05.03.10.

Pavi, V.P. *et al.* (2015) 'Microwave-assisted hydrodistillation of juniper berry essential oil: kinetic modeling and chemical composition'. doi:10.1002/jctb.4653.

Pourbafrani, M. *et al.* (2010) 'Production of biofuels, limonene and pectin from citrus wastes', *Bioresource Technology*, 101(11), pp. 4246–4250. doi:https://doi.org/10.1016/j.biortech.2010.01.077.

Radwan, M.N. *et al.* (2020) 'A solar steam distillation system for extracting lavender volatile oil', *Energy Reports*, 6, pp. 3080–3087. doi:https://doi.org/10.1016/j.egyr.2020.11.034.

Raeissi, S. *et al.* (2008) 'Ethane as an alternative solvent for supercritical extraction of orange peel oils', *The Journal of Supercritical Fluids*, 45(3), pp. 306–313. doi:https://doi.org/10.1016/j.supflu.2008.01.008.

Romdhane, M. and Tizaoui, C. (2005) 'The kinetic modelling of a steam distillation unit for the extraction of aniseed (Pimpinella anisum) essential oil', *Journal of Chemical Technology and Biotechnology J Chem Technol Biotechnol*, 80, pp. 759–766. doi:10.1002/jctb.1221.

Rossi, P. *et al.* (2011) 'D-limonene and geranial fractionation from lemon essential oil by molecular distillation', *Latin American Applied Research*, 41, pp. 81–85.

Roth, T., Uhlenbrock, L. and Strube, J. (2020) 'Distinct and quantitative validation for predictive process modelling in steam distillation of caraway fruits and lavender flower following a Quality-By-Design (QbD) approach', *Processes*, 8(5). doi:10.3390/PR8050594.

Russo, R. *et al.* (2013) 'Implication of limonene and linalyl acetate in cytotoxicity induced by bergamot essential oil in human neuroblastoma cells', *Fitoterapia*, 89, pp. 48–57. doi:https://doi.org/10.1016/j.fitote.2013.05.014.

Santiago, B. *et al.* (2020) 'Identification of environmental aspects of citrus waste valorization into D-limonene from a biorefinery approach', *Biomass and Bioenergy*, 143, p. 105844. doi:10.1016/J.BIOMBIOE.2020.105844.

Sarpietro, M.G. *et al.* (2021) 'Interaction of limonene, terpineol, and 1,8 cineol with a model of biomembrane: A DSC study', *Thermochimica Acta*, 700, p. 178938. doi:10.1016/J.TCA.2021.178938.

Sharma, K. *et al.* (2017) 'Converting citrus wastes into value-added products: Economic and environmently friendly approaches', *Nutrition*, 34, pp. 29–46. doi:10.1016/J.NUT.2016.09.006.

Sharma, P. *et al.* (2013) 'Isolation and characterization of hesperidin from orange peel', *Indo American Journal of Pharmaceutical Research.*, 2013, pp. 3892–3897.

Siddiqui, S.A. *et al.* (2022) 'Extraction and purification of d-limonene from orange peel wastes: Recent advances', *Industrial Crops and Products*, 177(December 2021), p. 114484. doi:10.1016/j.indcrop.2021.114484.

Silva, L. V. *et al.* (2005) 'Comparison of hydrodistillation methods for the deodorization of turmeric', *Food Research International*, 38(8–9), pp. 1087–1096. doi:10.1016/J.FOODRES.2005.02.025.

Sovová, H. and Aleksovski, S.A. (2006) 'Mathematical model for hydrodistillation of essential oils', *J*, 21, pp. 881–889. doi:10.1002/ffj.

Su, H., Tan, F. and Xu, Y. (2016) 'Enhancement of biogas and methanization of citrus waste via biodegradation pretreatment and subsequent optimized fermentation', *Fuel*, 181, pp. 843–851. doi:https://doi.org/10.1016/j.fuel.2016.05.055.

SUBBA, M.S., SOUMITHRI, T.C. and RAO, R.S. (1967) 'Antimicrobial Action of Citrus Oils', *Journal of Food Science*, 32(2), pp. 225–227. doi:https://doi.org/10.1111/j.1365-2621.1967.tb01299.x.

Vankar Padma S (2004) *Essential Oils and Fragrances from Natural Sources*, *Resonance*. Available at: https://www.ias.ac.in/article/fulltext/reso/009/04/0030-0041.

Vieira, A.J. *et al.* (2018) 'Limonene: Aroma of innovation in health and disease', *Chemico-Biological Interactions*, 283, pp. 97–106. doi:https://doi.org/10.1016/j.cbi.2018.02.007.

Waheed, A. *et al.* (2020) 'Kinetic model and optimization for enzyme-assisted hydrodistillation of d-limonene-rich essential oil from orange peel', *Flavour and Fragrance Journal*, 35(5), pp. 561–569. doi:https://doi.org/10.1002/ffj.3598.

Wang, L. and Weller, C.L. (2006) 'Recent advances in extraction of nutraceuticals from plants', *Trends in Food Science & Technology*, 17(6), pp. 300–312. doi:10.1016/J.TIFS.2005.12.004.

Wilkins, Mark R, Widmer, W.W. and Grohmann, K. (2007) 'Simultaneous saccharification and fermentation of citrus peel waste by Saccharomyces cerevisiae to produce ethanol', *Process Biochemistry*, 42(12), pp. 1614–1619. doi:https://doi.org/10.1016/j.procbio.2007.09.006.

Wilkins, Mark R., Widmer, W.W. and Grohmann, K. (2007) 'Simultaneous saccharification and fermentation of citrus peel waste by Saccharomyces cerevisiae to produce ethanol', *Process Biochemistry*, 42(12), pp. 1614–1619. doi:10.1016/J.PROCBIO.2007.09.006.

Xavier, V.B. *et al.* (2011) 'Mathematical modeling for extraction of essential oil from Baccharis spp. by steam distillation', *Industrial Crops and Products*, 33(3), pp. 599–604. doi:https://doi.org/10.1016/j.indcrop.2010.12.019.

Zema, D.A. *et al.* (2018) 'Valorisation of citrus processing waste: A review', *Waste Management*, 80, pp. 252–273. doi:10.1016/J.WASMAN.2018.09.024.

JALGAONKAR, K. R., JHA, S. K., & PAL, R. K. (2013). Effect of species and particle size on essential oil yield of citrus peel (Citrus spp). *Indian Journal of Agricultural Sciences 83(12)*, 1285–1288.

Bhattacharya, S. (2021). Central Composite Design for Response Surface Methodology and Its Application in Pharmacy. In P. Kayaroganam, *Response Surface Methodology in Engineering Science* (pp. 1-19). London: IntechOpen.

Chisoro-Dube , S., & Simon , R. (2021). Innovation and inclusion in South Africa's citrus industry. *"Innovation and inclusion in Agro Processing*, 1-7.

Dahm, K. D., & Visco, D. P. (2015). *Fundamentals of Chemical Engineering Thermodynamics* (SI ed.). Stamford, CT, USA: Cengage.

Denny, E. (1979). Steam distillation of the superficial essential oils: Hypotheses from studies with lavenders and mints. *Perfumer Flavorist*, 14-23.

DeWasch, A. P., & Froment, G. F. (1972). Heat transfer in packed beds. *Chemical Engineering Science, Vol 27,*, 567-576.

DO, D. N., PHAM, N., & LAM, T. (2019). Kinetic Modeling of Hydrodistillation of Essential Oil Production from Orange (Citrus sinensis) Peels on Pilot Scale. *AJ C SIAN OURNAL OF HEMISTRY*, 2298-2302.

Guenther, E. (1948). *The essential oils.* New York: D. Van Nostrand Company.

Kapas, A. (2011). THE KINETIC OF ESSENTIAL OIL SEPARATION FROM FENNEL BY MICROWAVE ASSISTED HYDRODISTILLATION (MWHD). *UPB Scientific Bulletin, Series B: Chemistry and Materials Science*, 113-120.

Koul, V., Gandotra, B., & Koul, S. (2004). Kinetic studies of hydrodistillation process showed that the extraction of orange peels essential oil follows first order kinetic (R2 > 0.95) (DO, PHAM, & LAM, 2019). *Kinetic studies of hydrodistillation process showed that the extraction of orange peels essential oil follows first order kinetic (R2 > 0.95) (DO, PHAM, & LAM, 2019)*, 135-139.

Mahara, S., & McGaw, D. (2020). Mathematical Model for the Removal of Essential Oil Constituents during Steam Distillation Extraction. *Processes*, 400-413.

Masango, P. (2001). *Towards Understanding Steam Distillation of Essential Oils by Differential Quantification of Principal Components Using Capillary Gas Chromatography.* University of Surrey.

Morin, P., Gunther, C., Peyron, L., & Richard, H. (1985). Etude des phénomènes physico-chimiques intervant lors du procédé d'hydrodistillation. *Bull. Soc. Chim. Fr*, 921-930.

Nazlina, Z., Chan, M., & Angelynn, J. (2017). Kinetic Study of Hydrodistillation of Citrus Sinensis and Quality of the Oil. *International Journal of Engineering & Technology*, 42-46.

Peng, D. -Y., & Robsinson, D. B. (1976). A New Two-Constant Equation of State. *Ind. Eng. Chem. Fund., 15*, 59-64.

Perry, R. H. (1984). *Perry's Chemical engineers' handbook.* New York : McGraw-Hill.

Renon, H., & Prausnitz, J. M. (1968). Local compositions in thermodynamic excess functions for liquid mixtures. *AIChE J., 14*, 135-144.

Tripathi, A. (2021, October 6). *What is the Coefficient of Determination: R Square*. Retrieved October 20, 2022, from Data Science Duniya: https://ashutoshtripathi.com/2019/01/22/what-is-the-coefficient-of-determination-r-square/

Appendix A. Project proposal and signed meetings

Appendix B. Experimental Results

Data Run 1

Table 18:Heating power of 800 W and constant mass loading of 150 g (Run 1)

Time (min)	Initial Volume (ml)	Final Volume (ml)	Essential Oil Volume (ml)
0	0	0	0
10	37.7	37	0.7
20	28.4	27.3	1.1
30	19.9	18.6	1.3
40	14.6	12.9	1.7
50	7.9	6.2	1.7
60	19.8	18.1	1.7
70	13	11.3	1.7

Table 19: Heating power of 800 W and constant mass loading of 150 g (Run 2)

Time (min)	Initial Volume (ml)	Final Volume (ml)	Essential Oil Volume (ml)
0	0	0	0
10	40.6	39.8	0.8
20	27.9	26.7	1.2
30	30.5	28.9	1.6
40	31.7	29.9	1.8
50	19.8	17.8	2
60	30.1	28	2.1
70	24.7	22.6	2.1

Table 20:Heating power of 800 W and constant mass loading of 150 g (Run 3)

Time (min)	Initial Volume (ml)	Final Volume (ml)	Essential Oil Volume (ml)
0	0	0	0
10	8.8	8.5	0.3
20	8.4	8	0.7
30	7.8	7.2	1.3
40	8.5	7.9	1.9
50	9.2	9	2.1
60	8.9	8.9	2.1
70	9.7	9.7	2.1

Table 21:Heating power of 1000 W and constant mass loading of 150 g (Run 1)

Time (min)	Initial Volume (ml)	Final Volume (ml)	Essential Oil Volume (ml)
0	0	0	0
10	4.2	2.4	1.8
20	5.9	5	2.7
30	6	5.9	2.8
40	7.7	7.7	2.8
50	8.6	8.6	2.8
60	4.3	4.3	2.8
70	9.2	9.2	2.8

Table 22: Heating power of 1000 W and constant mass loading of 150 g (Run 2)

Time (min)	Initial Volume (ml)	Final Volume (ml)	Essential Oil Volume (ml)
0	0	0	0
10	7.4	6.8	0.6
20	5.3	4.7	1.2
30	9	8.4	1.8
40	7.1	6.6	2.3
50	8.5	8.2	2.6
60	7.3	7.3	2.6
70	4.7	4.7	2.6

Table 23: Heating power of 1000 W and constant mass loading of 150 g (Run 3)

Time (min)	Initial Volume (ml)	Final Volume (ml)	Essential Oil Volume (ml)
0	0	0	0
10	8.4	7.5	0.9
20	7.8	7.2	1.5
30	8.3	7.6	2.2
40	7.2	7	2.4
50	9.6	9.6	2.4
60	8.4	8.4	2.4
70	7.5	7.5	2.4

Table 24:Heating power of 1200 W and constant mass loading of 150 g (Run 1)

Time (min)	Initial Volume (ml)	Final Volume (ml)	Essential Oil Volume (ml)
0	0	0	0
10	3.4	2.6	0.8
20	6.7	5.1	2.4
30	6.9	6.8	2.5
40	2.9	2.9	2.5
50	7.7	7.7	2.5
60	8.4	8.4	2.5
70	4.3	4.3	2.5

Table 25:Heating power of 1200 W and constant mass loading of 150 g (Run 2)

Time (min)	Initial Volume (ml)	Final Volume (ml)	Essential Oil Volume (ml)
0	0	0	0
10	5.4	4.3	1.1
20	8.4	7.9	1.6
30	6.6	6.3	1.9
40	5.6	5.5	2
50	6.4	6.4	2
60	8.8	8.8	2
70	8.4	8.4	2

Table 26:Heating power of 1200 W and constant mass loading of 150 g (Run 3)

Time (min)	Initial Volume (ml)	Final Volume (ml)	Essential Oil Volume (ml)
0	0	0	0
10	5.4	3.5	1.9
20	5.8	5.6	2.1
30	7.3	7.3	2.1
40	6.5	6.5	2.1
50	4.7	4.7	2.1
60	8.1	8.1	2.1
70	8.8	8.8	2.1

Table 27:Heating power of 1400 W and constant mass loading of 150 g (Run 1)

Time (min)	Initial Volume (ml)	Final Volume (ml)	Essential Oil Volume (ml)
0	0	0	0
10	6	5.7	0.3
20	7.7	7.3	0.7
30	6.6	6.4	0.9
40	7.1	6.9	1.1
50	9.2	9.2	1.1
60	8.1	8.1	1.1
70	6.6	6.6	1.1

Table 28:Heating power of 1400 W and constant mass loading of 150 g (Run 2)

Time (min)	Initial Volume (ml)	Final Volume (ml)	Essential Oil Volume (ml)
0	0	0	0
10	6.4	6.3	0.1
20	4.1	3.2	1
30	4.8	4.2	1.6
40	9.6	9.6	1.6
50	6.5	6.5	1.6
60	7.1	7.1	1.6
70	9.3	9.3	1.6

Table 29:Heating power of 1400 W and constant mass loading of 150 g (Run 3)

Time (min)	Initial Volume (ml)	Final Volume (ml)	Essential Oil Volume (ml)
0	0	0	0
10	6.9	6.2	0.7
20	7.6	6.8	1.5
30	5.4	5.4	1.5
40	9.1	9.1	1.5
50	7.3	7.3	1.5
60	4.6	4.6	1.5
70	5.8	5.8	1.5

Data Run 2

Table 30:Mass loading of 50 g and constant heating power of 1000 W (Run 1)

Time (min)	Initial Volume (ml)	Final Volume (ml)	Essential Oil Volume (ml)
0	0	0	0
10	37.9	37.6	0.3
20	38.5	38.1	0.4
30	27.7	27.3	0.4
40	18.9	18.5	0.4
50	6.5	6.1	0.4
60	25.8	25.5	0.3
70	14.4	14.1	0.3

Table 31:Mass loading of 50 g and constant heating power of 1000 W (Run 1)

Time (min)	Initial Volume (ml)	Final Volume (ml)	Essential Oil Volume (ml)
0	0	0	0
10	25.5	25.3	0.2
20	17.6	17.3	0.3
30	7	6.7	0.3
40	5.4	5.1	0.3
50	20.7	20.4	0.3
60	14.3	13.9	0.4
70	9.4	9	0.4

Table 32:Mass loading of 50 g and constant heating power of 1000 W (Run 3)

Time (min)	Initial Volume (ml)	Final Volume (ml)	Essential Oil Volume (ml)
0	0	0	0
10	4.6	4.1	0.5
20	6.1	6	0.6
30	7.4	7.4	0.6
40	7.8	7.8	0.6
50	8.5	8.5	0.6
60	9.1	9.1	0.6
70	7.6	7.6	0.6

Table 33:Mass loading of 100 g and constant heating power of 1000 W (Run 1)

Time (min)	Initial Volume (ml)	Final Volume (ml)	Essential Oil Volume (ml)
0	0	0	0
10	27	26.6	0.4
20	14.4	13.2	1.2
30	18.6	17.3	1.3
40	11.7	10.4	1.3
50	23.6	22.3	1.3
60	20.5	19.1	1.4
70	21.5	20.1	1.4

Table 34:Mass loading of 100 g and constant heating power of 1000 W (Run 2)

Time (min)	Initial Volume (ml)	Final Volume (ml)	Essential Oil Volume (ml)
0	0	0	0
10	3.5	2.4	1.1
20	3.4	3.2	1.3
30	7.8	7.8	1.3
40	8.2	8.2	1.3
50	8.6	8.6	1.3
60	7.9	7.9	1.3
70	6.6	6.6	1.3

Table 35:Mass loading of 100 g and constant heating power of 1000 W (Run 3)

Time (min)	Initial Volume (ml)	Final Volume (ml)	Essential Oil Volume (ml)
0	0	0	0
10	4.8	3.6	1.2
20	5.6	5.3	1.5
30	4.6	4.6	1.5
40	8.2	8.2	1.5
50	7	7	1.5
60	8.6	8.6	1.5
70	7.4	7.4	1.5

Table 36:Mass loading of 150 g and constant heating power of 1000 W (Run 1)

Time (min)	Initial Volume (ml)	Final Volume (ml)	Essential Oil Volume (ml)
0	0	0	0
10	43.6	42.4	1.2
20	40.3	37.8	2.5
30	30.5	28.1	2.4
40	26.3	24	2.3
50	20	17.7	2.3
60	17.1	14.8	2.3
70	12.9	10.6	2.3

Table 37:Mass loading of 150 g and constant heating power of 1000 W (Run 2)

Time (min)	Initial Volume (ml)	Final Volume (ml)	Essential Oil Volume (ml)
0	0	0	0
10	9.2	7.7	1.5
20	8.7	8.2	2
30	4.2	4.1	2.1
40	6.8	6.6	2.3
50	5.2	5.2	2.3
60	6.1	6.1	2.3
70	4.8	4.8	2.3

Table 38:Mass loading of 150 g and constant heating power of 1000 W (Run 3)

Time (min)	Initial Volume (ml)	Final Volume (ml)	Essential Oil Volume (ml)
0	0	0	0
10	5	3.2	1.8
20	5.2	4.6	2.4
30	5.4	5.4	2.4
40	5.7	5.7	2.4
50	8.1	8.1	2.4
60	6.2	6.2	2.4
70	7.8	7.8	2.4

Table 39:Mass loading of 200 g and constant heating power of 1000 W (Run 1)

Time (min)	Initial Volume (ml)	Final Volume (ml)	Essential Oil Volume (ml)
0	0	0	0
10	35.1	33.3	1.8
20	29.1	25.9	3.2
30	22.1	19	3.1
40	17	13.9	3.1
50	10.4	7.3	3.1
60	5.5	2.4	3.1
70	7.1	4.1	3

Table 40:Mass loading of 200 g and constant heating power of 1000 W (Run 2)

Time (min)	Initial Volume (ml)	Final Volume (ml)	Essential Oil Volume (ml)
0	0	0	0
10	8.5	7.2	1.3
20	8.8	8	2.1
30	8.3	7.7	2.7
40	9.6	9.3	3
50	6.2	6	3.2
60	8.2	8.2	3.2
70	8.9	8.9	3.2

Table 41:Mass loading of 200 g and constant heating power of 1000 W (Run 3)

Time (min)	Initial Volume (ml)	Final Volume (ml)	Essential Oil Volume (ml)
0	0	0	0
10	3.5	2.9	0.6
20	4.5	3.4	1.7
30	4.8	3.6	2.9
40	4.6	4.3	3.2
50	5.1	4.9	3.4
60	6.7	6.7	3.4
70	8.7	8.7	3.4

Data Run 3: Central Composite Design

Table 42: Mass loading of 75 g and heating power of 800 W (Run 1)

Time (min)	Initial Volume (ml)	Final Volume (ml)	Essential Oil Volume (ml)
0	0	0	0
10	5.7	5.6	0.1
20	7.2	6.8	0.5
30	7.5	7.2	0.8
40	9.2	8.9	1.1
50	6.9	6.9	1.1
60	7.3	7.3	1.1
70	8.4	8.4	1.1

Table 43:Mass loading of 178 g and heating power of 800 W (Run 2)

Time (min)	Initial Volume (ml)	Final Volume (ml)	Essential Oil Volume (ml)
0	0	0	0
10	6.6	6.2	0.4
20	9.4	8.2	1.6
30	8	7.2	2.4
40	7.2	6.5	3.1
50	7.3	6.9	3.5
60	7.9	7.7	3.7
70	9.2	9.2	3.7

Table 44:Mass loading of 75 g and heating power of 1200 W (Run 3)

Time (min)	Initial Volume (ml)	Final Volume (ml)	Essential Oil Volume (ml)
0	0	0	0
10	5.8	5.7	0.1
20	7.2	6.2	1.1
30	8.1	8	1.2
40	8.6	8.6	1.2
50	7.2	7.2	1.2
60	9.2	9.2	1.2
70	7.5	7.5	1.2

Table 45:Mass loading of 75 g and heating power of 1200 W (Run 4)

Time (min)	Initial Volume (ml)	Final Volume (ml)	Essential Oil Volume (ml)
0	0	0	0
10	6.9	6.6	0.3
20	8.6	7.5	1.4
30	9.2	7.4	3.2
40	8.6	8.4	3.4
50	5.7	5.6	3.5
60	8.2	8.2	3.5
70	6.5	6.5	3.5

Table 46:Mass loading of 125 g and heating power of 717 W (Run 5)

Time (min)	Initial Volume (ml)	Final Volume (ml)	Essential Oil Volume (ml)
0	0	0	0
10	6.4	4.6	1.8
20	5.7	5.3	2.2
30	4.6	4.4	2.4
40	5.5	5.4	2.5
50	7.7	7.7	2.5
60	8.2	8.2	2.5
70	6.6	6.6	2.5

Table 47:Mass loading of 125 g and heating power of 1400 W (Run 6)

Time (min)	Initial Volume (ml)	Final Volume (ml)	Essential Oil Volume (ml)
0	0	0	0
10	4.6	3.7	0.9
20	5.2	4.1	2
30	5.9	5.8	2.1
40	7	6.9	2.2
50	8.6	8.6	2.2
60	7.3	7.3	2.2
70	9.5	9.5	2.2

Table 48:Mass loading of 50 g and heating power of 1000 W (Run 7)

Time (min)	Initial Volume (ml)	Final Volume (ml)	Essential Oil Volume (ml)
0			0.00
10			0.33
20			0.43
30			0.43
40			0.43
50			0.43
60			0.43
70			0.43

Table 49:Mass loading of 200 g and heating power of 1000 W (Run 8)

Time (min)	Initial Volume (ml)	Final Volume (ml)	Essential Oil Volume (ml)
0			0.00
10			1.23
20			2.33
30			2.90
40			3.10
50			3.23
60			3.23
70			3.23

Table 50:Mass loading of 125 g and heating power of 1000 W (Run 9)

Time (min)	Initial Volume (ml)	Final Volume (ml)	Essential Oil Volume (ml)
0	0	0	0
10	5	3.9	1.1
20	5.2	4.2	2.1
30	4.9	4.8	2.2
40	5.4	5.4	2.2
50	8.1	8.1	2.2
60	7.4	7.4	2.2
70	6.7	6.7	2.2

Table 51:Mass loading of 125 g and heating power of 1000 W (Run 10)

Time (min)	Initial Volume (ml)	Final Volume (ml)	Essential Oil Volume (ml)
0	0	0	0
10	5.2	4.6	0.6
20	5.9	5	1.5
30	4.7	4.6	1.6
40	7.9	7.6	1.9
50	8.2	8.2	1.9
60	9.4	9.4	1.9
70	7.5	7.5	1.9

Data Run : Heating Mantle Calibration

Table 52: Temperature rise as a function of time at heating power of 800 W (Run1)

Time	Temperature
0	18.9
1	21.8
2	25.3
3	29.4
4	34.1
5	38.6
6	41.7
7	46.5
8	49.7
9	53.4
10	58.9
11	61.4
12	65.2
13	70.1
14	70.8

Table 53: Temperature rise as a function of time at heating power of 1000 W (Run1)

Time	Temperature
0	28.8
1	35.4
2	37
4	53.5
5	60
6	66.8
7	73.4
8	80
9	87.6
10	92.7
11	99.1

Table 54:Temperature rise as a function of time at heating power of 1200 W (Run1)

Time	Temperature
0	19.1
1	23.6
2	30.6
3	37.8
4	44.7
5	52.2
6	58.8
7	65.5
8	74.3
9	78.8
10	85.7
11	92.1

Table 55:Temperature rise as a function of time at heating power of 1400 W (Run1)

Time	Temperature
0	18.8
1	22.5
2	29.8
3	37.8
4	46.2
5	54.6
6	60.3
7	68.1
8	76.9
9	83.9
10	87

Table 56:Temperature decrease as a function of time at heating power of 800 W (Run1)

Time	Temperature
15	70.4
16	69.9
17	69.8
18	69.6
19	69.4
20	68.8
21	68.4
22	68.4
23	68.3
24	67.9
25	67.8
26	67.5
27	67.3
28	67.1
29	66.8

Table 57:Temperature decrease as a function of time at heating power of 1000 W (Run1)

Time	Temperature
11	98.9
12	98.6
13	98.4
14	98
15	97.7
16	97.3
17	96.7
18	96.4
19	98
20	95.5
21	95.3
22	94.7

Table 58:Temperature decrease as a function of time at heating power of 1200 W (Run1)

Time	Temperature
11	91.8
12	91.4
13	90.9
14	90.5
15	90.4
16	89.9
17	89.8
18	89.5
19	89.1
20	88.7
21	88.3
22	88.1

Table 59:Temperature decrease as a function of time at heating power of 1400 W (Run1)

Time	Temperature
11	87
12	85.8
13	85.4
14	85.1
15	84.8
16	84.4
17	84.3
18	84.1
19	83.9
20	83.6
21	83.1

Table 60:Temperature rise as a function of time at heating power of 800 W (Run 2)

Time	Temperature
0	18.6
1	22
2	26.1
3	30.1
4	34
5	38.1
6	42.3
7	46.4
8	50.6
9	54.2
10	58.4
11	62.4
12	66
13	70.3
14	73.7

Table 61:Temperature rise as a function of time at heating power of 1000 W (Run 2)

Time	Temperature
0	18.5
1	22.9
2	29
3	36.1
4	43.4
5	50
6	56.5
7	63.4
8	70.2
9	77.2
10	83.4

Table 62:Temperature rise as a function of time at heating power of 1200 W (Run 2)

Time	Temperature
0	19.7
1	23.8
2	30.5
3	38.2
4	45.2
5	52.6
6	60.8
7	66.7
8	74.3
9	81.2
10	87.6

Table 63:Temperature rise as a function of time at heating power of 1400 W (Run 2)

Time	Temperature
0	16.1
1	18.2
2	24.2
3	32.3
4	40.3
5	47.9
6	56.5
7	63.7
8	70.3
9	79.3
10	89

Table 64:Temperature decrease as a function of time at heating power of 800 W (Run2)

Time	Temperature
15	75.3
16	74.8
17	74.1
18	73.8
19	73.7
20	73.7
21	73.3
22	73.1
23	72.8
24	72.5
25	72.4
26	72.1
27	72
28	71.5
29	71.2

Table 65:Temperature decrease as a function of time at heating power of 1000 W (Run2)

Time	Temperature
11	85.6
12	85.5
13	85.3
14	85.2
15	84.9
16	84.6
17	84.3
18	84
19	83.7
20	83.4
21	83.1

Table 66:Temperature decrease as a function of time at heating power of 1200 W (Run2)

Time	Temperature
11	90.5
12	90.5
13	90.1
14	89.9
15	89.7
16	89.2
17	89.1
18	88.8
19	88.5
20	88.1
21	87.8

Table 67:Temperature decrease as a function of time at heating power of 1400 W (Run2)

Time	Temperature
11	92.6
12	92.6
13	92
14	91.7
15	91.4
16	90.9
17	90.5
18	90
19	89.6
20	89
21	88.6

Table 68::Temperature rise as a function of time at heating power of 800 W (Run 3)

Time	Temperature
0	19.3
1	22.2
2	27
3	31.1
4	35.4
5	40.2
6	44.3
7	48.6
8	53
9	57.4
10	61.7
11	66.2
12	70.3

Table 69::Temperature rise as a function of time at heating power of 1000 W (Run 3)

Time	Temperature
0	18.8
1	23.3
2	30.3
3	36.8
4	43.9
5	51.4
6	57.3
7	64
8	70.9
9	77.6
10	84

Table 70:Temperature rise as a function of time at heating power of 1200 W (Run 3)

Time	Temperature
0	20
1	25.1
2	32.3
3	38.6
4	46.7
5	53.8
6	59.8
7	67.1
8	74
9	80.9
10	87.8

Table 71:Temperature rise as a function of time at heating power of 1400 W (Run 3)

Time	Temperature
0	18.8
1	23.5
2	31.4
3	39.5
4	46.9
5	54.6
6	62.4
7	70.3
8	77.2
9	85.2
10	92.6

Table 72: Temperature decrease as a function of time at heating power of 800 W (Run 3)

Time	Temperature
15	80.2
16	80
17	79.7
18	79.5
19	79.3
20	78.9
21	78.7
22	78.5
23	78.2
24	77.8
25	77.7
26	77.4
27	77.1
28	76.8
29	76.6

Table 73:Temperature decrease as a function of time at heating power of 1000 W (Run3)

Time	Temperature
11	85.8
12	85.7
13	85.4
14	85.2
15	84.8
16	84.6
17	84.3
18	84.1
19	83.8
20	83.4
21	83.1

Table 74:Temperature decrease as a function of time at heating power of 1200 W (Run3)

Time	Temperature
11	90.5
12	90
13	90
14	89.7
15	89.4
16	89.1
17	88.9
18	88.6
19	88.2
20	87.9
21	87.6

Table 75:Temperature decrease as a function of time at heating power of 1400 W (Run3)

Time	Temperature
11	94.4
12	94.2
13	93.8
14	93.5
15	93.2
16	92.8
17	92.6
18	92.2
19	91.7
20	91.2
21	90.9

Data Run 4: D-Limonene concentration data

Table 76: D-limonene concentration data obtained from Gas chromatography Flame ionisation detector

Sample No.	**1**	**2**	**3**	**4**	**5**	**6**	**7**	**8**	**9**	**10**
Standard (2-Pentanol) Amount (mg)	34.4	33.7	38.9	23	25.1	36.5	25.1	35.5	27.1	25.4
Standard 2-Pentanol) Area	10702281	10464087	10369292	8683310	7718956	11730906	7580049	9562696	8083591	7420216
D-Limonene Area	20704906	34324477	1923501	34487092	30481550	32198542	21693141	22726188	29818987	25612283
D-Limonene Amount (mg)	52.95373	87.95766	5.741615	72.68424	78.86665	79.71475	57.15646	67.12986	79.54246	69.76003
Sample No.	**11**	**12**	**13**	**14**	**15**	**16**	**17**	**18**	**19**	**20**
Standard (2-Pentanol) Amount (mg)	30.6	28.9	29.9	31.2	36.5	25.1	34.3	29.6	28.6	37.1
Standard 2-Pentanol) Area	10603236	9570135	10822710	11091134	14703907	9775278	17556012	12385568	13586290	15321608
D-Limonene Area	2101145	30318424	635466	28977941	28494989	30700585	0	22924014	31532039	23207677
D-Limonene Amount (mg)	4.82481	72.84967	1.396911	64.86155	56.28203	62.72381	0	43.59208	52.81513	44.71388
Sample No.	**21**	**22**	**23**	**24**	**25**	**26**	**27**	**28**	**29**	**30**
Standard (2-Pentanol) Amount (mg)	29.8	32.1	29.6	28	24.4	37.6	23.8	34.8	30.5	38.2
Standard 2-Pentanol) Area	14628918	14125356	13928633	12691548	11709324	15016451	13753544	13753544	8895337	10453897
D-Limonene Area	874203	29848648	27910939	29334758	28191917	26300070	0	28759197	28950770	30267687
D-Limonene Amount (mg)	1.41696	53.97237	47.19531	51.49524	46.74377	52.39847	0	57.90053	78.98393	88.00464

data highlighted in red was discarded and not considered in any calculations

Data run 5: Moisture content

Table 77: Moisture content runs

Run Number	**Run 1**	**Run 2**	**Run 3**	**Average**
Solid's content (%)	15.570	15.320	20.420	17.1± 2.3
Moisture content (%)				82.9± 2.3
Mass of Clementine peel used (g)	0.501	0.111	0.098	

Data Run 4: D-Limonene concentration data

Data obtained from the analytical department

Appendix C. Processed Data

Data run 1: Single-factor Runs

Table 78: Average Yield data at a mass loading of 150g and heating power of 800W.

Time (min)	Essential Oil Volume (ml)	Yield (ml/g)	%	Standard deviation
0	0.00	0.000		
10	0.60	0.004	0.40	0.14
20	1.00	0.007	0.67	0.14
30	1.40	0.009	0.93	0.09
40	1.80	0.012	1.20	0.05
50	1.93	0.013	1.29	0.11
60	1.97	0.013	1.31	0.13
70	1.97	0.013	1.31	0.13

Table 79: Average Yield data at a mass loading of 150g and heating power of 1000W.

Time (min)	Essential Oil Volume (ml)	Yield (ml/g)	%	Standard deviation
0	0.00	0		
10	1.10	0.007	0.73	0.34
20	1.80	0.012	1.20	0.43
30	2.27	0.015	1.51	0.27
40	2.50	0.017	1.67	0.14
50	2.60	0.017	1.73	0.11
60	2.60	0.017	1.73	0.11
70	2.60	0.017	1.73	0.11

Table 80: Average Yield data at a mass loading of 150g and heating power of 1200W.

Time (min)	Essential Oil Volume (ml)	Yield (ml/g)	%	Standard deviation
0	0	0		
10	1.27	0.008	0.84	0.31
20	2.03	0.014	1.36	0.22
30	2.17	0.014	1.44	0.17
40	2.20	0.015	1.47	0.14
50	2.20	0.015	1.47	0.14
60	2.20	0.015	1.47	0.14
70	2.20	0.015	1.47	0.14

Table 81: Average Yield data at a mass loading of 150g and heating power of 1400W.

Time (min)	Essential Oil Volume (ml)	Yield (ml/g)	%	Standard deviation
0	0	0.0000	0	0
10	0.37	0.0024	0.24	0.17
20	1.07	0.0071	0.71	0.22
30	1.33	0.0089	0.89	0.21
40	1.40	0.0093	0.93	0.14
50	1.40	0.0093	0.93	0.14
60	1.40	0.0093	0.93	0.14
70	1.40	0.0093	0.93	0.14

Table 82: Average Yield data at a mass loading of 50g and heating power of 1000W.

Time (min)	Essential Oil Volume (ml)	Yield (ml/g)	%	Standard deviation
0	0.00	0.0000	0.00	0.00
10	0.33	0.0067	0.67	0.31
20	0.43	0.0087	0.87	0.31
30	0.43	0.0087	0.87	0.31
40	0.43	0.0087	0.87	0.31
50	0.43	0.0087	0.87	0.31
60	0.43	0.0087	0.87	0.31
70	0.43	0.0087	0.87	0.31

Table 83: Average Yield data at a mass loading of 100g and heating power of 1000W.

Time (min)	Essential Oil Volume (ml)	Yield (ml/g)	%	Standard deviation
0	0	0.000	0.00	0
10	0.90	0.009	0.90	0.44
20	1.33	0.013	1.33	0.15
30	1.37	0.014	1.37	0.12
40	1.37	0.014	1.37	0.12
50	1.37	0.014	1.37	0.12
60	1.40	0.014	1.40	0.10
70	1.40	0.014	1.40	0.10

Table 84: Average Yield data at a mass loading of 150g and heating power of 1000W.

Time (min)	Essential Oil Volume (ml)	Yield (ml/g)	%	Standard deviation
0	0.00	0.000	0.00	0.00
10	1.50	0.010	1.00	0.16
20	2.30	0.015	1.53	0.14
30	2.30	0.015	1.53	0.09
40	2.33	0.016	1.56	0.03
50	2.33	0.016	1.56	0.03
60	2.33	0.016	1.56	0.03
70	2.33	0.016	1.56	0.03

Table 85: Average Yield data at a mass loading of 200g and heating power of 1000W.

Time (min)	Essential Oil Volume (ml)	Yield (ml/g)	%	
0	0.00	0.000	0.00	0.00
10	1.23	0.006	0.62	0.25
20	2.33	0.012	1.17	0.32
30	2.90	0.015	1.45	0.08
40	3.10	0.016	1.55	0.04
50	3.23	0.016	1.62	0.06
60	3.23	0.016	1.62	0.06
70	3.20	0.016	1.60	0.08

Data run 1: Kinetic modelling data for Single factor experiments

Table 86: Kinetic modelling at 1000 W heating power & 50 g mass loading(Run 1)

Run 1	50 g and 1000W
Average yield(%) (ml/g)	0.625
Equilibrium yield(%) (ml/g)	0.732
Process constant	0.196
Sum of square error (SSD)	0.057
The total sum of squares (SST)	0.515
the sum of Squared regression (SSR)	0.456
Coefficient of Determination(R^2)	0.885

Table 87: Kinetic modelling at 1000 W heating power & 50 g mass loading(Run 2)

Run 2	50 g and 1000W
Average yield(%) (ml/g)	0.55
Equilibrium yield(%) (ml/g)	0.7240
Process constant	0.0720
Sum of square error (SSD)	0.0364
The total sum of squares (SST)	0.460
the sum of Squared regression (SSR)	0.440
Coefficient of Determination(R^2)	0.956

Table 88: Kinetic modelling at 1000 W heating power & 50 g mass loading(Run 1)

Run 3	50 g and 1000W
Average yield(%) (ml/g)	1.025
Equilibrium yield(%) (ml/g)	1.2050
Process constant	0.1814
Sum of square error (SSD)	0.0009
The total sum of squares (SST)	1.235
the sum of Squared regression (SSR)	1.233
Coefficient of Determination(R^2)	0.998

Table 89: Kinetic modelling at 1000 W heating power & 100 g mass loading(Run 1)

Run 1	100 g and 1000W
Average yield(%) (ml/g)	1.0375
Equilibrium yield(%) (ml/g)	1.442
Process constant	0.060
Sum of square error (SSD)	0.115
The total sum of squares (SST)	1.979
the sum of Squared regression (SSR)	1.720
Coefficient of Determination(R^2)	0.869

Table 90:Kinetic modelling at 1000 W heating power & 100 g mass loading(Run 2)

Run 2	100 g and 1000W
Average yield(%) (ml/g)	1.1125
Equilibrium yield(%) (ml/g)	1.305
Process constant	0.189
Sum of square error (SSD)	0.001
The total sum of squares (SST)	1.449
the sum of Squared regression (SSR)	1.447
Coefficient of Determination(R^2)	0.999

Table 91: Kinetic modelling at 1000 W heating power & 100 g mass loading(Run 3)

Run 3	100 g and 1000W
Average yield(%) (ml/g)	1.275
Equilibrium yield(%) (ml/g)	1.509
Process constant	0.165
Sum of square error (SSD)	0.003
The total sum of squares (SST)	1.935
the sum of Squared regression (SSR)	1.928
Coefficient of Determination(R^2)	0.996

Table 92: Kinetic modelling at 1000 W heating power & 150 g mass loading(Run 1)

Run 1	150 g and 1000W
Average yield(%) (ml/g)	1.275
Equilibrium yield(%) (ml/g)	1.589
Process constant	0.103
Sum of square error (SSD)	0.143
The total sum of squares (SST)	2.377
the sum of Squared regression (SSR)	2.131
Coefficient of Determination(R^2)	0.897

Table 93: Kinetic modelling at 1000 W heating power & 150 g mass loading(Run 2)

Run 2	150 g and 1000W
Average yield(%) (ml/g)	1.23333
Equilibrium yield(%) (ml/g)	1.5311
Process constant	0.1026
Sum of square error (SSD)	0.0049
The total sum of squares (SST)	1.973
the sum of Squared regression (SSR)	1.978
Coefficient of Determination(R^2)	1.003

Table 94: Kinetic modelling at 1000 W heating power & 150 g mass loading(Run 3)

Run 3	150 g and 1000W
Average yield(%) (ml/g)	1.35
Equilibrium yield(%) (ml/g)	1.6141
Process constant	0.1450
Sum of square error (SSD)	0.0075
The total sum of squares (SST)	2.220
the sum of Squared regression (SSR)	2.201
Coefficient of Determination(R^2)	0.992

Table 95: Kinetic modelling at 1000 W heating power & 200 g mass loading(Run 1)

Run 1	200 g and 1000W
Average yield(%) (ml/g)	1.275
Equilibrium yield(%) (ml/g)	1.5744
Process constant	0.1091
Sum of square error (SSD)	0.0700
The total sum of squares (SST)	2.225
the sum of Squared regression (SSR)	2.092
Coefficient of Determination(R^2)	0.940

Table 96: Kinetic modelling at 1000 W heating power & 200 g mass loading(Run 2)

Run 2	200 g and 1000W
Average yield(%) (ml/g)	1.16875
Equilibrium yield(%) (ml/g)	1.6927
Process constant	0.0508
Sum of square error (SSD)	0.0068
The total sum of squares (SST)	2.350
the sum of Squared regression (SSR)	2.309
Coefficient of Determination(R^2)	0.983

Table 97: Kinetic modelling at 1000 W heating power & 200 g mass loading(Run 3)

Run 3	200 g and 1000W
Average yield(%) (ml/g)	1.1625
Equilibrium yield(%) (ml/g)	2.038
Process constant	0.032
Sum of square error (SSD)	0.155
The total sum of squares (SST)	3.334
the sum of Squared regression (SSR)	2.845
Coefficient of Determination(R^2)	0.853

Table 98: Kinetic modelling at 800 W heating power & 150 g mass loading(Run 1)

Run 1	150 g and 800W
Average yield(%) (ml/g)	0.825
Equilibrium yield(%) (ml/g)	1.215
Process constant	0.0481
Sum of square error (SSD)	0.0158
The total sum of squares (SST)	1.199
the sum of Squared regression (SSR)	1.176
Coefficient of Determination(R^2)	0.980

Table 99: Kinetic modelling at 800 W heating power & 150 g mass loading(Run 2)

Run 2	150 g and 800W
Average yield(%) (ml/g)	0.967
Equilibrium yield(%) (ml/g)	1.515
Process constant	0.0402
Sum of square error (SSD)	0.00401
The total sum of squares (SST)	1.724
the sum of Squared regression (SSR)	1.735
Coefficient of Determination(R^2)	1.006

Table 100: Kinetic modelling at 800 W heating power & 150 g mass loading(Run 3)

Run 3	150 g and 800W
Average yield(%) (ml/g)	0.875
Equilibrium yield(%) (ml/g)	2.218
Process constant	0.0168
Sum of square error (SSD)	0.119
The total sum of squares (SST)	2.368
the sum of Squared regression (SSR)	2.015
Coefficient of Determination(R^2)	0.851

Table 101: Kinetic modelling at 1000 W heating power & 150 g mass loading(Run 1)

Run 1	150 g and 1000W
Average yield(%) (ml/g)	1.542
Equilibrium yield(%) (ml/g)	1.894
Process constant	0.112
Sum of square error (SSD)	0.0206
The total sum of squares (SST)	3.088
the sum of Squared regression (SSR)	3.027
Coefficient of Determination(R^2)	0.980

Table 102: Kinetic modelling at 1000 W heating power & 150 g mass loading(Run 2)

Run 2	150 g and 1000W
Average yield(%) (ml/g)	1.142
Equilibrium yield(%) (ml/g)	2.208
Process constant	0.0260
Sum of square error (SSD)	0.0614
The total sum of squares (SST)	3.177
the sum of Squared regression (SSR)	2.929
Coefficient of Determination(R^2)	0.922

Table 103: Kinetic modelling at 1000 W heating power & 150 g mass loading(Run 3)

Run 3	150 g and 1000W
Average yield(%) (ml/g)	1.183
Equilibrium yield(%) (ml/g)	1.725
Process constant	0.0502
Sum of square error (SSD)	0.0492
The total sum of squares (SST)	2.549
the sum of Squared regression (SSR)	2.393
Coefficient of Determination(R^2)	0.939

Table 104: Kinetic modelling at 1200 W heating power & 150 g mass loading(Run 1)

Run 1	150 g and 1200W
Average yield(%) (ml/g)	1.308
Equilibrium yield(%) (ml/g)	1.752
Process constant	0.0702
Sum of square error (SSD)	0.227
The total sum of squares (SST)	3.039
the sum of Squared regression (SSR)	2.574
Coefficient of Determination(R^2)	0.847

Table 105: Kinetic modelling at 1200 W heating power & 150 g mass loading(Run 2)

Run 2	150 g and 1200W
Average yield(%) (ml/g)	1.050
Equilibrium yield(%) (ml/g)	1.360
Process constant	0.0795
Sum of square error (SSD)	0.00302
The total sum of squares (SST)	1.571
the sum of Squared regression (SSR)	1.557
Coefficient of Determination(R^2)	0.991

Table 106: Kinetic modelling at 1200 W heating power & 150 g mass loading(Run 3)

Run 3	150 g and 1200W
Average yield(%) (ml/g)	1.208
Equilibrium yield(%) (ml/g)	1.402
Process constant	0.2352
Sum of square error (SSD)	0.000134
The total sum of squares (SST)	1.684
the sum of Squared regression (SSR)	1.684
Coefficient of Determination(R^2)	1.000

Table 107: Kinetic modelling at 1400 W heating power & 150 g mass loading(Run 1)

Run 1	150 g and 1400W
Average yield(%) (ml/g)	0.525
Equilibrium yield(%) (ml/g)	0.817
Process constant	0.0419
Sum of square error (SSD)	0.0136
The total sum of squares (SST)	0.564
the sum of Squared regression (SSR)	0.513
Coefficient of Determination(R^2)	0.909

Table 108:Kinetic modelling at 1400 W heating power & 150 g mass loading(Run 2)

Run 2	150 g and 1400W
Average yield(%) (ml/g)	0.758
Equilibrium yield(%) (ml/g)	1.239
Process constant	0.0385
Sum of square error (SSD)	0.175
The total sum of squares (SST)	1.537
the sum of Squared regression (SSR)	1.144
Coefficient of Determination(R^2)	0.744

Table 109: Kinetic modelling at 1400 W heating power & 150 g mass loading(Run 3)

Run 3	150 g and 1400W
Average yield(%) (ml/g)	0.808
Equilibrium yield(%) (ml/g)	1.0329
Process constant	0.0877
Sum of square error (SSD)	0.0437
The total sum of squares (SST)	0.991
the sum of Squared regression (SSR)	0.900
Coefficient of Determination(R^2)	0.909

Kinetic modelling for Central composite design data:

Table 110: Kinetic modelling at 800 W heating power & 72 g mass loading(Run 1)

Run 1: 800 W heating power & 72 g mass loading	
Average yield(%) (ml/g)	1.01
Equilibrium yield(%) (ml/g)	2.031
Process constant	0.025
Sum of square error (SSD)	0.199
The total sum of squares (SST)	2.961
the sum of Squared regression (SSR)	2.390
Coefficient of Determination(R^2)	0.807

Table 111:Kinetic modelling at 800 W heating power & 178 g mass loading(Run 2)

Run 2 : 800 W heating power & 178 g mass loading	
Average yield(%) (ml/g)	1.292
Equilibrium yield(%) (ml/g)	3.045
Process constant	0.019
Sum of square error (SSD)	0.145
The total sum of squares (SST)	4.860
the sum of Squared regression (SSR)	4.246
Coefficient of Determination(R^2)	0.873

Table 112: Kinetic modelling at 1200 W heating power & 72 g mass loading(Run 3)

Run 3: 1200 W heating power & 72 g mass loading	
Average yield(%) (ml/g)	1.25
Equilibrium yield(%) (ml/g)	1.823
Process constant	0.053
Sum of square error (SSD)	0.556
The total sum of squares (SST)	3.742
the sum of Squared regression (SSR)	2.702
Coefficient of Determination(R^2)	0.722

Table 113: Kinetic modelling at 1200 W heating power & 178 g mass loading(Run 4)

Run 4: 1200 W heating power & 178 g mass loading	
Average yield(%) (ml/g)	1.320
Equilibrium yield(%) (ml/g)	2.512
Process constant	0.028
Sum of square error (SSD)	0.514
The total sum of squares (SST)	5.182
the sum of Squared regression (SSR)	3.963
Coefficient of Determination(R^2)	0.765

Table 114: Kinetic modelling at 717 W heating power & 125 g mass loading(Run 5)

Run 5: 717 W heating power & 125 g mass loading	
Average yield(%) (ml/g)	1.64
Equilibrium yield(%) (ml/g)	1.993
Process constant	0.122
Sum of square error (SSD)	0.006
The total sum of squares (SST)	3.341
the sum of Squared regression (SSR)	3.353
Coefficient of Determination(R^2)	1.004

Table 115: Kinetic modelling at 1283 W heating power & 125 g mass loading(Run 6)

Run 6: 1283 W heating power & 125 g mass loading	
Average yield(%) (ml/g)	1.38
Equilibrium yield(%) (ml/g)	1.826
Process constant	0.073
Sum of square error (SSD)	0.100
The total sum of squares (SST)	3.056
the sum of Squared regression (SSR)	2.799
Coefficient of Determination(R^2)	0.916

Table 116:Kinetic modelling 1000 W heating power & 50 g mass loading (Run 7)

Run 7: 1000 W heating power & 50 g mass loading	
Average yield(%) (ml/g)	
Equilibrium yield(%) (ml/g)	0.873
Process constant	0.152
Sum of square error (SSD)	0.002
The total sum of squares (SST)	0.649
the sum of Squared regression (SSR)	0.645
Coefficient of Determination(R^2)	0.994

Table 117:Kinetic modelling 1000 W heating power & 200 g mass loading(Run 8)

Run 8: 1000 W heating power & 200 g mass loading	
Average yield(%) (ml/g)	0.733
Equilibrium yield(%) (ml/g)	1.702
Process constant	0.056
Sum of square error (SSD)	0.022
The total sum of squares (SST)	2.487
the sum of Squared regression (SSR)	2.372
Coefficient of Determination(R^2)	0.954

Table 118: Kinetic modelling at 1000 W heating power & 125 g mass loading(Run 9)

Run 9: 1000 W heating power & 125 g mass loading	
Average yield(%) (ml/g)	1.42
Equilibrium yield(%) (ml/g)	1.811
Process constant	0.088
Sum of square error (SSD)	0.076
The total sum of squares (SST)	2.954
the sum of Squared regression (SSR)	2.767
Coefficient of Determination(R^2)	0.937

Table 119: Kinetic modelling at 1000 W heating power & 125 g mass loading (Run 9)

Run 10: 1000 W heating power & 125 g mass loading	
Average yield(%) (ml/g)	1.13
Equilibrium yield(%) (ml/g)	1.617
Process constant	0.054
Sum of square error (SSD)	0.069
The total sum of squares (SST)	2.335
the sum of Squared regression (SSR)	2.130
Coefficient of Determination(R^2)	0.912

Heating mantle calibration processed data:

Table 120: Gradient used to calculate the rate of heating at 800W (Run 1)

800W RUN 1	Heating
Gradient, $\frac{\dot{Q}}{mc_p}$	3.90
y-intercept	18.40
Sum of square error	11.06

Table 121: Gradient used to calculate the rate of heating at 1000W (Run 1)

1000W	RUN 1
Gradient, $\frac{\dot{Q}}{mc_p}$	6.55
y-intercept	27.40
Sum of square error	18.13

Table 122: Gradient used to calculate the rate of heating at 1200W (Run 1)

1200W	RUN 1
Gradient, $\frac{\dot{Q}}{mc_p}$	6.86
y-intercept	17.63
Sum of square error	7.72

Table 123: Gradient used to calculate the rate of heating at 1400W (Run 1)

14000W	RUN 1
Gradient, $\frac{\dot{Q}}{mc_p}$	7.30
y-intercept	16.78
Sum of square error	24.46

Table 124: : Gradient used to calculate the rate of cooling at 800W (Run 1)

800W RUN 1	Cooling
Gradient, $\frac{\dot{Q}}{mc_p}$	0.25
y-intercept	73.96
Sum of square error	0.27

Table 125: Gradient used to calculate the rate of cooling at 1000W (Run 1)

1000W RUN 1	Cooling
Gradient, $\frac{\dot{Q}}{mc_p}$	0.33
y-intercept	102.55
Sum of square error	3.82

Table 126: Gradient used to calculate the rate of cooling at 1200W (Run 1)

1200W RUN 1	Cooling
Gradient, $\frac{\dot{Q}}{mc_p}$	0.33
y-intercept	95.28
Sum of square error	0.12

Table 127:Gradient used to calculate the rate of cooling at 1400W (Run 1)

1400W RUN 1	Cooling
Gradient, $\frac{\dot{Q}}{mc_p}$	0.32
y-intercept	89.81
Sum of square error	0.85

Table 128: : Gradient used to calculate the rate of heating at 800W (Run 2)

800W RUN 2	Heating
Gradient, $\frac{\dot{Q}}{mc_p}$	3.99
y-intercept	18.27
Sum of square error	0.84

Table 129: Gradient used to calculate the rate of heating at 1000W (Run 2)

1000W RUN 2	Heating
Gradient, $\frac{\dot{Q}}{mc_p}$	6.66
y-intercept	16.74
Sum of square error	5.20

Table 130: Gradient used to calculate the rate of heating at 1200W (Run 2)

1200W RUN 2	Heating
Gradient, $\frac{\dot{Q}}{mc_p}$	7.03
y-intercept	17.64
Sum of square error	8.43

Table 131: Gradient used to calculate the rate of heating at 1400W (Run 2)

1400W RUN 2	Heating
Gradient, $\frac{\dot{Q}}{mc_p}$	7.51
y-intercept	11.34
Sum of square error	40.356

Table 132: Gradient used to calculate the rate of cooling at 800W (Run 2)

800W RUN 2	Cooling
Gradient, $\frac{\dot{Q}}{mc_p}$	0.26
y-intercept	78.79
Sum of square error	0.47

Table 133: Gradient used to calculate the rate of cooling at 1000W (Run 2)

1000W RUN 2	Cooling
Gradient, $\frac{\dot{Q}}{mc_p}$	0.26
y-intercept	88.68
Sum of square error	0.12

Table 134: Gradient used to calculate the rate of cooling at 1200W (Run 2)

1200W RUN 2	Cooling
Gradient, $\frac{\dot{Q}}{mc_p}$	0.28
y-intercept	93.75
Sum of square error	0.10

Table 135: Gradient used to calculate the rate of cooling at 1400W (Run 2)

1400W RUN 2	Cooling
Gradient, $\frac{\dot{Q}}{mc_p}$	0.42
y-intercept	97.48
Sum of square error	0.20

Table 136: : Gradient used to calculate the rate of heating at 800W (Run 3)

800W RUN 3	Heating
Gradient, $\frac{\dot{Q}}{mc_p}$	4.32
y-intercept	18.44
Sum of square error	1.40

Table 137: Gradient used to calculate the rate of heating at 1000W (Run 3)

1000W RUN 3	Heating
Gradient, $\frac{\dot{Q}}{mc_p}$	6.66
y-intercept	17.45
Sum of square error	3.65

Table 138: Gradient used to calculate the rate of heating at 1200W (Run 3)

1200W RUN 3	Heating
Gradient, $\frac{\dot{Q}}{mc_p}$	6.89
y-intercept	18.85
Sum of square error	3.17

Table 139: Gradient used to calculate the rate of heating at 1400W (Run 3)

1400W RUN 3	Heating
Gradient, $\frac{\dot{Q}}{mc_p}$	7.55
y-intercept	17.02
Sum of square error	5.29

Table 140: Gradient used to calculate the rate of cooling at 800W (Run 3)

800W RUN 3	Cooling
Gradient, $\frac{\dot{Q}}{mc_p}$	0.26
y-intercept	84.19
Sum of square error	0.04

Table 141: Gradient used to calculate the rate of cooling at 1000W (Run 3)

1000W RUN 3	Cooling
Gradient, $\frac{\dot{Q}}{mc_p}$	0.27
y-intercept	88.95
Sum of square error	0.05

Table 142: Gradient used to calculate the rate of cooling at 1200W (Run 3)

1200W RUN 3	Cooling
Gradient, $\frac{\dot{Q}}{mc_p}$	0.28
y-intercept	93.59
Sum of square error	0.08

Table 143: Gradient used to calculate the rate of cooling at 1400W (Run 3)

1400W RUN 3	Cooling
Gradient, $\frac{\dot{Q}}{mc_p}$	0.35
y-intercept	98.45
Sum of square error	0.11

Table 144: Physical data of water used to determine rate of heat trasnferred to/from the water obtained from (Perry, 1984)

Water heat capacity	J/kg.K	4182
Volume of water	L	2
Density of water	kg/m3	998
Mass of water	kg	1.996
Seconds in 1 minute	seconds	60

Table 145: The actual power at the induction cooker power ratings for 800W, 1000W, 1200 W and 1400 W.

Power Rating	Gradient	Power (J/s)
800	3.814	531
1000	6.340	882
1200	6.628	922
1400	7.088	986

D-Limonene concentration data

Table 146: D-Limonene concentration at the various heating power and mass loading conditions

Run #	Heating power, X_1	Mass loading X_2	D-Limonene amount (mg)			Average amount (mg)	Standard deviation	Volume of essential oil (ml)	mg/ml
1	800	72	52.95			52.95	0.00	1.10	48.14
2	800	178	87.96	72.85	53.97	71.59	13.90	3.70	19.35
3	1200	72			47.20	47.20	0.00	1.20	39.33
4	1200	178	72.68	64.86	51.50	63.01	8.75	3.50	18.00
5	717	125	78.87	56.28	46.74	60.63	13.47	2.50	24.25
6	1283	125	79.71	62.72	52.40	64.95	11.26	2.20	29.52
7	1000	50	57.16			57.16	0.00	0.43	131.78
8	1000	200	67.13	43.59	57.90	56.21	9.68	3.23	17.39
9	1000	125	79.54	52.82	78.98	70.45	12.47	2.20	32.02
10	1000	125	69.76	44.71	88.00	67.49	17.75	1.90	35.52

GC Analysis

The calibration is the ratio of the signal (peak area) of the analyte over the signal (peak area) of internal standard versus the amount ratios of analyte to internal standard for a known range of standard amounts. This is referred to as a ratio calibration (Figure 1). When analysing the sample, a known weight of internal standard is added to the sample. The amount of analyte can then be calculated from the calibration graph since the peak areas are obtained from the chromatogram and the amount of the analyte is the only unknown. The amount of analyte is then calculated from the regression line formulae. Note: It is not necessary to measure the amount of solvent used in preparing the samples, since the ratio of the analyte to internal standard is fixed and will remain fixed when diluting the sample with solvent. Only the internal standard and the sample mass added to the solvent should be accurately weighed and recorded in your notebook.

Standard preparation method

1. Accurately weigh 30 µl of the internal standard into a 2ml vial. Use a 4- or 5-decimal balance. Record weight.
2. Accurately weigh 10 µl of each compound into the same vial and record the weight for each component added.
3. Add ± 1.5 ml of solvent (analytical grade methanol). This weight does not have to be recorded.
4. Cap the vial and mix well.
5. Pipette 100µl of the mixture from the first vial into a 2nd vial. (Dilution)
6. Add ± 1.5ml of solvent (analytical grade methanol) to the 2nd vial and mix.
7. The above steps describe the preparation of Standard #1. Repeat the steps for the rest of the standards.

Sample preparation method

1. Accurately weigh 30 µl of the internal standard into a 2ml vial. Use a 4- or 5-decimal balance. Record weight.
2. Accurately weigh 80 µl of sample into the same vial. Record weight.
3. Add ± 1.5ml of solvent (analytical grade methanol).
4. Cap the vial and mix well.
5. Pipette 100µl of the mixture from the first vial into a 2nd vial. (Dilution)
6. Add ± 1.5ml of solvent to the 2nd vial and mix.
7. Submit the 2nd set of sample vials for GC analysis; send the internal standard weights added to each sample to the analyst.

General Notes:

- Weigh the least volatile components first.
- Weigh volatile solvents in capped vials ◊ Tare the balance with the capped vial, quickly remove the cap and add sample, cap immediately and weigh again, etc.

- Use new septa for your sample vials when working with volatile solvents.
- The weights are critical and must be accurate; the volume of solvent added is approximate quantities since an internal standard calibration (calibration with ratios) is used.
- The results will be in mg. Since the initial weight of the samples is known, percentage weight or molar ratios can be calculated.

Calibration curve

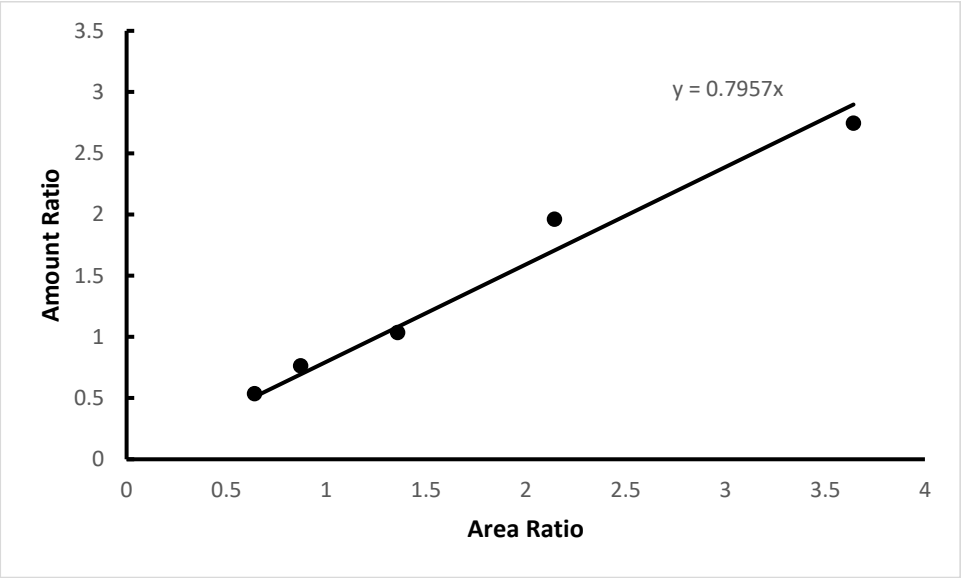

Figure 24: Calibration curve used to determine the mass of D-limonene present in the samples

Table 147: GC-FID results used for the calibration curve

	Amount ratio	Area ratio
Level 1	0.53617	0.640249
Level 2	0.762931	0.871697
Level 3	1.03356	1.35799
Level 4	1.96087	2.14356
Level 5	2.744	3.64216

The calibration curve is used to determine the composition of D-Limonene (expressed in milligrams) present in the analysed samples. When the samples are sent, the mass of the internal standard(which in this case was 2-Pentanol) must also be attached. The resulting data from the Gas Chromatography-Flame Ionisation Detector will be expressed in terms of Area. Knowing these areas, the mass of internal standard added to the sample and the calibration curve slope, the composition of D-limonene is calculated using:

$$limonene\ amount(mg) = \frac{Limonene\ Area}{Standard\ Area} * Standard\ amount(mg) * Calibration\ curve\ slope$$

Appendix D. Typical Calculations

Required mass for each run

$$Mass\ of\ citrus\ peel = citrus\ peel + water$$

Mass of citrus peel required for 50 g, 100 g, 150 g and 200 g dry citrus peel mass:

Measured moisture content:

$$water\ content = 82.9\ \%$$

$$solids\ content = 100 - 82.9\ \% = 17.1\%$$

The mass required for 50 g:

$$Mass\ required\ for\ 50\ g = 50\ g * \frac{100}{solids\ content(\%)}$$

$$Mass\ required\ for\ 50\ g = 50\ g * \frac{100}{17.1} = 292.4g$$

The mass required for 100 g:

$$Mass\ required\ for\ 100\ g = 100\ g * \frac{100}{17.1} = 584.8g$$

The mass required for 150 g:

$$Mass\ required\ for\ 150\ g = 150\ g * \frac{100}{17.1} = 877.2g$$

The mass required for 200 g:

$$Mass\ required\ for\ 200\ g = 200\ g * \frac{100}{17.1} = 1169.6g$$

For each run, the volume of extracted essential oil is measured every 10 minutes for 70 minutes. The volume is measured in ml.

Essential Oil yield

$$Yield(\%) = \frac{volume\ of\ Essential\ oil\ collected\ (ml)}{Dry\ mass\ of\ citrus\ peel\ added(g)} * 100$$

$$Dry\ mass\ of\ citrus\ peel\ added = \frac{Mass\ of\ citrus\ peel\ added}{100} * solids\ content(\%)$$

Example: mass loading of 50g

Time (min)	Initial Volume (ml)	Final Volume (ml)	Essential Oil Volume (ml)
10	37.7	37	0.7

$$Volume\ of\ Essential\ oil\ collected\ (ml) = 37.7 - 37 = 0.7\ ml$$

$$Dry\ mass\ of\ citrus\ peel\ added(g) = 50g$$

$$Yield(\%) = \frac{volume\ of\ Essential\ oil\ collected\ (ml)}{Dry\ mass\ of\ citrus\ peel\ added(g)} * 100 = \frac{0.7}{50} * 100$$

$$Yield(\%) = 1.4\ \%$$

Model fitting

The model fitting was executed using Microsoft excel, the model parameters and constants are obtained by minimising the sum of the square difference between the theoretical and actual yield of Essential oil at the relevant time point.

$$Sum\ of\ Square\ Error(SSE) = \sum_{t=o}^{t=70} (y_{actual} - y_{model})^2$$

Evaluating the model fit:

The model fit is evaluated using the coefficient of determination, R^2.

$$R^2 = \frac{SSR}{SST}$$

$$SSR = \sum_{i} (\hat{y_i} - \bar{y})^2$$

$$SST = \sum_{i} (y_i - \bar{y})^2$$

SSR is the sum of Squared regression which is known as the variation explained by the model.

SST is the total variation in the data also known as the sum of the squared total.

y_i is the predicted value of y for observation i

$\bar{y}$ is the mean of value y

y_i is the y value for observation i.

If the fit is good, R^2 is close to 1.

Calibration of the Induction Cooker (Heating mantle)

The amount of heat gained or lost by a sample is given by the formula:

$$Q(J) = mc_p\Delta T$$

In the calibration experimental runs, the mass of water added was kept constant by using a volume of 2L which is 1.996 kg.

The heat capacity of water, c_p is 4182 J/kg.K.

Since the goal is to calculate the heat gain rate(Power), the above formula is divided by time to yield:

$$\frac{Q}{t}\left(\frac{J}{s}\right) = \frac{mc_p\Delta T}{t}$$

Plotting the change in temperature as a function yields a straight line of the form:

$$y = mx + c$$

Rearranging the calorimetric equation into the form of temperature as a function of time yield:

$$\Delta T = \frac{\dot{Q}}{mc_p} * t$$

The gradient of the above equation is used to calculate the heating power at the specified induction cooker heat rating.

$$\frac{\dot{Q}}{mc_p} = gradient$$

$$\dot{Q} = mc_p * gradient$$

1000W: Heating			
Run 1			
Time (min)	Temperature (°C)	Theoretical (°C)	Square error
0	28.8	27.40	1.96
1	35.4	33.95	2.09
2	37	40.51	12.31
4	53.5	53.62	0.01
5	60	60.17	0.03
6	66.8	66.72	0.01
7	73.4	73.28	0.01
8	80	79.83	0.03
9	87.6	86.39	1.48
10	92.7	92.94	0.06
11	99.1	99.49	0.15

The y-intercept of the plot of temperature against time is calculated by fitting this data to a straight-line equation and using goal seek solver in excel. In solver, the parameters are obtained by minimising the sum of square error between the experimental and calculated data. The results from goal seek solver are in the table below:

m	6.55
c	27.40
SSD	18.13

With the intercept known, the next step is calculating the heating power:

$$\dot{Q} = mc_p * intercept = 6.55\frac{\mathrm{K}}{min} * \ 1.996\ \mathrm{kg} * 4182\frac{\mathrm{J}}{\mathrm{kg.\,K}} * \frac{1\ min}{60 seconds}$$

$$\dot{Q} = 911\frac{J}{s}$$

The same procedure is followed for the cooling down process of the heated water.

Determining D-Limonene concentration

The Example used in the sample calculations is for Sample 10(1000W and 125 dry mass):

Internal Standard Report

Data File:	C:\ChromQuest\Enterprise\Projects\Default\Data\Jaco 2022\10_272022\Sample 010 27102022.dat
Method:	C:\ChromQuest\Enterprise\Projects\Default\Method\Limonene-test-2021.met
Acquired:	2022/10/27 13:26:39
Printed:	2022/10/28 10:35:25

Sample Name:	Sample 010
Sample Amt:	1
Internal Std. Amt:	25.4
Multiplier:	1

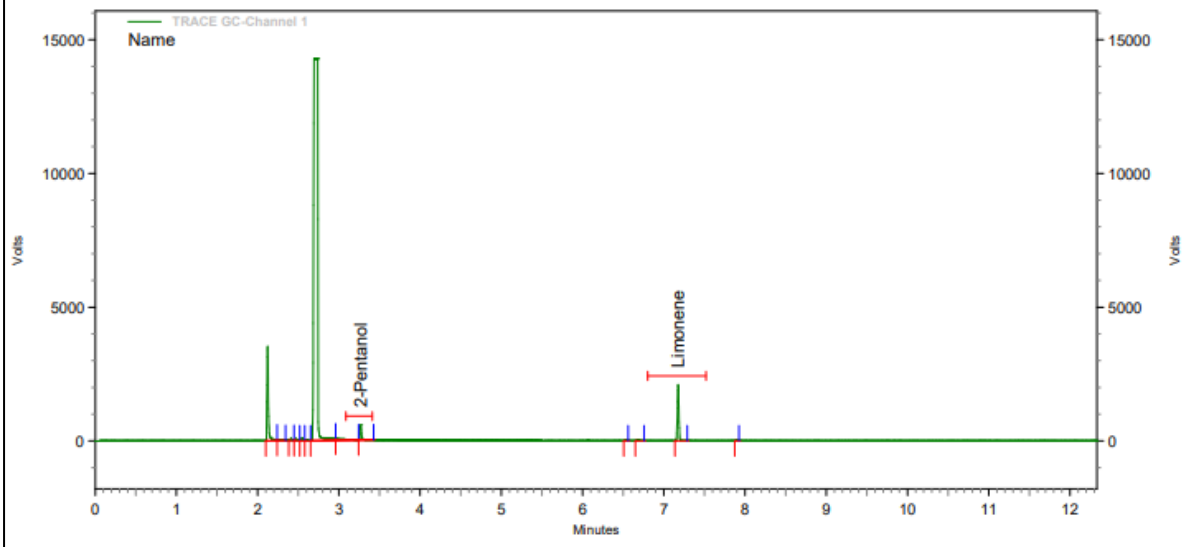

Channel A

TRACE GC-Channel 1
Results (System (2022/10/28 10:35:24) (Reprocessed))

Name	Time	Area	Amount
	2.122	41489581	0.000
	2.255	646604	0.000
	2.410	829330	0.000
	2.473	803440	0.000
	2.547	1193717	0.000
	2.610	277670	0.000
	2.693	503188874	0.000
	2.973	5458972	0.000
2-Pentanol	3.268	7420216	0.000
	6.528	123101	0.000
	6.678	433740	0.000
Limonene	7.177	25612283	69.760
	7.895	125206	0.000

Figure 25: Report of the GC-FID analysis of sample 10 to determine the composition of D-Limonene in mg

Sample No.	10
Std Amount (mg)	25.4
STD Area	7420216
Limonene Area	25612283
Limonene Amount (mg)	69.76003

$$limonene\ amount(mg) = \frac{Limonene\ Area}{Standard\ Area} * Standard\ amount(mg) * Calibration\ curve\ slope$$

$$limonene\ amount(mg) = \frac{25612283}{7420216} * 25.4 * 0.795$$

$$limonene\ amount(mg) = 69.76\ mg$$

The amount of D-limonene in mg is then converted to a concentration. The concentration is expressed as:

$$limonene\ concentration\left(\frac{mg}{ml}\right) = \frac{Limonene\ amount(mg)}{Volume\ of\ essential\ oil(ml)}$$

For this sample, sample 10, the volume of essential oil that was extracted was 1.90 ml.

$$limonene\ concentration\left(\frac{mg}{ml}\right) = \frac{69.76\ mg}{1.90\ ml} = 36.72\frac{mg}{ml}$$

Appendix D-Experimental Problem Encountered

Pressure Build-up

Pressure builds up when there is no opening for the collecting chamber. The problem with pressure building up in the column is that none of the vapours flows up the column but is rather forced to all report to the bottoms which causes potential losses in essential oil. Solution:

D-Limonene losses to the bottom

Sieve hole size

To improve the contact surface area between the citrus waste and steam, citrus waste was first ground as a pre-treatment method. Citrus waste that was formed after grinding was small and fine. Because the particles were too small, a lot of solid material passed through the primary sieve employed in the column. A sieve with more restricted holes was employed to address this problem. There were still material losses that were reported to the bottoms even though the amount of solid material lost via the sieve holes was reduced. Unground citrus waste material was used as opposed to narrower sieve holes. Due to the unground material's high particle sizes, nothing solid was able to pass through the sieve holes. It was also suggested to employ another approach rather than solely using unground material. A sieve with even smaller holes was used to make sure the grounded material could still be used. In addition to the earlier sieves, the sieve with smaller sieve holes was utilized. No solid material was reported to the bottoms in this configuration. Due to the issue with the sieve pores being too small, it was now possible to examine how grinding citrus waste may affect the amount of limonene that could be extracted from the material.

Cooling rate/ Vapor losses

The operating temperature for the steam distillation is between 90 a 100. At these elevated temperatures, sufficient cooling is required to incoming vapours to liquid. Initially, a small cooling water bath was employed supplemented with ice. However, this setup was not practical because after around 20 to 30 minutes all the ice melted, and the water was extremely hot. Due to the water being hot, the temperature was not cold enough to cool incoming vapours from the column. Since vapours were reported to the collecting chamber, essential oil vapours were lost to the atmosphere through the vent of the collecting chamber. Another problem encountered by the lack of cooling was that every time the cooling water got heated, the hot cooling water needed to be replaced with new cooling water and more ice need to be added. During the time the cooling water needed to replace, the steam distillation operation needs to be paused which is not ideal considering ideally the process needs to be allowed to run for several hours without any disturbances as this potentially affects the final yield of essential oils. To counter this problem the cooling system needed to be changed. A cooling system with a large surface area was used to increase cooling duty was used that incorporated connecting the cooling pipes to a tap which would provide continuous cool water that would not

require the distillation being paused whilst hot water is replaced with new chilly water. With this new cooling system, unnecessary disturbances to the process were reduced and there was sufficient cooling which ensured that no vapours were reported to the collecting chamber.